HIGH ENERGY SHOCK WAVE INDUCED BIOLOGICAL EFFECTS IN DIFFERENT TUMOR MODELS

G.A.H.J. SMITS

HIGH ENERGY SHOCK WAVE INDUCED BIOLOGICAL EFFECTS IN DIFFERENT TUMOR MODELS

Geert A.H.J. Smits

HIGH ENERGY SHOCK WAVE INDUCED BIOLOGICAL EFFECTS IN DIFFERENT TUMOR MODELS

Een wetenschappelijke proeve op het gebied van de
Medische Wetenschappen, in het bijzonder de Geneeskunde

PROEFSCHRIFT (THESIS)

ter verkrijging van de graad van doctor aan
de Katholieke Universiteit te Nijmegen,
volgens besluit van het college van decanen
in het openbaar te verdedigen op
donderdag 18 juni 1992
des namiddags om 15.30 uur precies

door

Gerardus Anthonius Hubertus Johannes Smits
geboren op 25 juni 1961 te Maastricht

Promotor: Prof. Dr. F.M.J. Debruyne

Co-promotores: Dr. G.O.N. Oosterhof
                  Dr. J.A. Schalken

aan: Mirjam

        mijn ouders

CONTENTS

Chapter 1

INTRODUCTION

INTRODUCTION

Clinical aspects of high energy shock waves

The search for less invasive and more efficient treatment modalities in the destruction of concrements has concentrated on the use of mechanic and acoustic energy. Using continuous wave ultrasound in early experiments, stonegrinding was achieved but (in vivo) severe tissue damage was seen (Coats 1956). In the seventies new methods using acoustic energy were developed resulting in various forms of lithotripsy (Preminger 1985, Finlayson 1989). Lithotripsy was then performed after the introduction of (flexible) probes via the ureter or by percutaneous access. Stone disintegration was obtained by the use of unfocussed shock waves which can be generated in several ways (Rous 1987). Electrohydrolic destruction can be achieved by the discharge of a capacitor via a spark gap at the tip of the probe. The resulting plasma explosion at a distance of several mm from the stone gives rise to the formation of an unfocussed shock wave which disintegrates the concrement. Unfocussed shock waves can also be generated by dielectrical breakdown in liquid or by a thermic pulse in the concrement generated either by a Nd-YAG laser or a pulsed dye laser. Alternatively, stone disintegration can be obtained by the transmission of externally generated continuous wave ultrasound via a rigid wire which is in contact with the concrement.

In addition to the development of these endourologic techniques, efforts were made to obtain contact-free destruction of concrements. Eventually the use of focussed high energy (acoustic) shock waves (HESW) resulted in the possibility of non-invasive treatment of uro-lithiasis. Based on the electrohydraulic principle, the first patent application was in 1973 for the Dornier Systems GmbH (Reichenberger 1988) and in 1974 succesful stone disintegration with little (damaging) absorption of HESW in soft tissues was reported (Forssmann 1977). The first publication on the introduction of HESW in clinical practice was in 1980, after initial experiments had confirmed the safety of this non-invasive therapy. In addition to the electrohydrolic generation, other techniques for shock wave generation suitable for non-invasive treatment have been developed.

Currently extracorporeal shock wave lithotripsy (ESWL) is the method of choice for the treatment of most renal and ureteral calculi (Assismos 1989). Exposure to shock waves for stone disintegration by commercially available lithotriptors has proven to

be relatively safe. At this moment 80 to 85% of all patients with symptomatic urinary tract calculi can be treated by ESWL. Since 1986, ESWL has been extended to the fragmentation of gall stones (Sauerbruch 1986, Sackmann 1988). The application of ESWL to gall-bladder stones however, is very limited for various anatomical and physiological reasons. Biliary lithotripsy is burdened with a high retreatment rate due to incomplete fragmentation and requires additional measures. Due to the high viscosity of the gall-bladder fluid the cavitational activity of HESW, which is an essential part of the mechanism of stone fragmentation, is hindered. Additional dissolving of biliary stones can be achieved by using chemolysis (Ponchon 1989). More recently efforts were made to increase the cavitational activity of the shock waves by decreasing the viscosity of the biliary fluid (Sass 1990).

Physical aspects of shock wave generation

Focussed acoustic shock waves are generated by an emitter outside the body and transmitted as pulsed longitudinal waves through a fluid coupling medium and the body tissue to the target. Two basic types of shock wave emitters are available:
Point and line sources; these sources are based on the generation of exploding plasma, thus resulting in an acoustic shock wave which can be focussed by elliptic or near-elliptic reflectors. Since the initial velocity of the radial propagation of the shock wave is significantly higher than the speed of sound (in water) one speaks of supersonic emitters. Exploding plasma is generated by the sudden release of energy, spark-gap emission, explosion of lead azid pellets or beam focussing of a pulsed laser (Kambe 1985, Chapman 1987, Kuwahara 1987). The shock wave generation by plasma explosion over a high voltage spark gap in water is a commonly used point source and applied in the electrohydrolic lithotriptors. After reflection, the shock wave is concentrated: its pressure increases significantly and its duration shortens.
Two-dimensional sources; these sources are based on the displacement of the surface of the emitter by which a pulsed acoustic plane wave is generated. During propagation the pulse is distorted and changes to a sawtooth form.
Two types of two-dimensional sources are clinically used for ESWL: the piezoceramic (PC) and the electromagnetic (EM) emitter. In the PC emitter the piezoceramic elements are arranged spherically. By capacitor discharge, the length of the elements changes due to a piezoelectrical effect. By displacement of their surface an acoustic pulse is generated. The acoustic pulses are focussed by acoustic

lenses if the elements are planary arranged.

The electromagnetic (EM) shock wave generator will be described more extensively because this type was used in the studies described in this thesis. The EM emitter works similar to a loudspeaker system. The shock wave source consists of a slab coil which is mounted on a hard, electrical insulating carrier separated by a thin insulating layer from an opposing metallic membrane. A capacitor discharge acts across the slab coil and induces eddy currents in the membrane. By repulsion the membrane is displaced and an acoustic pulse is emitted into the adjacent medium. During its path through water the pulse steepens and forms a shock wave. Finally the shock wave front is focussed by an acoustic, concave lens (figure 1).
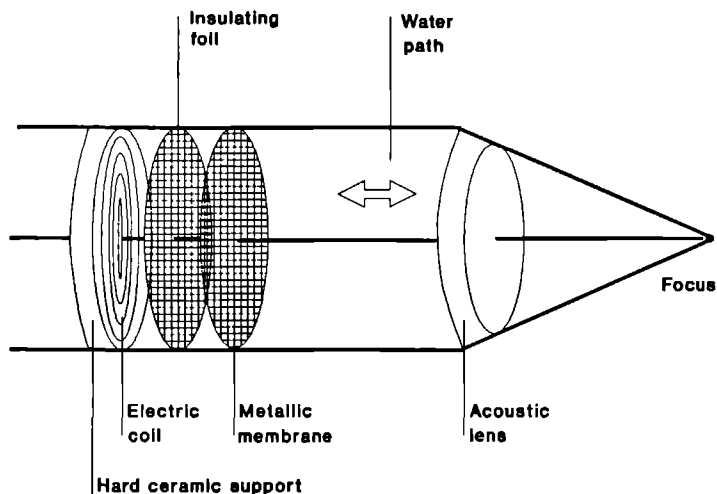
Fig. 1.
Electromagnetic shock wave generator system.

Although quantitative differences exist between the emitters, they all have in common that the acoustic pulses can be focussed into a target area of interest in the body. Variation of shock wave generation and focussing geometries results in differences in the acoustic output (Coleman 1989).

Pressure wave forms can be defined by the positive and negative peak pressures, the pulse rise time and the pulse width (Barnett 1989), allowing for the determination of the boundaries of a focal area or volume (e.g., defined as 50% of P_{max}, the -6

dB zone). In addition, the relative acoustic energy emitted in a single pulse can be calculated within prescribed areas. (Coleman 1989, Vergunst 1990). Pressure measuring techniques play an important role in shock wave technology. Several types of piezoelectric hydrophones like the tourmaline and the polyvinylidene difluoride (PVDF) membrane or needle hydrophones have been developed but all have their limitations (Pfeiler 1989, Coleman 1989). The high pressure amplitudes, the very short pressure rise times, and in particular the negative pressures make measurements difficult. Until now, apart from the peak pressures, the role of these parameters with respect to stone disintegration and biological effects are unclear. More recently, new probes which registrate the shock wave profile more accurately have been developed (Siemens, personal communication).

The electromagnetic emitter used in our experiments is the commercially available lithotriptor Lithostar (Siemens AG, Germany). The shape of a typical focussed shock wave as measured by a PVDF needle hydrophone (Müller 1985) and a 100 MHz oscilloscope is shown in figure 2.

The maximum pressure (P_{max}) can be varied from 10 to 37.5 MPa. The negative peak pressure (P_{neg}) remains relatively constant (3.8 to 4.9 MPa respectively). The pulse rise time (t_r), defined as the time necessary for the pressure to rise from 10% to 90% of the value of Pmax, ranges from 50 to 150 nsec respectively. The half width time (t_w,) defined as the width of the initial positive pressure half cycle at half amplitude, is 290 to 400 nsec respectively. The focus (defined as 50% of P_{max} (-6 dB)) is 'cigar-like shaped' (figure 3), i.e., about 95mm in the axial direction and 9 mm wide in the transversal plane, at the discharge setting (18.4 kV, P_{max}: 37.5 MPa) used in our experiments. The shock waves generated by electromagnetic sources are highly reproducible; pulse to pulse variation in the P_{max} is approximately 3% in the Lithostar (Oosterhof 1989, Vergunst 1989, Coleman 1989).
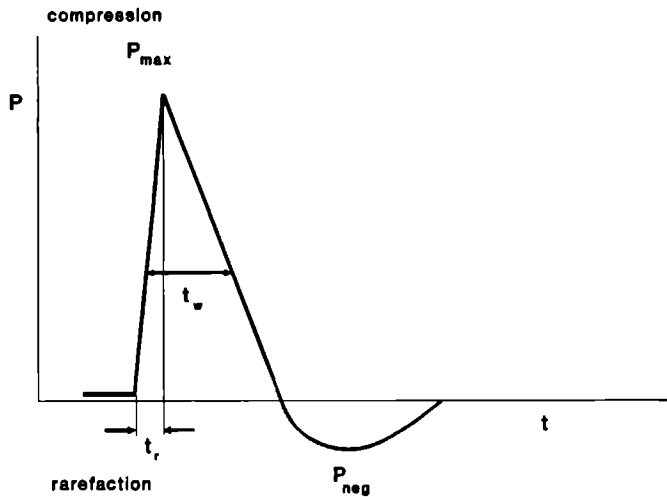
Fig. 2
Parameters of a focused shock wave. Pressure maximum (P_{max}), pressure rise time (t_r), half width time (t_w) and negative peak pressure (P_{neg}).

In addition, an experimental type of emitter was used in our experiments. The technical part is equivalent to the commercially available Lithostar *Plus* (Siemens AG), but the set-up was designed to perform experimental in vitro and in vivo studies. The shape of the shock wave profile of this generator is in principle congruent with the shock wave shown in figure 2. However, with the experimental set-up, the positive pressures can be varied from 25 to 65 MPa (P_{neg}: 4.7 to 5.7 MPa). The pulse rise time ranges from 300 to 50 nsec respectively. In addition, the focal area is relativelly smaller.
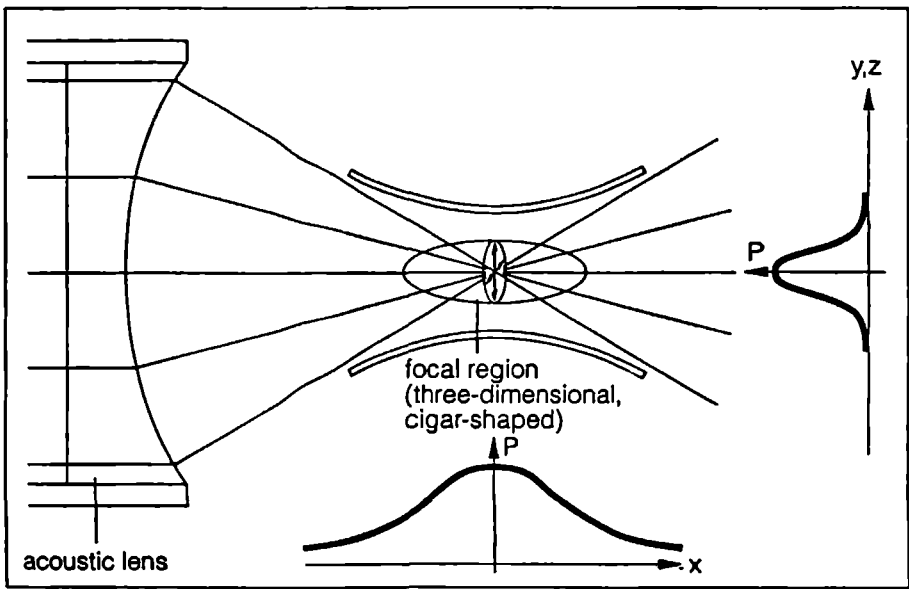
Fig. 3:
Depiction of the three-dimensional, cigar-like shaped, focal region by means of an isobar.

The mechanism of stone destruction by HESW is still not completely understood. The explanation proposed by Chaussy is that the sound impedance changes when the shock wave comes into contact with an interface, so that the compression phase is reflected depending on the acoustic quality of this interphase (Chaussy 1986). Pressure gradients and tear and shear forces due to absorption and/or internal reflection were thought to be of relevance.

More recently it has been shown that the occurence of acoustic cavitation is an essential part of the mechanism of stone fragmentation (Coleman 1987, Sass 1991). Cavitation can be defined as "any observable activity involving bubbles" (Crum 1986), i.e., the formation or movement of gas bubbles in a fluid, resulting from rapid pressure drops. The gasses in solution form gas bubbles during the rapid transformation of the positive pressure of the shock wave into the negative pressure phase. Bonding of fluid molecules can no longer follow the change in pressure and tear apart, leading to vapor bubble formation The bubble radius increases rapidly in magnitude over the negative portion of the acoustic cycle and eventually may

15

collapse (transient cavitation) or remain present (stable cavitation) (Miller 1987).
The collapsing vapor-filled cavities are thought to be responsible for a number of secondary effects. Calculations suggest temperatures and pressures to be as high as 5000 K and 1000 MPa, respectively, due to the extremely violent collapse of gas bubbles (Lauterborn 1980, Suslick 1990, Jeffries 1992). High speed cavitation microjets (water hammer blows of microjets) are generated by asymmetrical collapse of a cavitation to a boundary and create jetlike blasts of material (Coleman 1987, Crum 1988, Dear 1988). During the collaps secondary shock waves are formed.

HESW induced biological effects

Prior to clinical shock wave application for the destruction of kidney stones, Chaussy and co-workers performed studies on the pathophysiologic effects of shock wave exposure in vivo. Exposure of the thoracic area led to extensive damage of pulmonary tissue causing the death of the animals, whereas exposure of the abdomen of rats did not result in pathological changes after 24 hours or 2 weeks (Chaussy 1980).

In contrast to the low rate of side effects observed initially, more recently numerous reports show evidence of severe acute effects and chronic complications after shock wave treatment (Baumgartner 1987, Begun 1989, Fisher 1988, Haupt 1989, Hill 1990, Knapp 1988). Biological effects like injuries of living organisms (Carstensen 1990a, Hartman 1990, Miller 1985), organs or tissues in vivo (Abrahams 1988, Carstensen 1990b, Delius 1987,1988,1990ab, Gunasekaran 1989, Karlsen 1991, Newman 1987) and cells in culture (Bräuner 1989, Brümmer 1989, Clayman 1991) exposed to the focal area of shock waves have been described. The observed effects are confined to the focal area of the lithotryptor. Various histopathological and pathophysiological effects of shock waves on organs or tissues have been described (Brümmer 1990). The majority of the data concerns effects on the vascular system (Brendel 1987, Goetz 1988, Kaude 1985, Knapp 1988, Prat 1991b, Recker 1989, Weber 1992, Williams 1988).

The consequences of shock waves on living tissue, i.e., the extent and mechanism of cellular and tissue damage, are poorly understood. These may be be explained by the sudden pressure changes and/or the induction of cavitations and cavitation related phenomena since biological systems are known to possess cavitation nuclei. Conventional wisdom has come to relate the likelihood of the occurence of transient

cavitation to the magnitude of the negative pressure in the acoustic wave. The shock wave area of a lithotripter provides an ideal system to study the effects of acoustic cavitation (Coleman 1987).

Cavitation in vitro is a complicated and typically uncontrolled process which is very difficult to study in a manner amenable to detailed analysis of biological effects (Miller 1987). Presently, there are no conclusive experimental results on cavitation thresholds in biological media for transient shock waves. The variability of the occurence of cavitation nuclei during exposure may in fact explain the discrepancies in results of studies on HESW induced biological effects (Carstensen 1987). Several critical factors should be considered in the assessment of the effects of HESW induced cavitation in vitro (Bräuner 1989, Laudone 1989). Thus it is unclear to what extent the in vitro observed phenomena occur in vivo. Recent studies have revealed the in vivo occurence of cavitations in the focal beam of a lithotryptor (Delius 1988, Brody 1991, Prat 1991a, Mayer 1990).

A number of cavitation related phenomena which could be of relevance in the induction of bio-effects have been described (Miller 1987). These include the formation of radicals (short living highly reactive molecules or atoms) with concomitant chemical activity (Coackley 1978, Crum 1986, Morgan 1988). Recent in vitro studies have shown evidence for the generation of intracellular free radicals (Suhr 1991).

The gas bubbles that are formed during the cavitation process collapse and may result in the emission of a tissue destructing liquid jet. Induction of hydrodynamic shear stresses and intracellular microstreaming results in viscous shearing stress (Miller 1987). As mentioned earlier, during the collapse (implosion) of HESW induced gas bubbles, the compression of gas results in a local increase of temperature up to several thousand Kelvin without heat exchange with the surrounding medium. Thermal injury (macroscopic heating) is not very likely to be the cause of tissue or cell damage by HESW, since the low frequency shock waves are not absorbed well by the tissue (Filipczynski 1990). Further research on HESW cytotoxicity in vivo is necessary and will be crucial to increase our knowledge on the mechanism of action and the extent of HESW induced bioeffects.

This may not only contribute to a better understanding of a safe operation with this type of ultrasound equipment for stone disintegration, but especially to the use of the HESW field in new (experimental) applications to living tissue.

HESW are easy to apply in a non-invasive way, can be focussed in the body very accurately in a small area of interest, exert their effect only in this area, and are known not to induce systemic side effects. Thus, HESW are likely to be useful in a non-invasive tumor therapy.

In 1985, Russo and associates first published results on in vitro exposure of tumor cells to HESW and noted a dose-dependent cytotoxic effect. Further in vitro investigations on single cell suspensions showed that application of the shock waves, when focussed on single cell suspensions of (tumor)cells, resulted in cell permeability changes, an impaired clonogenic potential, and a decreased tumorigeneity in vivo (Brümmer 1989, Berens 1990, Chen 1991, Gambihler 1990, Kohri 1990, Oosterhof 1989, Prat 1991a). Intact cells contained swollen mitochondria with distended cristae suggesting sub-cellular, not necessarily irreversible damage. Some authors suggested that the HESW induced intra-cellular damage may not be manifest immediately (Berens 1990). Exposure of multi-cellular tumor spheroids showed an alteration in cell shape, perinuclear cisternae, and vacuolisation of the cytoplasm (Bräuner 1989).

In in vivo experiments, exposure of tumors to shock waves resulted in a growth delay (Russo 1985, Chaussy 1986). Since these initial experiments, a number of studies using different tumor types have been published (Debus 1991, Delius 1989, Holmes 1990, Hoshi 1991, Lee 1990, Randazzo 1988, Weiss 1990). In most studies only a temporary anti-tumor effect was observed and the only specific histopathological events observed were necrotic regions indistinguishable from spontaneous necrosis.

Since, at the time we stared our studies, in 1988, little was known about the factors that might influence the effects of shock waves on tumor cells, as well as the underlying mechanisms of HESW induced tumor growth suppression, the aim of this thesis was to investigate these aspects in more detail, both in vitro as well as in vivo.

In chapter 1 the historical background of the clinical introduction of high energy shock waves (HESW) is described. Furthermore several relevant physical aspects of HESW and the generators are discussed. Finally, the knowledge concerning HESW induced bioeffects, particularly on tumor tissue is reviewed.

In chapter 2 we deal with the importance of experimental set up in determining in vitro the effects of HESW. Furthermore, the sensitivity of various cell types for acoustic shock waves was determined. From chapter 3 on we exclusively deal with in vivo administration of HESW, since we learned from the previous studies(chapter 2) that the experimental set up critically determines the observed effect, hence the relevance for in vivo tumor treatment was at least questionable. In this chapter 3 we describe how we empirically determine the effectiveness of several HESW (combination) treatment regimens on tumor growth. In order to better understand the critical factors that influence the in vivo antitumor effect, knowledge that is essential for the rational design of further treatment schemes, we used various methods to unravel the mechanisms involved in the tumor growth suppression. For the histopathological analyses (electron and light microscopy) the animals had to be sacrificed. Nuclear magnetic resonance spectroscopy (MRS) provided us with the possibility to study the biochemical changes in a non-invasive longitudinal way. Thus we studied normal tissue (muscle) in chapter 4 and tumors in chapter 5. These studies suggested that especially in tumors perfusion was strongly affected by HESW treatment. We therefore recruited MRS to directly measure tumor blood flow. After intra-tumoral injection of D_2O the exclusion of the tracer was measured and the effects of HESW on tumor blood flow were determined.

REFERENCES

Abrahams C., Lipson S., Ross L. Pathologic changes in the kidneys and other organs of dogs undergoing extracorporeal shock wave lithotripsy with tubless lithotripter.
J. Urol., 140, 391, 1988.

Assismos D.G., Boyce W.H, Harrison L.H., McCollough D.L., Kroovand R.L. The role of open stone surgery since extracorporeal shock wave lithotripsy J. Urol., 142, 263, 1989.

Barnett S.B. Parameters for bioeffects experiments, overview.
Ultrasound in Med. & Biol., 15, sup.1, 75, 1989.

Baumgartner B R., Dickney K.W., Ambrose S.S., Walton K.N., Nelson R.C., Bernadino M.E. Kidney changes after extracorporeal shock wave lithotripsy appearing on MR imaging.
Radiology, 163, 531, 1987.

Begun F.P., Lawson R.K., Kearns C M., Tieu T.M. Electrohydrolic shock wave induced renal injury.
J. Urol., 142, 155, 1989

Berens M E., Welander C E., Griffin A.S., McCullough D L. Effect of acoustic shock waves on clonogenic growth and drug sensitivity of human tumor cells in vitro. J. Urol., 142, 1090, 1989.

Bräuner T., Brummer F., Hulser D F. Histopathology of shock wave treated tumor cell suspensions and multicell tumor spheroids. Ultrasound Med. Biol, 15, 451, 1989.

Brendel W., Delius M, Goetz A. Effect of shock waves on the microvasculature.
Prog. Appl. Microcirc., 12, 41, 1987.

Brody J.M., Siebert W.F., Cattau E L., Kawas F., Goldberg J.A., Zeman R K. Detection of tissue injury after extracorporeal lithotripsy of gall stones. J. Clin. Gastroenterology, 13, 348, 1991.

Brummer F., Brenner J, Bräuner T., Hulser D F. Effect of shock waves on suspended and immobilized L1210 cells. Ultrasound Med. Biol., 15, 451, 1989.

Brummer F, Bräuner T., Hulser D F Biological effects of shock waves. World J. Urol, 8, 224, 1990.

Carstensen E.L. Acoustic cavitation and the safety of diagnostic ultrasound.
Ultrasound Med. Biol., 13, 597, 1987.

Carstensen E.L., Campbell D S., Hoffman D, Child S Z., Ayme-Bellegarda. Killing of Drosophila larvae by the fields of an electrohydrolic lithotripter. Ultrasound Med. Biol, 16, 687, 1990a.

Carstensen E.L., Hartman C., Child S.Z., Cox C A., Mayer R., Schenk E. Test for kidney hemorrhage following exposure to intense, pulsed ultrasound Ultrasound Med. Biol., 16, 681, 1990b.

Chapman W.H., Mayo M.E., Norton B F. Alternative forms of extracorporeal shock-wave lithotripsy.
In. Stone disease, diagnosis and management, Rous S.N., Ed. Grune & Stratton, 311, 1987

Chaussy Ch., Brendel W., Schmiedt E. Extracorporeally induced destruction of kidney stones by shock waves. The Lancet, 1265, 1980.

Chaussy Ch., Randazzo R F., Fuchs G.J. The effects of extracorporeal shock waves on FANFT bladder tumors in C3H/He mice. J. Urol., 139, 324, 1986.

Chen C.L., Guo Z.H., Zhao Y., Pu J.X, Chen Z.X, Zhang R. Suppressive effect of high energy shock waves on tumor cells. Chin. Med. J. Engl, 104, 548, 1991.

Clayman R.V., Long S., Marcus M High energy shock waves: in vitro effects.
Am. J. Kidney Dis., 17, 436, 1991.

Coackley W.T., Nyborg W.L. Ultrasound: Its applications in Medicin and Biology, ed. Fry F.J. Elsevier Amsterdam, 77, 1978.

Coats E.C. The application of ultrasonic energy to urinary and biliary calculi. J. Urol., 75, 865, 1956.

Coleman A.J., Saunders J.E., Crum L.A., Dyson M. Acoustic cavitation generated by an extracorporeal shockwave lithotripter. Ultrasound Med. Biol., 13, 69, 1987.

Coleman A.J., Saunders J.E. A survey of acoustic output of commercial extracorporeal shock wave lithotripters. Ultrasound Med. Biol., 15, 213, 1989.

Crum L.A., Fowlkes J.B. Acoustic cavitation generated by microsecond pulses of ultrasound. Nature, 391, 52, 1986.

Crum L.A. Cavitation on microjets as a contributory mechanism for renal calculi disintegration in ESWL. J. Urol., 140, 1587, 1988.

Dear J.P., Field J.E., Walton A.J. Gas compression and jet formation in cavities collapsed by shock wave. Nature, 332, 505, 1988.

Debus J., Peschke P., Hahn E.W., Lorenz W.J., Lorenz A., Ifflaender H., Zabel H.J., van Kaick G., Pfeiler M. Treatment of the Dunning prostate rat tumor R3327-AT1 with pulsed high energy ultrasound shock waves (PHEUS): growth delay and histomorphologic changes. J. Urol., 146, 1143-1146, 1991.

Delius M., Heine G., Stark J., Remberger K., Brendel W. Biological effects of shock waves: lung hemorrhage by shock waves in dogs; pressure dependence. Ultrasound Med. Biol., 13, 61, 1987.

Delius M., Enders G., Xuan Z., Liebich H-G., Brendel W. Biological effects of shock waves: kidney damage by shock waves in dogs - dose dependence. Ultrasound Med. Biol., 14, 117, 1988.

Delius M., Weiss N., Gambihler S., Goetz A., Brendel W. Tumor therapy with shock waves requires modified lithotripter shock waves. Naturwissenschaften 76, 573, 1989.

Delius M., Denk R., Berding C., Liebich H-G., Jordan M., Brendel W. Biological effects of shock waves: cavitation by shock waves in piglet liver. Ultrasound Med. Biol., 16, 467, 1990a.

Delius M., Jordan M., Liebich H-G., Brendel W. Biological effects of shock waves: effect of shock waves on the liver and gall-bladder wall of dogs; administration rate dependence. Ultrasound Med. Biol., 16, 459, 1990b.

Filipczynski L., Piechocki M. Estimation of the temperature increase in the focus of a lithotripter for the case of high rate administration. Ultrasound Med. Biol., 16, 149, 1990.

Finlayson B., Ackermann D. Overview of surgical treatment with special reference to lithotripsy. J. Urol., 141, 778, 1989.

Fisher N., Mller H.M., Gulhan A., Sohn M., Deutz Fj., Rubben H., Lutzeyer W. Cavitation effects: possible cause of tissue injury during extracorporeal shock wave lithotripsy. J. Endourol., 2, 215, 1988.

Folberth W. Non-invasive treatment of urinary and biliary stones with extracorporeal shock wave lithotripsy. Atomkernenergie-Kerntechnik, 53, 1989.

Forssmann B., Hepp W., Chaussy Ch., Eisenberger F. Eine methode zur berührungsfreie Zertrümmerung von Nierensteinen durch Stosswellen. Biomed. Technik, 22, 164, 1977.

Gambihler S., Delius M., Brendel W. Biological effects of shock waves: cell disruption, viability, and proliferation of L1210 cells exposed to shock waves in vitro. Ultrasound Med. Biol., 16, 587, 1990.

Glickson J.D., Wehrle J.P., Rajan S.S., Li S.J., Steen R.G. NMR spectroscopy of tumors. In: Pettegrew J.W. (ed.) NMR, priciples and applications to biomedical research, Springer-Verlag, New York, 1990.

Goetz A.E., Königsberger R., Hammersen F., Conzen P., Delius M., Brendel W. Acute shock wave induced effects on the microcirculation. In: Steiner R. (ed.) Laser Lithotripsy, Springer Verlag Berlin Heidelberg, 1988.

Gunasekaran S., Donovan J.M., Chvapil M., Drach G. Effects of extracorporeal shock wave lithotripsy on the structure and function of rabbit kidney. J. Urol., 141, 1250, 1989.

Hartman C., Cox C.A., Brewer L., Child S.Z., Cox C.F., Carstensen E.L. Effect of lithotripter fields on the development of chick embryos. Ultrasound Med. Biol., 16, 581, 1990.

Haupt G., Haupt A., Donovan J.M., Drach G.W., Chaussy C. Short-term changes of laboratory values after extracorporeal shock wave lithotripsy: a comparitive study. J. Urol., 142, 259, 1989.

Hill D.E., McDougal W.S., Stephens H., Fogo A., Koch M.O. Physiological and pathological alterations associated with ultrasonically generated shock waves. J. Urol., 144, 1531, 1990.

Holmes R.P., Yeaman L.I., Li W., Hart L.J., Wallen C.A., Woodruff R.D., McCullough D.L.: The combined effects of shock waves and cisplatin therapy on rat prostate tumors.
J. Urol., 144, 159, 1990.

Hoshi S., Orikasa S., Kuwahara M., Suzuki K., Yoshikawa K., Saitoh S., Ohyama C., Satoh M., Kawamura S., Nose M. High energy underwater shock wave treatment on implanted urinary bladder cancer in rabbits. J. Urol., 146, 439, 1991.

Jeffries J.B., Copeland R.A., Suslick K.S., Flint E.B. Thermal equilibration during cavitation.
Science, 256, 248, 1992.

Kambe K., Kuwahara M., Kurosu S. Underwater shock wave focussing - an application to extracorporeal lithotripsy. Proc. 15th Intern. Symp. on shock waves and shock tubes, 641, 1985.

Karlsen S.J., Smevik B., Hovig T. Acute morphological changes in canine kidneys after exposure to extracorporeal shock waves. Urol. Res., 19, 105, 1991.

Kaude J.V., Williams C.M., Millner M.R., Scot K.N., Finlayson B. Renal morphology and function immediately after extracorporeal shock-wave lithotripsy. AJR., 145, 305, 1985.

Knapp P.M., Kulb T.B., Lingeman J.E., Newman D.M., Mertz J.H.O., Mosbaugh P.G., Steele R.E. Extracorporeal shock wave induced perirenal hematoma. J. Urol., 139, 700, 1988.

Kohri K., Uemura T., Iguchi M., Kurita T. Effect of high energy shock waves on tumor cells. Urol. Res., 18, 101, 1990.

Kuwahara M., Kambe K., Kuroso S., Kageyama S., Ioritani N., Orikasa S., Takayama K. Clinical application of extracorporeal shock wave lithotripsy using microexplosions. J. Urol., 137, 837, 1987.

Laudone V.P., Morgan T.R., Huryk R.F., Heston W.D.W., Fair W.R. Cytotoxicity of high energy shock waves: methodologic considerations. J. Urol., 141, 965, 1989.

Lauterborn W. Cavitation and inhomogeneities in underwater accoustics.
Springer-Verlag, Berlin, 1980.

Lee K.E., Smith P., Cocket A.T. Influence of high energy shock waves and cisplatin on antitumor effect in murine bladder cancer. Urology, 36, 440, 1990.

Mayer R., Schenk E., Child S., Norton S., Cox C., Hartman C., Cox C., Carstensen. Pressure

threshold for shock wave induced renal hemorrhage. J. Urol., 144, 1505, 1990.

Miller D.L., Microstreaming shear as a mechanism of cell death in elodea leaves exposed to ultrasound. Ultrasound Med. Biol., 11, 285, 1985.

Miller D.L. A review of the ultrasonic bioeffects of microsonation, gas-body activation, and related cavitation-like phenomena. Ultrasound Med. Biol., 13, 443, 1987.

Morgan T.R., Laudone V.P., Heston W.D.W., Zeitz L. and Fair W.R. Free radical production by high energy shock waves; comparison with ionizing irradiation. J. Urol., 139, 18, 1988.

Müller M., Platte M. Einsatz einer breitbandigen Piezodrucksonde auf PVDE-Basis zur Untersuchung konvergierender Stosswellen in Wasser. Acustica, 58, 215, 1985.

Newman R.C., Hackel R.L., Senior D.F., Brock K.A., Feldman J. ESWL pathological effects on canine renal tissues. Urology, 29, 194, 1987.

Oosterhof G.O.N., Smits G.A.H.J., de Ruyter J.E., van Moorselaar R.J.A., Schalken J.A., Debruyne F.M.J. The in vitro effect of electromagnetically generated shock waves on the Dunning R3327 P-AT-2 rat prostatic cancer cell line. Urol. Res., 17, 13, 1989.

Oosterhof G.O.N., Smits G.A.H.J., de Ruyter J.E., Schalken J.A., Debruyne F.M.J. In vivo effects of high energy shock waves on urological tumors; an evaluation of treatment modalities.
J. Urol., 144, 785, 1990a.

Oosterhof G.O.N., Smits G.A.H.J., de Ruyter J.E., Schalken J.A., Debruyne F.M.J. Effects of high energy shock waves combined with biological response modifiers or adriamycine on a human kidney cancer xenograft. Urol. Res., 18, 419, 1990b.

Pfeiler M., Matura E., Iffländer H., Seyler G. Lithotripsy of renal and biliary calculi: physics, technology and medical-technical application. Electromedica 57, 52, 1989.

Ponchon T., Barkun A., Pujol B., Mestas J.L., Lambert R. Gallstone disappearance following extracorporeal lithotripsy and oral bile acid solution. Gastroenterology, 97, 457, 1989.

Prat F., Chapelon J.Y., Chauffert B., Ponchon T., Cathignol D. Cytotoxic effects of acoustic cavitation on HT-29 cells and a rat peritoneal carcinomatosis in vitro.
Cancer Res., 51, 3024, 1991a.

Prat F., Ponchon T., Berger F., Chapelon Y., Gagnon P., Cathignol D. Hepatic lesions in the rabbit induced by acoustic cavitation. Gastroenterology, 100, 1345, 1991b.

Preminger G.M., Peterson R., Peters P.C., Pak C.Y.C. The current role of medical treatment of nephrolithiasis; the impact of improved techniques of stone removal. J. Urol., 134, 6, 1985.

Randazzo R.F., Chaussy C.G. Fuchs G.J. Bhutta S.M., Lovrekovich H., de Kernion J.B. The in vitro and in vivo effects of extracorporeal shock waves on malignant cells. Urol. Res., 16, 419, 1988.

Recker F., Rübben H., Bex A., Constantinides C. Morphological changes following ESWL in the rat kidney. Urol. Res., 17, 229, 1989.

Reichenberger H. Lithotrypter systems. Proceedings of the IEEE., 76, 1236, 1988.

Rous S.N. Ed. Stone Disease, Diagnosis and Managment. Orlando, Grune & Stratton, 1987.

Russo P., Heston W.D.W., Fair W.R. Suppression of in vitro and in vivo tumor growth by high energy shock waves. Surg. Forum, 36, 645, 1985.

Russo P., Stephenson R., Mies C., Huryk R., Heston W.D.W., Melamed M.R., Fair W.R. High energy shock waves suppress tumor growth in vitro and in vivo. J. Urol., 135, 626, 1986.

Russo P., Mies C., Huryk R., Heston W.D.W., Fair W.R. Histopathologic and ultrastructural correlates of tumor growth suppression by high energy shock waves. J. Urol., 137, 338, 1987.

Sackmann M. Shock-wave lithotripsy of gall-bladder stones. N. Engl. J. Med., 318, 393, 1988.

Sass W., Bräunlich M., Dreyer H-P., Matura E., Folberth W., Priesmeyer H-G., Seifert J. The mechanisms of stone disintegration by shock waves. Ultrasound Med. Biol. 17, 239-243, 1991.

Sauerbruch T., Delius M., Paumgartner G., Holl J., Wess O., Weber W., Hepp W., Brendel W. Fragmentation of gallstones by extracorporeal shock waves. N. Engl. J. Med., 314, 818, 1986.

Suhr D., Brümmer F., Hülser D.F. Cavitation-generated free radicals during shock wave exposure: investigations with cell-free solutions and suspended cells. Ultrasound Med. Biol., 17, 761, 1991.

Suslick K.S. Sonochemistry. Science, 247, 1440, 1990.

Vergunst H., Terpstra O.T., Schröder F.H., Matura E. Assessment of shock wave pressure profiles in vitro; clinical implications. J. Lithotripsy & Stone Dis., 1, 289, 1989.

Weber C., Moran M., Braun E.J., Drach G.W. Injury of rat renal vessels following extracorporeal shock wave treatment. J. Urol., 147, 476, 1992.

Weiss N., Delius M., Gambihler S., Dirschedl P., Goetz A., Brendel W. Influence of the shock wave application mode on the growth of A-MEL3 and SSK2 tumors in vivo. Ultrasound Med. Biol., 16, 595, 1990.

CYTOTOXIC EFFECTS OF HIGH ENERGY SHOCK WAVES
IN DIFFERENT IN VITRO MODELS;
Influence of the experimental set-up

Geert A.H.J. Smits, Gosse O.N. Oosterhof, Anja E. de Ruyter,
Jack A. Schalken, Frans M.J. Debruyne

Department of Urology, University Hospital Nijmegen, The Netherlands

ABSTRACT

High energy shock waves (electromagnetically generated, Siemens Lithostar) were studied for their effects in vitro on different (tumor) cell types. Cells were exposed to the shock waves as a single cell suspension or as a cell pellet on the bottom of a test tube. In both cases, a dose dependent direct cytotoxicity, established by trypan blue dye exclusion, was observed after treatment with 1000 or 2000 shock waves. Also, the antiproliferative capacity as determined by clonogenic potential (double layer soft agar) and growth rate (plastic) were affected in this way. However, comparing the results after treatment in suspension or pellet, a discrepancy was evident, i.e. the cell lines showed a different susceptibility in pellet vs. suspension. Also the differential sensitivity of the cell types varied in these two treatment models. Furthermore the outcome depended on the cell concentration; direct cytotoxicity in a cell suspension was more pronounced at higher cell concentrations, while in a pellet this was increased by reducing the number of cells. Finally, no shock wave induced cytotoxicity could be seen after fixation of cells in gelatine or by placing the pellet on a bottom layer of gelatine. Pressure measurements revealed no adequate explanation for this phenomenon.

These results indicate that in vitro effects depend on the way cells are exposed to the shock waves and can be greatly influenced by changing the conditions of the micro-environment. Therefore, precise descriptions of the experimental set-up and careful interpretations of their outcome are obligatory.

INTRODUCTION

Since Russo et al. (1985, 1986) showed that electrohydraulically generated high energy shock waves (HESW) can be cytotoxic to tumor cells in vitro and in vivo, several investigators reported similar observations (Berens 1989, v.Dongen 1989, Laudone 1989, Oosterhof 1989, 1990a,b, Randazzo 1988, Russo 1985, 1986).

Although the precise mode of action of HESW is not yet understood, several possible mechanisms for shock wave induced cytotoxicity are suggested. Thermal injury seems most unlikely (Miller 1987), and among the non-thermal effects, cavitation (gas body activation) with subsequent secondary shock waves, hydro-dynamic jets and free radical generation are supposed to be responsible for the cellular damage observed (Coleman 1987, Crum 1986, Miller 1987, Morgan 1988). Most of the in vitro experiments were performed by exposing (tumor-) cells as a single cell suspension to shock waves generated by different types of (experimental) lithotriptors.

Several critical factors within the design and interpretation of HESW experiments concerning the cytotoxic potential of shock waves in vitro were described. It is known that in vitro exposures tend to enhance cavitation mechanisms (Miller 1987). In addition, more recently, Laudone et al. (1989) showed that the composition of containment vessel, presence or absence of acoustic interfaces and environmental factors significantly alter the outcome of the experiments. Brümmer and Bräuner et al. (1989) conclude that cell damage after treatment of cells or multicellular spheroids in suspension must be attributed to shearing and acceleration forces, since embedding these cells or cultures in agar completely protects the cells from damage by HESW. These studies demonstrate the importance of the in vitro experimental set-up in studies on the cytotoxic effects of HESW.

Furthermore, different types of (experimental) lithitriptors vary in their acoustic parameters (Coleman 1989). Indeed, physical and biological factors must be considered in the assessment of the effects of HESW in vitro.

In order to get more insight in the way cells are damaged by HESW in vitro, we treated (tumor-) cells under various experimental conditions. Also, we investigated wether the cytotoxic effect of HESW depends on the cell type used.

MATERIALS AND METHODS

Cell lines

Three tumor cell lines and one fibroblast cell line were used. The Dunning R3327 PAT-2 prostatic carcinoma was generously provided by Dr. John Isaacs (Baltimore, Md, USA). The Gural human kidney tumor cell line was provided by Dr. S.O. Warnaar (Leiden, The Netherlands). The Caki-2 human kidney tumor cell line (HTB-47) and fibroblast cell line (CCL-64) were obtained from the American type culture collection. The cell lines were cultured in RPMI-1640 medium (Gibco) enriched with 10% fetal calf serum (Gibco), 1% L-glutamine, 100,000 U/L penicillin, 100,000 μg/L streptomycin and 2.2% HEPES, and were grown as monolayer cultures at 37° C in a humidified atmosphere of 5% CO_2 in air. Cell cultures were routinely tested for mycoplasma contamination using Hoechst staining kit (Flow Laboratories).

Sample preparation

Just before HESW exposure, cells were trypsinized using 0.25 mg/ml trypsine and 0.1% EDTA and resuspended in enriched RPMI medium. Cells were exposed to HESW in completely filled polyethylene test tubes (diameter 9 mm, rounded bottom, Alpha Laboratories) as:
(*a*) single cell suspension (s.c.s.) in enriched medium.
(*b*) s.c.s. with gelatine 15% in enriched medium.
(*c*) cell pellet covered by gelatine 15% in enriched medium.
(*d*) cell pellet between gelatine 15% in enriched medium.
Sample (*b*) was prepared by mixing the s.c.s. with a sterile and purified gelatine (Merck) solution in enriched medium at 37° C. The solution solidified at 4° C (30"). For the pellet samples, the cells were pelleted (800 g, 5 min.) in the test tube directly on the bottom, sample (*c*), or on a bottom layer of gelatine 15% in enriched medium, sample (*d*).
Pilot experiments revealed that exposing a pellet, covered by enriched medium without addition of gelatine, resulted in distortion of the pellet, whereby a fraction of cells became suspended. Therefore, we applicated an additional cover layer of 15% gelatine on the pellet, in order to immobilize the pellet properly and avoid these side effects.

HESW treatment

For these studies the commercially available lithotriptor (Siemens, Lithostar) was used. Cells were exposed to the shock waves in an experimental set-up as described earlier (Oosterhof 1989). In brief, the shock wave tube of the lithotriptor was in contact with a water filled plexiglass container over a silicon membrane in its lateral side. Optimal contact was ensured by a gel placket and lubricating gel. The test tube was submerged in the water, and positioned in the centre of the focal area (fluoroscopically controlled).

Shock waves were applied at an energy output level of 18.4 kV (corresponding with P_{max} 37.5 MegaPascal (MPa) and P_{neg} 5.0 MPa in water) with a frequency of 80/min. The temperature of the water was 22° C or 37° C .

Pressure measurements

Several physical factors can significantly influence the actual exposure and thus the result of the experiments. Therefore, in order to get an optimal and reproducible set-up, pressure measurements were performed using a piezoelectric crystal transducer (Imotec) connected with a 100 mHz oscilloscope (Gould DSO, 4072). In this way the spatial-peak temporal-peak positive (P_{max}) and negative (P_{neg}) pressures were determined (Coleman 1989).

To determine the field of pressures, the piezoelectrical sensor was placed at different sites in the water bath. To exclude a possible absorption of shock waves by the polyethylene test tube, pressures were also registered in the radiological focus with and without shielding the transducer by the tube.

Finally, pressure measurements were performed in the test tube filled with different concentrations of gelatine.

Trypan-blue dye exclusion

Cell viability was determined before and after HESW treatment by adding 15 μl trypan-blue solution (25 mg in 5 ml 3% acetic acid) to 15 μl cell suspension and simultaneously counting colored and not colored cells using a Bürker Türk hemocytometer.

Cloning in soft agar

For the tumor cell lines the anchorage-independent clonogenic potential was evaluated by the modified double layer soft agar culture system as initially described by Salmon and Hamburger (1977). In brief, petri-dishes (35 mm diameter) were seeded with the treated or sham treated cells in doubly enriched CMRL-1066 (Gibco) with 0.3% agar in the top layer, on a bottom layer of doubly enriched McCoy's-5A (Gibco) medium with 0.5% agar. The cultures were reincubated at $37^{\circ}C$ and 6% CO_2 in a humidified atmosphere. As a cytotoxic control, $HgCl_2$ (0.37 mM) was used in an overlayer of 200 μl/dish.

The dynamic growth of colonies was detected and followed by counting the dishes using the Omnicon FAS-2 automated colony counter (Milton Roy Inc.) (Herman 1983). With this method the number of colonies produced was determined at day 21.

Proliferation on plastic

Unlike tumor cells, fibroblasts do not form colonies in soft agar (Hamburger 1977). Therefore, the proliferative capacity of the CCL-64 fibroblasts was determined by their growth on plastic substrate. Viable cells (10^5) were inoculated in triple in a series of 75 cm^2 culture flasks (Costar), and grown at 37° C and 6% CO_2. After several periods of time (3, 24, 48 and 72 hours), trypsinized cells were counted by means of a hemocytometer, and viability was determined by the trypan blue dye exclusion. Growth curves were obtained by serial plotting the measurements of time of culture and the corresponding log of the mean total cell number at that respective time point.

Influence of the experimental set-up; physical aspects

To study possible alterations in acoustic output due to the use of the test tube or the gelatine application, and to avoid the risk of error from missing the region of maximum pressure, pressure measurements were carried out under all exposure conditions.

Focal area

Characterization of the acoustical field generated by this lithotriptor showed a similar focal area ($P_{max}50$) as determined earlier (Oosterhof 1989), and is in agreement with data recently published (Coleman 1989). Of interest is the marked pressure drop in the lateral plane of the focal area. Its diameter is only 6 mm, i.e. the peak positive pressure in the centre of the focal area is 37.5 megapascal (MPa), at the edge 20 MPa, and 2 mm outside the focal area 7.5 MPa (18.4 kV). This small diameter stresses the importance of a precise position of the test tube in the water bath. In addition this pressure drop exists also in the test tube (diameter 9 mm).

The test tube

In order to study the influence of the polyethylene tube, pressure profiles were determined in the water bath with and without shielding the piezoelectric transducer by the test tube. These measurements showed no significant differences in P_{max} and P_{neg} indicating that there is no pressure loss due to this tube used (data not shown).

Gelatine in the medium.

Measurements in a rising concentration of gelatine (0-20%) medium in the test tube showed a gradual decrease of temporal peak pressures; P_{max} from 37.5 to 31.0 MPa and P_{neg} from 5.5 to 4.3 MPa. Pulse to pulse variation was 3%.

a. Influence of non-physiologic conditions

Temperature

Cell suspensions or cell pellets were immobilized by adding gelatine up to 15 % in enriched medium. Due to liquification at 37° C these experiments were carried out at 22° C. Therefore it was of importance to establish wether the temperature influenced the antiproliferative effects of HESW. PAT-2 cells when exposed in suspension at 22 or 37°C showed no significant difference in the fraction of viable cells or number of colonies formed in the soft agar clonogenic assay (viability: 96/53% c.q. 97/56%, number of colonies: 330/90 c.q. 680/213 control/treated).

Gelatine application

Manipulation of cells for HESW exposure (gelatine embedding, or pelleting for three hours, the time needed to carry out the experiments), did not significantly alter cell viability (2-4 % decrease according to the dye exclusion).

b. Influence of the micro-environment; cell surroundings and cell concentration

In order to study these biological parameters four different samples *(a,b,c,d)* were prepared as described above.

single cell suspension (a)

It appeared that for the cell suspensions the fraction of viable cells decreased with an increasing number of shock waves (Fig. 1).

This viability was also influenced by the cell concentration; cell damage was more pronounced in a sample containing a higher concentration of cells. Comparing samples with an equal cell concentration, a differential sensitivity towards HESW became evident. The kidney tumor cell lines (Caki-2 and Gural) were most sensitive (Fig. 1), and 2000 HESW resulted in 40-60% cell loss (debris) in contrast to the PAT-2 and CCL-64 cell lines (0-5%).

As we reported earlier (Oosterhof 1989), PAT-2 cells show a decreased anchorage independent clonogenic potential when treated as a single cell suspension. Similar but more pronounced results were obtained for the kidney tumor cell lines Caki-2 and Gural (Table 1).

Table 1.

Colonies formed (% of control) at day 21 in the double layer soft agar clonogenic assay, after exposure to 2000 HESW of a single cell suspension (sample (a)) or a cell pellet (sample (c)).

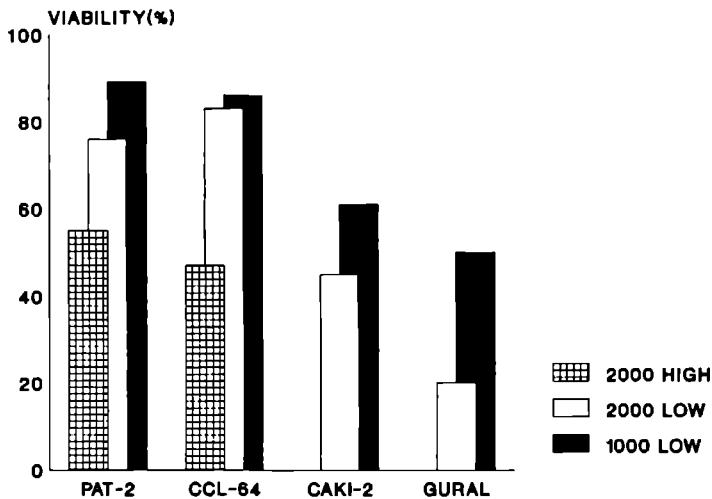|	suspension (a)	pellet (c)
PAT-2	50%	80%
Gural	15%	70%
CAKI	30%	n.d.

Fig. 1.
Viability, according to the trypan blue dye exclusion test, after exposure to 1000 or 2000 HESW of single cell suspensions (sample (a)) with high (30.10^6 cells/ml) or low (5.10^6 cells/ml) concentration of cells.

As stated before, proliferation of fibroblasts cannot be evaluated in the double layer soft agar assay. Therefore, we evaluated the growth potential of the CCL-64 cell line by the proliferation on plastic substrate. 24 Hours after exposure of the suspension, sham treated cells had a 98% viability and were in the beginning of their exponential growth phase, whereas treated cells (high concentration, direct cytotoxicity 47%) showed a 78% viability followed by a lagged growth curve (Fig. 4a).

single cell suspension in gelatine (b)

Treatment of a PAT-2 or Gural single cell suspension in gelatine showed no significant increase in non-viable cells, even after exposing the cells to three sessions of 4000 shock waves within 48 hours. Also the clonogenic potential in soft agar was not affected.

pellet on the bottom of the test tube (c)

The pellet was immobilized in order to prevent distortion and subsequent partial resuspension in the covering solution. Therefore, the pellet was kept in place by a 15% gelatine 'plug'. Exposure of 40.10^6 cells as a cell pellet, lying directly on the bottom of the test tube, resulted in a dose dependent reduction of fraction of viable cells. In contrast to the suspension this effect was enhanced by decreasing the number of cells (10.10^6) in the pellet and thus decreasing the volume of the pellet ("thick" vs. "thin" pellet). In this pellet model also a difference in sensitivity for different cell types was seen (Fig. 2).

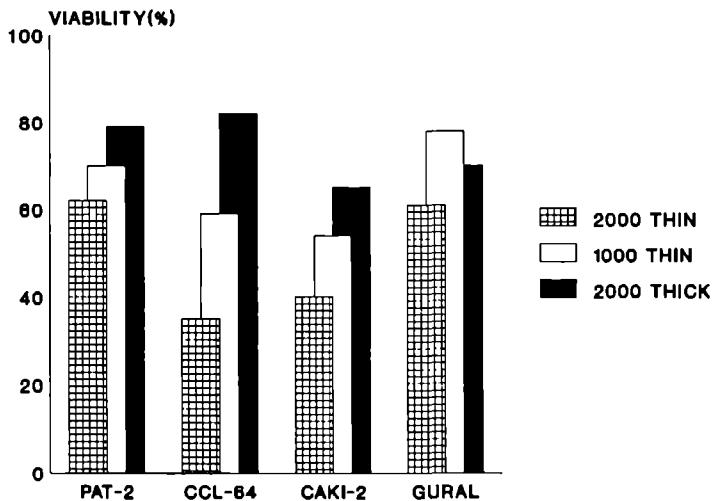**Fig. 2.**
Viability, according to the trypan blue dye exclusion test, after exposure to 1000 or 2000 HESW of cell pellets (sample (c)) of different thickness. (thin: 10.10^6 cells; thick 40.10^6 cells).
Treatment of CCL-64 in a thin cell pellet (10.10^6cells) showed similar results as in a suspension but after a prolonged lag phase the cells had an unaffected exponential growth (Fig. 4b).

Exposure of PAT-2 cells in a pellet fixed by a 15% gelatine plug showed an impaired clonogenicity in soft agar. Concerning the Gural cells, the growth potential was affected when cells were exposed as a thin pellet (Table 1). This result was less evident in a thick pellet. Similar observations were obtained with the Caki-2 cell line.

Comparing the effects of 2000 shock waves on the single cell suspension (sample (*a*)) and pellet (sample(*c*)) we observed a differential sensitivity of the four cell lines. Gural cells were less sensitive to exposure in a cell pellet than a suspension, while the CCL-64 fibroblasts were more sensitive to exposure in a pellet (Fig. 3).
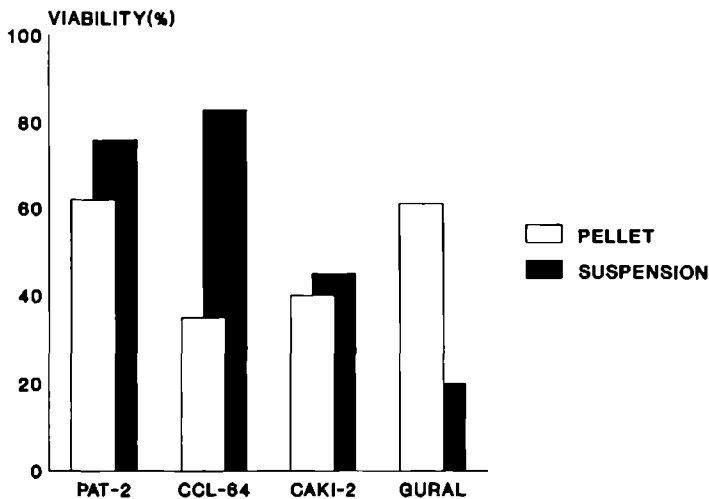
Fig. 3.
Viability, according to the trypan blue dye exclusion test, after exposure to 2000 HESW of a single cell suspension (sample (*a*), 5.10^6 cells/ml), or a cell pellet (sample (*c*), 10.10^6 cells).

pellet surrounded by gelatine ("sandwich pellet") (d)

When the pellet was placed on a bottom of 15% gelatine medium and a gelatine plug was placed on the pellet ("sandwich pellet") no direct cytotoxicity or antiproliferative effects were detected in the four cell lines used.

35

Fig.4a

Fig.4b

Fig. 4a and b.
Proliferative capacity (number of viable cells) on plastic substrate of CCL-64 fibroblasts at different hours after exposure to 2000 HESW as a single cell suspension (sample (*a*) **(Fig. 4a)** or a cell pellet (sample (*c*) **(Fig. 4b)**.
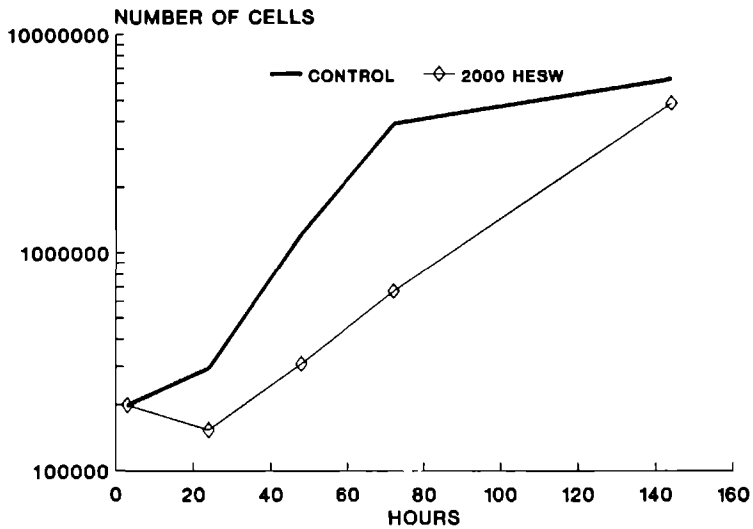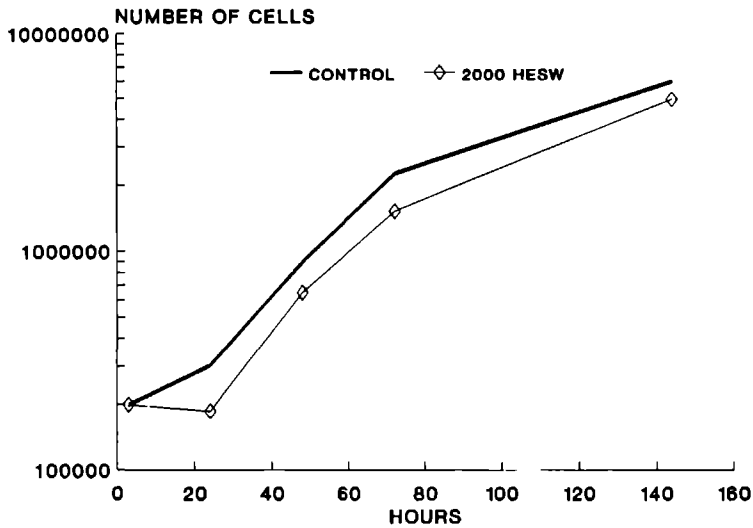
36

DISCUSSION

The effects of HESW on (tumor-) cells has been point of interest in the last years. Cytotoxic and antiproliferative effects on tumor cells are described in vitro. Recently, it was suggested that these results can be attributed to secondary effects and are influenced by experimental factors (Bräuner 1989, Brümmer 1989, Laudone 1989, Miller 1987). Therefore, we exposed several (tumor) cell lines to electromagnetically generated shock waves under different experimental conditions, and evaluated several critical physical and biological aspects. In brief, cells were treated as cell suspension or as cell pellets in polyethylene tubes.

For the cell suspensions it appeared that the fraction of non viable cells was more pronounced by applying more HESW or increasing the number of cells in the test tube (Fig. 1). Concerning this last phenomenon, the cell concentration dependent decrease in viability may indicate that cell damage can be attributed to secondary shock wave effects (jet streams, shearing forces, collisions). With regard to the pressure measurements performed, the marked pressure drop in the lateral plane can be responsible for acceleration forces in that direction and might contribute in these effects. The cell concentration dependent increase in direct cytotoxicity seems in contradiction with an earlier report (van Dongen 1989), where cell kill appeared to be independent of cell density i.e. using concentrations of $1-4.10^6$ cells/ml, the amount of non viable cells after treatment remained approximately equal. In our studies, higher cell concentrations were more effectively treatable by HESW. Unlike in the earlier report, the range in which we tested varied tenfold. This might explain the discrepancy. Also unlike this report, we found no change in viability or clonogenic potential, as a percentage of the control, by decreasing the temperature (22 instead of 37° C) during shock wave exposure of PAT-2 prostatic carcinoma cells as a single cell suspension. The differences in experimental set-up and the temperature range tested, might explain this discrepancy.

By immobilizing PAT-2 or Gural cells in suspensions by means of gelatine, no change in viability or clonogenic potential was detected, even after 3 sessions of 4000 HESW in 48 hours. It seems that this cannot be explained by the minor decrease in P_{max} or P_{neg} due to the gelatine used. In contrast, in the gelatine medium, cavitations were macroscopically observed to a far lesser extent as compared to medium containing no gelatine. It is known that mechanisms involving cavitation-related effects depend on the characteristic of the pulse rather than the

overall averaged intensity, and on the physico-elastic properties of the medium. Indeed, the key characterization of in vitro experiments is the determination of wether, or not, cavitations occur (Miller 1987). Thus the absence of decrease in viability or clonogenic potential might be explained by a decrease in cavitations.

In the pellet model also a dose related direct cytotoxicity was evident (Fig. 3). This is of great interest since, assuming that under this condition acceleration forces and collisions are avoided, shock waves can have a direct impact on immobilized cells. In contrast with the cell suspension model, this direct cytotoxicity was enhanced by reducing the number of cells in the pellet.

What makes the immobilized cells in the pellet susceptible to shock waves? A difference (albeit slight) in acoustic impedance between the test tube wall and the pellet covered by gelatine 15% medium, and the existence of cavitation like phenomena within the pellet might explain this susceptibility. The observation that exposing a smaller pellet resulted in a greater decrease in viability is in agreement with this hypothesis, and suggests shock wave induced effects nearby the wall of the tube. This is upheld by the fact that viability was not affected when the cells were exposed in a pellet surrounded by gelatine ("sandwich pellet"). Thus, immobilized cells are affected by HESW when exposed in a pellet on the bottom of the test tube and not when surrounded by gelatine. The pellet system, where fixed cells are subject to these phenomena (acoustic impedance and cavitation), might resemble the in vivo situation and could serve as a more reliable model for studying in vitro effects of HESW.

In conclusion, both a single cell suspension and a cell pellet exposed to HESW result in a dose-response decrease in viability. These effects are influenced by several critical physical and biological factors and depend mainly on the way how cells are exposed to the shock waves. Our results indicate that immobilized cells can be affected by HESW when acoustic impedance and cavitation effects can be exerted. Overall, cell lines have a differential sensitivity for HESW. Also an individual cell line shows a model dependent susceptibility towards the shock waves. The in vitro studies of shock wave induced bio-effects, their interpretations and considerations in possible ways of action are therefore restricted to the particular experimental model used. In addition they are of limited relevance for implications of the use of HESW in vivo. However, in vitro model systems with differential sensitivities for HESW can be used to study shock wave induced bio-effects on a (tumor) cellular level.

Further investigations are required but need a careful interpretation.

ACKNOWLEDGEMENTS

REFERENCES

Berens M.E., Welander C.E., Griffin A.S., McCullough D.L. Effect of acoustic shock waves on clonogenic growth and drug sensitivity of human tumor cells in vitro. J. Urol., 142, 1090, 1989.

Bräuner T., Brümmer F., Hülser D.F. Histopathology of shock wave treated tumor cell suspensions and multicell tumor spheroids. Ultrasound Med. Biol., 15, 451, 1989.

Brümmer F., Brenner J., Bräuner T., Hülser D. F. Effects of shock waves on suspended and immobilized L1210 cells. Ultrasound Med. Biol., 15, 229, 1989.

Coleman A.J., Saunders J.E., Crum L.A., Dyson M. Acoustic cavitation generated by an extracorporal shockwave lithotriptor. Ultrasound Med. Biol., 13, 69, 1987.

Coleman A.J., Saunders J.E. A survey of the acoustic output of commercial extracorporal shock wave lithotriptors. Ultrasound Med. Biol., 15, 213, 1989.

Crum L.A., Fowlkes J.B. Acoustic cavitation generated by microsecond pulses of ultrasound. Nature, 319: 52, 1986.

Hamburger A.W., Salmon S.E. Primary bioassay of human tumor stem cells. Science, 197, 461, 1977.

Herman C.J., Pelgrim O.E., Kirkels W.J., Verheyen R., Debruyne F.M.J., Kenemans P., Vooys G.P. In-use evaluation of the Omnicon automate tumor colony counter. Cytometry, 3, 439, 1983.

Laudone V.P., Morgan T.R., Huryk R.F., Heston W.D.W., Fair W.R. Cytotoxicity of high energy shock waves: methodologic considerations. J. Urol., 141, 965, 1989.

Miller D.L. A review of the ultrasonic bio-effects of microsonation, gas-body activation, and related cavitation-like phenomena. Ultrasound Med. Biol., 13, 443, 1987.

Morgan T.R., Laudone V.P., Heston W.D.W., Zeitz L., Fair W.R. Free radical production by high energy shock waves - comparison with ionizing irradiation. J. Urol., 139, 18, 1988.

Oosterhof G.O.N., Smits G.A.H.J., de Ruyter J.E., Schalken J.A., Debruyne F.M.J. Effects of high energy shock waves combined with biological response modifiers or adriamycin on a human kidney cancer xenograft. Urol. Res., 18, 419, 1990.

Oosterhof G.O.N., Smits G.A.H.J., de Ruyter J.E., van Moorselaar R.J.A., Schalken J.A., Debruyne F.M.J. The in vitro effect of electromagnetically generated shock waves (Lithostar) on the Dunning R3327 PAT-2 rat prostatic cancer cell-line. Urol. Res., 17, 13, 1989.

Oosterhof G.O.N., Smits G.A.H.J., de Ruyter J.E., Schalken J.A., Debruyne F.M.J. In vivo effects of high energy shock waves on urological tumors, an evaluation of treatment modalities. J. Urol., 145, 171, 1991.

Randazzo R.F., Chaussy C.G., Fuchs G.J., Bhuta S.M., Lovrekovich H., de Kernion, J.B. The in vitro and in vivo effects of extracorporal shock waves on malignant cells. Urol. Res., 16, 419, 1988.

Russo P., Heston W.D.W., Fair, W.R. Suppression of in vitro and in vivo tumor growth by high energy shock waves. Surg. Forum, 36, 645, 1985.

Russo P., Stephenson R.A., Mies C., Huryk R., Heston W.D.W., Melamed M.R., Fair W.R. High energy shock waves suppress tumor growth in vitro and in vivo. J. Urol., 135, 626, 1986.

van Dongen J.W., van Steenbrugge G.J., Romijn J.C., Schröder, F.H. The cytocidal effect of high energy shock waves on human prostatic tumour cell lines. Eur. J. Clin. Oncol., 25, 1173, 1989.

EFFECTS OF HIGH ENERGY SHOCK WAVES
COMBINED WITH BIOLOGICAL RESPONSE MODIFIERS
IN DIFFERENT HUMAN KIDNEY CANCER XENOGRAFTS

Gosse O.N. Oosterhof, Geert A.H.J Smits, Anja E. de Ruyter,
Jack A. Schalken, Frans M.J. Debruyne

Department of Urology, University Hospital Nijmegen, The Netherlands

ABSTRACT

We have studied the effects of high energy shock waves (HESW) alone or in combination with Biological Response Modifiers (BRM's) on the growth of five human kidney cancer xenografts in mice. Exposure of the tumors to 3 sessions of 800 shock waves every 48 hours (P_{max} 37,5 MPa) on the commercially available Lithostar resulted in a temporary growth delay. The sensitivity for HESW is related to the doubling time of the tumor. Several days after stopping the HESW administration, the tumors regained their original growth potential with the same doubling time.

The systemic application of Tumor Necrosis Factor-alpha (TNF-α, 500 ng/g body weight, 5 times/week) and/or Interferon-alpha (IFN-α, 5.0 ng/g body weight, 3 times a week) subcutaneously around the tumor also had a limited effect on the growth of these established tumors (60-80 mm^3).

The combination of HESW with TNF-α and IFN-α resulted in an almost complete cessation of tumor growth in the NU-1 human kidney xenograft and had an additive antitumor effect in the NU-3. Synergism was also seen in the NU-1 and NU-3 with the combination of HESW and TNF-α, while the combination with IFN-α had only a limited effect on tumor growth. So TNF-α was the active agent that enhanced the anti-proliferative effects of shock waves.

The NC-65 tumor has the same doubling time as the NU-1 and NU-3, but the vascularization is less well developed. The anti-proliferative effect of HESW was not potentiated by TNF-α. In the more slowly growing NU-10 and NU-12, the combined treatment was synergistic in the well vascularized NU-10, but had no potentiating antitumor effect in the poorly vascularized NU-12.

We conclude that TNF is able to potentiate the anti-proliferative effect of shock waves. The differential sensitivity of the tumors for the combined treatment is likely to be related to the vascularization and doubling time of the tumor.

INTRODUCTION

Electromagnetically generated High Energy Shock Waves (HESW) can alter growth characteristics of tumor cells in vitro, depending on the experimental set-up (Oosterhof 1989, Smits 1991). Furthermore, HESW can provoke a temporary suppression of tumor growth in vivo (Oosterhof 1990a, 1990b, Randazzo 1988, Russo 1986, 1987). After some days the tumor starts growing again with the same doubling time. The shock waves result thus in an elongated lag-phase and do not have a permanent suppressive effect on tumor growth.

From earlier studies we know that the in vivo antitumor effect of HESW depends not only on the number of shock waves, but also on the number of shock wave sessions, the initial tumor burden and the tumor model used (Oosterhof 1990b). We have now studied different human kidney xenografts under standard experimental conditions (3 sessions of 800 shock waves with 18.4 kV; tumor volume at start of treatment of 60-80 mm^3).

The treatment of metastatic renal cell carcinoma in man with Biological Response Modifiers (BRM's) has gained more interest in the past years. Response rates of 25% are described and are probably due to a direct cytotoxic effect and an augmented host immune response. Results of treatment are, however, difficult to predict since there is no good correlation between the in vivo and in vitro sensitivity of the tumor(cells) for BRM's. The administration of BRM's in human kidney xenografts in mice may lead to a complete inhibition of the tumor, only if it is smaller than 5 mm^3. Established tumors are partially or completely insensitive for therapy (Beniers 1991). The antitumor effect of TNF is dose dependent, while the effect of IFN has an optimum dose, depending on the tumor tested. Treatment with BRM's alone should thus be considered as suboptimal.

To obtain a prolonged suppression of tumor growth, HESW should be combined with another treatment. The additive antitumor effect of the combination of HESW and chemotherapeutic drugs was described earlier (Oosterhof 1990a, Randazzo 1988). In another study we found a synergistic anti-proliferative effect of the combination of HESW and BRM's in the nude mouse xenograft system, and even tumor regression (Oosterhof 1990a). We therefore studied now the effects of BRM's (IFN-α, TNF-α, or both) on five different human kidney cancer xenografts.

MATERIALS AND METHODS

Animals

Xenografts were transplanted in six week old male Balb C nu/nu mice (Bornholt Gårt, Rye, Denmark). The mice were kept in groups of five in PAG type 2 cages (IFFA Credo) covered with an iso cap for sterile conditions. The mice were fed ad libitum with irradiated SRM food (Hope Farms, Woerden, The Netherlands) and drinking water was acidified with 0.7 ml concentrated HCl/ml.

Tumors

Five renal cell carcinoma xenografts were used. The NC-65 tumor, originally described by Hoëhn and Schröder (1978), was kindly provided by Dr. Romijn (Dept. of Urology, Erasmus University, Rotterdam, The Netherlands). The NU-1, NU-3, NU-10 and NU-12 tumors were established in our laboratory by serial subcutaneous transplantation of tumor pieces after original subcutaneous transplantation of small primary tumor pieces directly after nephrectomy. The tumors were transplanted subcutaneously as trocar pieces in the hind limb of the animals, under ether anesthesia. The histological features of the kidney cancer xenografts (NC-65, NU-1, NU-3, NU-10, NU-12) are summarized in table 1 (type of tumor cells, cell arrangement, nucleus, number of mitosis per high power field, vascularization, doubling time and the spontaneous development of the tumor when it reaches a volume of more than 200 mm^3).

HESW treatment

The shock waves were generated electromagnetically by the commercially available Lithostar (Siemens). The experimental set-up and way of administration of the shock waves were described earlier (Oosterhof 1989, 1990b). For HESW exposure the animals were placed in a water filled container (37^{0}C) and immobilized and fixed in a narrow plastic cylinder. At the site of the limb of the animal a 1.5 x 1.5 cm hole in the tube allows the shock waves to reach the tumor while the animal is protected by the tube against shock wave exposure at other sites.

Table 1. Histological characteristics of the five tumors.

histological features	NU-1	NU-3	NC-65	NU-10	NU-12
type of tumor cells	spindle cells of different size	eosinophilic	eosinophilic and granular type	large clear cells	clear cell
cell arrangement	sarcomatous	trabecular and anarchistic	compact pattern acinar	trabecular and of acini	trabecular acinar
nucleus	pleomorphic	moderate pleo- (G3)	polymorphic (G3) morphic (G2)	Grade 1	small nuclei (G2)
mitosis/10 hpf	25-30	25	1	1	<1
vascularization in the stroma	many small dis-	pronounced persed capilla- ries, collapsed	small collapsed capillaries in the stroma	well developed capillaries in the stroma	dilated capillaries in the capsule, few capillaries in the stroma
tumor doubling time (days)	3-4	3-4	3-4	7	7
spontaneous development when > 200 mm^3	haemorrhagic necrotic	ischemic + haemorrhagic necrosis	ischemic necrosis	haemorrhagic necrosis	cystic growth

With in vitro pressure measurements, using a piezoelectric film (Imotec) connected to an oscilloscope (Gould, DSO, 4072), determined the focal area (area limited by pressures which are half of the maximum pressure ($P_{max}50$)). It appeared that there is a pronounced pressure fall in the lateral plane, indicating the importance of immobilizing the animal and positioning the tumor precisely (Oosterhof 1989). The polyvinylidene difluoride (PVDF) needle hydrophone (Imotec) has abroad spectrum and an effective area of 0.5 mm^2 with a constant sensitivity of up to 5 MHz. Measurements are possible up to the focal point with a measuring range from 0 to 200 MPa.

When the tumor had reached the desired volume of 60-80 mm^3, the tumor bearing animals were randomly divided in a sham treated control group, a group receiving shock waves (three sessions of 800 shock waves (18.4 kV, 80 pulses/minute) on day 0, 2 and 4), a group receiving BRM's and a group receiving both treatment modalities. Each group consisted of 5 or 6 animals. The sham treated control animals were handled, anesthetized and RPMI medium, the dissolvent of the BRM's, was injected around the tumor identically with their treated counterparts for each session. At 18.4 kV the maximum pressure is 37.5 MPa. Its focal area ($P_{max}50$) with pressures above 18.7 MPa appeared to be about 90 mm long in the axial plane and 6 mm in the lateral plane. If correctly focussed the whole tumor of 60-80 mm^3 is thus effectively exposed to the pressures in the focal area. From earlier studies we know that tumor volume may influence the outcome of shock wave therapy: the smaller the tumor the more antitumor effect. On the other hand, the tumor should be big enough that spontaneous regtression is excluded and to allow accurate focus-sing. We therefore used tumors of the same size (60-80 mm^3). In order to be able to establish a additional or synergistic antitumor effect of a combined treatment, the effect of each treatment should be reproducible, clearly measurable and, finally, it should not lead to a complete or almost complete cessation of tumor growth. It resulted from our studies that three sessions of 800 shock waves, administered every 48 hours could lead to this suboptimal decrease in tumor growth (Oosterhof 1990a). Since the lithoptriptor we used is generating relatively low maximum and negative pressures, we used the maximum voltage setting (18.4 kV).

Human IFN-α and TNF-α, kindly supplied by Boehringer Ingelheim, Alkmaar, The Netherlands, were produced in Escherichia coli by recombinant DNA technology. The specific activity of IFN-α was 3.2 x 10^8 units/mg protein. It was measured by inhibition of encephalomyocarditis (EMC) virus replication in A549 cells with reference to the National Institute of Health (NIH) leucocyte IFN-α standard Go 23-901-527. The purity of IFN was > 98% as determined by SDS polyacrylamide gel electrophoresis, and the amount of endotoxin was less than 1.0 ng/mg. as based on the limulus amoebocyte lysate assay. The specific activity of TNF-α determined in the presence of actinomycin-D was 6x10^7 units/mg protein (the L-929 cytotoxicity assay). The purity was > 99% as determined by SDS polyacrylamide gel electrophoresis, and it contained 1.0 ng or less endotoxin/mg protein based on the limulus amebocyte lysate assay. The drugs were dissolved in the accessory dissolvent and diluted with unsupplemented RPMI medium (Gibco, Paisley, UK). After dilution, the drugs were stored in small aliquots at -80°C until use.

As BRM we used IFN-α (5.0 ng/g body weight, 3 times/week), TNF-α (500 ng/g body weight, 5 times/week) or the combination TNF-α (500 ng/g body weight, 5x/week) and IFN-α (5.0 ng/g body weight, 3 times/week).

Evaluation of tumor growth

The tumor volume was determined every other day by measuring with a precision sliding caliper the three dimensions, i.e. the maximum diameter (L) and the perpendicular diameters (W, H) and expressed as the tumor size index (TSI) calculated by the equation L x W x H x π/6. In this way tumor growth patterns were evaluated by calculating the mean tumor volume of the tumors in each group.

Statistical analysis

Per animal, loglinear regression over the first two weeks was used to estimate the growth rate (α), i.e. the number of times the tumor volume doubles per day (The doubling time equals 1/α). Treatment versus control differences in growth rate were then analyzed by two sided t-tests.

For combined treatments, two treatments were considered partly additive if the

decrease in growth rate, resulting from the combined treatment, was larger than the decreases resulting from each of the single treatments. They were considered synergistic if the decrease by the combined treatment was larger than the sum of the decreases by the single treatments (One sided t-tests, each $p < 0.05$). Two treatments were considered not significant if the decrease in growth rate by the combined treatment was not larger than the decreases resulting from each of the single treatments (Table 2).

RESULTS

Effect of HESW alone

Earlier studies revealed a significant differential sensitivity of tumors towards shock waves. Doubling time of the tumor and vascularization seemed to be of importance (Oosterhof 1990b). In the 5 tumors, that we exposed to 3 sessions of 800 shock waves, a temporary delay in growth was seen (Table 2). The tumors regained their original growth potential 5-10 days after stopping the HESW exposure. The slowly growing tumors (NU-10 and NU-12) were less susceptible to the shock wave administration (growth rate $(=\alpha)$ decreased from 0.13 to 0.11; Table 2) than the more rapidly growing NU-1, NU-3 and NC-65 (α decreased from 0.26 to 0.18; Table 2).
The duration of growth suppression was 5 days in all the tumors, except the NU-1 where it was 10 days, and was thus not related to the doubling time of the tumor.
In these experiments there was no animal mortality, neither from the HESW treatment alone nor from the combined treatments.

Effect of BRM's alone

The subcutaneous injection of BRM's around an established human kidney tumor results in a partial antitumor effect, depending on the tumor volume and the dose of TNF-α used (Beniers 1991). In the five tumors the same dosage of TNF-α (500 ng/g body weight 5x/week) was given and the initial tumor volume was identical. A differential sensitivity towards the different tumors was confirmed (Beniers 1991). The NU-10 tumor was most sensitive to TNF-α treatment (α decreased from 0.13 to 0.07), followed by the NU-1, while the NU-12 was almost insensitive (Table 2).

In earlier in vitro and in vivo studies an additional cytotoxic effect was observed when HESW was combined with chemotherapeutic drugs (Oosterhof 1989, Randazzo 1988). We could find a synergistic antitumor effect of the combination of 4 times 800 shock waves with BRM's in the NU-1 human kidney cancer xenograft, even resulting in a tumor regression (Oosterhof 1990a). To get more insight in this phenomenon we now studied the combination of a fixed number of shock waves (3 sessions of 800 shock waves every 48 hours with 18.4 kV, i.e 37 MPa) and different BRM's or combinations of BRM's in five human kidney cancer xenografts.

1. NU-1 human kidney tumor
Three sessions of 800 HESW on the human kidney tumor NU-1, implanted in the nude mouse caused a significant decrease in tumor growth rate (α decreased from 0.28 to 0.17; Table 2), but the tumor regained its original doubling time 10 days after stopping the HESW treatment. A temporary anti-proliferative effect could also be obtained by the administration of TNF-α plus IFN-α (growth rate decreased from 0.29 to 0.20; Table 2). The combination of three shock wave sessions and TNF-α plus IFN-alpha, however, had a synergistic antitumor effect (α = 0.04). Tumor growth was suppressed during 15 days and the tumor did not regain its original doubling time (Fig. 1a). The same results could be obtained by exposing the tumor to the combination of 3 sessions of HESW and TNF-α, suggesting that TNF-α is the active agent responsible for the synergism (Fig. 1b). This was confirmed by the fact that IFN-α had no potentiating antitumor effect when it was combined with HESW, although IFN-α alone had a clear effect on tumor growth (Table 2).

2. NU-3 human kidney tumor
The NU-3 human kidney cancer has almost the same doubling time (3-4 days; α = 0.26) and vascularization as the NU-1 tumor (Table 1). A synergistic antitumor effect could be obtained with the combination of HESW and TNF-α (Fig. 2b). IFN-α alone had no effect on tumor growth, and the anti-proliferative effect of HESW alone was even slightly suppressed when it was combined with IFN-alpha. Also the combination of shock waves with TNF-α plus IFN-α was less effective than the combination of shock waves and TNF-α: while the first was synergistic, the latter only had an additive antitumor effect (Fig. 2a and 2b; Table 2).

tumor model	treatment	first 10 days after treatment			Fig. in text and result
		α	s.e.m.	p	
NU-1	control	0.29	0.01	-	Fig. 1a
	TNF/IFN	0.20	0.03	0.01	
	3 x 800	0.17	0.01	0.01	
	combined	0.04	0.03	0.01	synergistic
NU-1	control	0.28	0.01	-	Fig. 1b
	TNF	0.23	0.02	0.0001	
	3 x 800	0.17	0.01	0.0001	
	combined	0.023	0.02	0.01	synergistic
NU-1	control	0.22	0.02	-	
	IFN	0.18	0.03	0.30	
	3 x 800	0.17	0.01	0.14	
	combined	0.17	0.01	0.27	not significant
NU-3	control	0.29	0.02	-	Fig. 2a
	TNF/IFN	0.23	0.01	0.002	
	3 x 800	0.18	0.01	0.0001	
	combined	0.09	0.03	0.58	additive
NU-3	control	0.23	0.01	-	Fig. 2b
	TNF	0.19	0.01	0.0001	
	3 x 800	0.19	0.02	0.0001	
	combined	0.04	0.03	0.005	synergistic
NU-3	control	0.26	0.01	-	
	IFN	0.25	0.02	0.34	
	3 x 800	0.18	0.01	0.0002	
	combined	0.21	0.01	0.12	not significant

Table 2.
Estimated growth rates (α), standard error of the mean (s.e.m.) and p-value. Loglinear regression calculation after treatment of different animal models with shock waves, BRM's or combination of these. Results of combined treatment were synergistic, additive or not significant.

tumor model	treatment	first 10 days after treatment			Fig. in text and result
		α	s.e.m.	p	
NC-65	control	0.30	0.01	-	Fig. 3a
	TNF/IFN	0.28	0.01	0.02	
	3 x 800	0.23	0.01	0.0002	
	combined	0.18	0.03	0.003	not significant
NC-65	control	0.29	0.01	-	Fig. 3b
	TNF	0.21	0.02	0.2	
	3 x 800	0.20	0.01	0.01	
	combined	0.22	0.02	0.03	not significant
NC-65	control	0.29	0.01	-	
	IFN	0.23	0.01	0.08	
	3 x 800	0.20	0.01	0.01	
	combined	0.21	0.01	0.03	not significant
NU-10	control	0.13	0.01	-	Fig. 4
	TNF	0.07	0.01	0.0001	
	3 x 800	0.11	0.01	0.0001	
	combined	0.03	0.01	0.03	synergistic
NU-12	control	0.14	0.01	-	Fig. 5
	TNF	0.13	0.02	0.50	
	3 x 800	0.11	0.03	0.37	
	combined	0.13	0.02	0.16	not significant

Table 2.
Estimated growth rates (α), standard error of the mean (s.e.m.) and p-value. Loglinear regression calculation after treatment of different animal models with shock waves, BRM's or combination of these. Results of combined treatment were synergistic, additive or not significant.
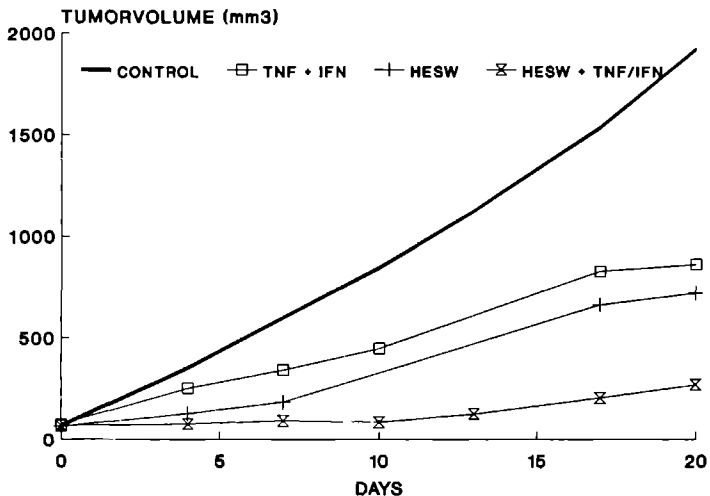
Fig. 1a.
Tumor volume after 3 exposures (every 48 hours) of 800 HESW (18.4 kV, 37.5 MPa) combined with TNF-α and IFN-α. NU-1 human kidney tumor in the nude mouse xenograft system.
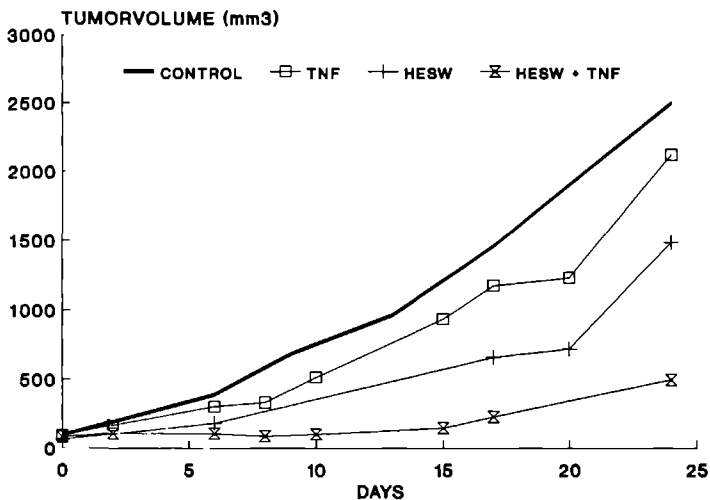

Fig. 1b.
Tumor volume after 3 exposures (every 48 hours) of 800 HESW (18.4 kV, 37.5 MPa) combined with TNF-α. NU-1 human kidney tumor in the nude mouse xenograft system.
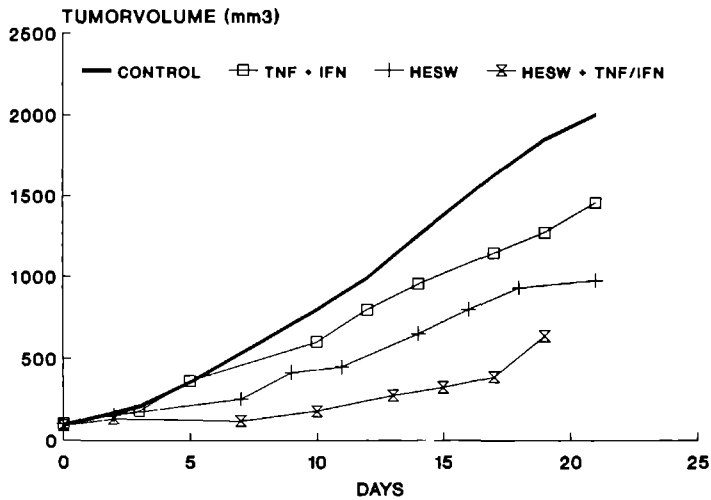
52

Fig. 2a.
Tumor volume after 3 exposures (every 48 hours) of 800 HESW (18.4 kV, 37.5 MPa) combined with TNF-α and IFN-α. NU-3 human kidney tumor in the nude mouse xenograft system.
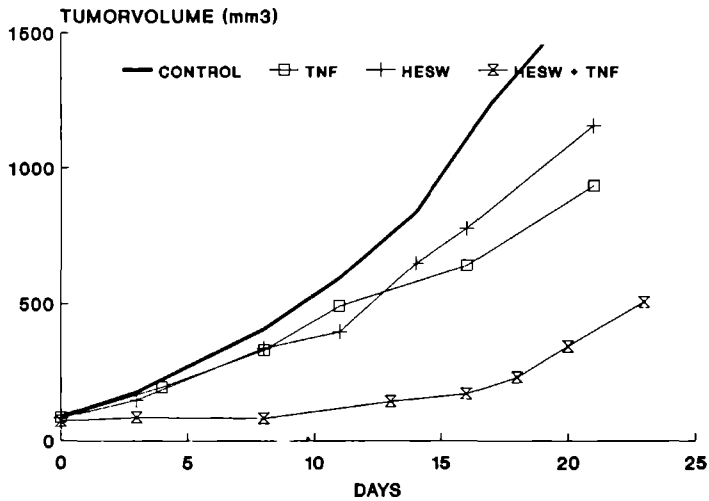

Fig. 2b.
Tumor volume after 3 exposures (every 48 hours) of 800 HESW (18.4 kV, 37.5 MPa) combined with TNF-α. NU-3 human kidney tumor in the nude mouse xenograft system.

53

3. NC-65 human kidney tumor

The NC-65 tumor has a doubling time of 3-4 days (α=0.29) and is thus comparable with the NU-1 and NU-3 tumor. Vascularization is, however, less well developed (Table 1). Treatment with shock waves alone or BRM's alone (TNF-α, IFN-α or both) had some anti-proliferative effect on tumor growth, but the combined treatment was not significantly more effective than each of the single treatments (Fig. 3a and 3b; Table 2).

From these results in the NU-1, NU-3 and NC-65 tumors, we concluded that TNF-α was the active potentiating agent when used in combination with shock waves. We therefore used only TNF-α in the other experiments.

Fig. 3a.
Tumor volume after 3 exposures (every 48 hours) of 800 HESW (18.4 kV, 37.5 MPa) combined with TNF-α and IFN-α. NC-65 human kidney tumor in the nude mouse xenograft system.

4. NU-10 human kidney tumor

The NU-10 human kidney tumor has a doubling time of 7.7 days (α = 0.13) and is thus not comparable with the NU-1, NU-3 and NC-65 tumor (Table 2). Vascularization is, however, well developed in the capsule of the tumor, while the capillaries in the stroma are inconspicuous (Table 1). Three sessions of 800 shock waves could add few to the anti-proliferative effect of TNF-α (Fig. 4). The original growth rate of 0.13 decreased to 0.11 by HESW alone and to 0.07 by TNF-α alone. The combination had a synergistic anti-proliferative effect on tumor growth (α = 0.03)
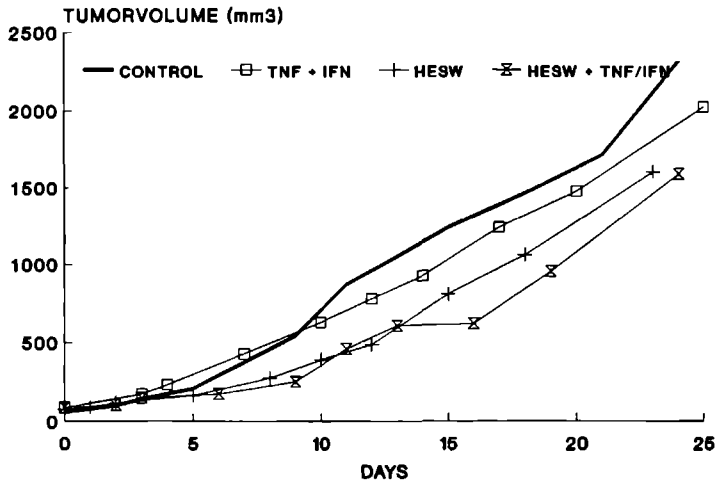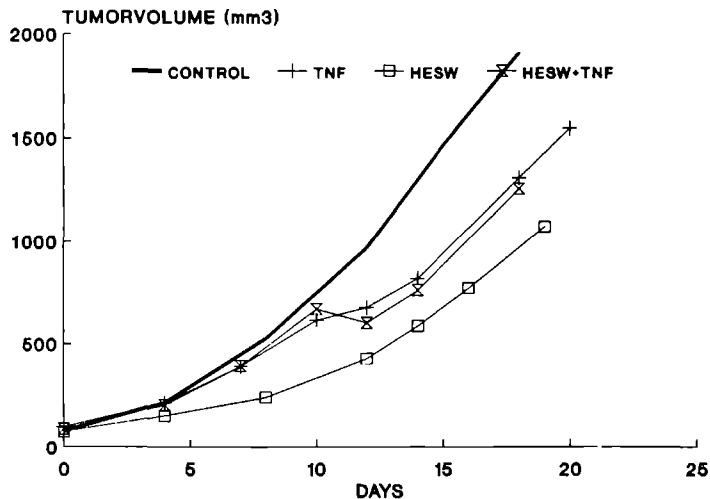
Fig. 3b.
Tumor volume after 3 exposures (every 48 hours) of 800 HESW (18.4 kV, 37.5 MPa) combined with TNF-α. NC-65 human kidney tumor in the nude mouse xenograft system.
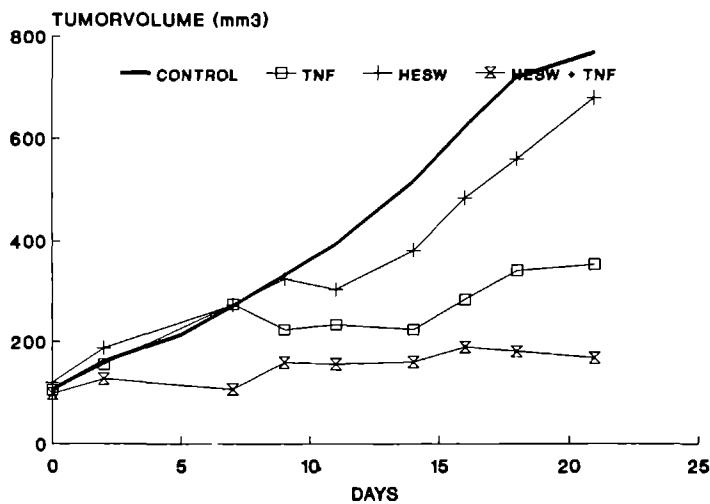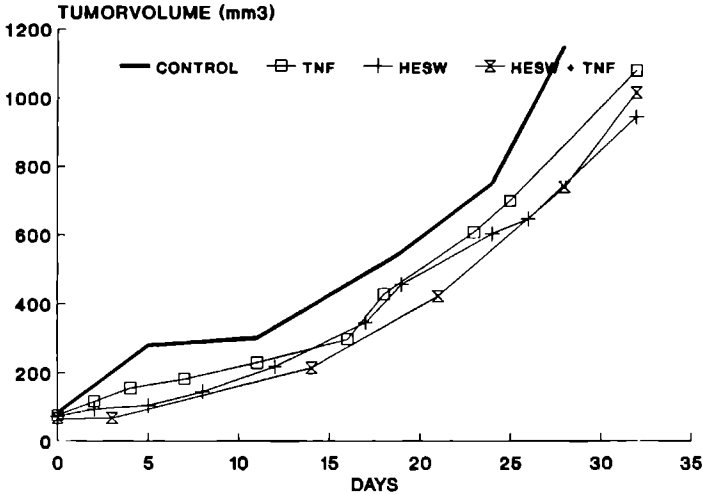

Fig. 4.
Tumor volume after 3 exposures (every 48 hours) of 800 HESW (18.4 kV, 37.5 MPa) combined with TNF-α. NU-10 human kidney tumor in the nude mouse xenograft system.

5. NU-12 human kidney tumor

The NU-12 tumor is not only poorly vascularized, with dilated capillaries in the stroma (Table 1) but has also a long doubling time ($\alpha = 0.13$; Table 2). Shock waves alone or TNF-α alone had almost no effect on tumor growth, nor had the combination (Fig. 5).

Fig. 5.
Tumor volume after 3 exposures (every 48 hours) of 800 HESW (18.4 kV, 37.5 MPa) combined with TNF-α. NU-12 human kidney tumor in the nude mouse xenograft system.

DISCUSSION

Temporal growth delay can be obtained by shock waves alone, depending on the doubling time and the initial size of the tumor. In the rapidly growing PAT-2 Dunning tumor (doubling time 1.2 - 1.6 days) no in vivo measurable effect on tumor growth could be obtained by shock waves alone (Oosterhof 1990b). Also, a tumor that is larger than the focal area of the lithotriptor will only be partially affected by the shock waves. This is of particular interest in the Lithostar with its small focal area in the lateral plane (P_{max} 50 is 6 mm large) (Oosterhof 1989). The pressure exerted in the center of the focal area is 37.5 MPa, at the edge 20 MPa and 2 mm outside the focal area 7.5 MPa (18.4 kV). For this reason we used tumors of the same size (60-80 mm^3) that were small enough to be exposed in toto to the

pressure of the focal area.

In the five human kidney cancers we treated with three sessions of 800 shock waves, a temporary growth delay could be found, related to the doubling time. The tumors regained their original doubling time 5-10 days after stopping the shock wave exposure. Slowly growing tumors (i.e. NU-10 and NU-12) are less susceptible to shock wave exposure alone (α decreased from 0.13 to 0.11 i.e. 15%) than the more rapidly growing tumors NU-1, NU-3 and NC-65 (α decreased from 0.26 to 0.18 i.e. 30%). The sensitivity of the tumors for shock waves is thus related to the doubling time.

The effects of the administration of BRM's to human kidney xenografts depend on the initial tumor volume. Established tumors are insensitive or partially sensitive for therapy (Beniers 1991). The anti-tumor effect of TNF is dose dependent, while the effect of IFN has an optimum dose, depending on the tumor tested.

Since we could not obtain a complete destruction of even a small tumor with the serial exposure of shock waves every 48 hours, we studied the combination of two treatment modalities that might have a potentiating antitumor effect. In the NU-1 tumor we could provoke a complete regression of small tumors with the combination of four shock wave sessions and TNF-α plus IFN-alpha, whereas each treatment alone only had a limited and temporary effect on tumor growth (Oosterhof 1990a). Thus, the combination of these two suboptimal treatments was synergistic. Is this effect reproducible in any kidney cancer xenograft or is it dependent on certain factors related to the tumor or to the BRM's ?

In order to get more insight in the effects of IFN-α, TNF-α or combination of these, we first exposed the NU-1, NU-3 and NC-65 kidney tumor to 3 sessions of 800 shock waves combined with these different BRM treatments. When BRM's are used in the athymic nude mice, only the non-T-cell mediated effects can be studied. IFN-α alone had some effect on the growth rate of the NU-1 tumor, but combination with HESW had no additive anti-proliferative effect (Table 2). In the NU-3 tumor this combination was even less effective than the administration of shock waves alone (Table 2). When the shock waves were combined with TNF-α in the NU-1 and NU-3 tumor, a synergistic anti-proliferative effect was observed. These findings suggested that TNF-α was the agent responsible for potentiating the antitumor effect of shock waves. This was confirmed by the fact that, when the NU-1 tumor was exposed to shock waves and TNF-α plus IFN-α, the anti-proliferative effects were similar to those obtained by the combination of shock waves and TNF-alpha.

We thus concluded that TNF-α is responsible for potentiating the anti-proliferative effect of the shock waves.

Although the precise mode of action of HESW is not yet understood, several possible mechanisms for shock wave induced cytotoxicity are suggested. Thermal injury seems most unlikely since the low frequency shock waves are not absorbed much by the tissue. Of non-thermal effects, cavitation (gas body activation) with subsequent secondary shock waves, hydrodynamic jets and free radical generation are supposed to be responsible for the cellular damage observed.

The negative peak pressure of the shock wave is essential for the development of cavitations and one might conclude that, the lower the negative pressure, the more cavitation will occur and thus more tissue damage. Indeed, in vitro studies comparing different lithotriptors demonstrated that the lithotriptor with the lowest maximum pressure and negative peak pressure showed the lowest amount of cell damage. We do not know whether this accounts also for the in vivo situation, since no comparative studies have yet been performed.

Biological systems are known to possess cavitation nuclei, and it seems thus likely that shock waves may also induce cavitation in vivo. The gas bubbles that are formed during the cavitation process collaps and may results in the emission of a tissue destructing liquid jet. In vitro studies indicated that immobilized cells can be affected by shock waves when acoustic impedance and cavitation effects can be exerted. In vivo shock waves act mainly on the vasculature. This phenomenon may be explained by the acoustic impedance between the vessel containment and the endothelial cell membrane. Cavitation effects thus result in damaging the endothelial cells. How can the synergistic effect of the combination of HESW and TNF-α be explained? The effects of shock waves alone on tissue are: vasoconstriction of the small arterioles, stasis within the capillaries, micro-haemorrhages, ruptures of endothelial cells, defects in vascular basal membranes, leakage from venules of macromolecules and extravasation of red blood cells (Brendel 1987). TNF-α is known to have a direct cytotoxic effect on the endothelial cells. Histologic examinations of the NU-1 tumor, several days after exposure to the combination of 4 sessions of 800 shock waves and TNF-α plus IFN-α, showed a pronounced vasodilatation, leucocyte migration and infiltration, and fibrin clots within the capillaries (Oosterhof 1990a). It appeared that both shock waves and TNF-α act on the microcirculation. Combination of these actions result in an enhanced damage of tumor vascularization and may thus explain the potentiated antitumor effect.

The tumors that are well vascularized are thus more susceptible for the combined treatment.

This hypothesis was confirmed by the results obtained in the NU-10 and NU-12 tumors. Both tumors are slowly growing and the effects of shock waves alone are very limited (Table 2, Fig. 4 and 5). The peritumoral administration of TNF-α leads to a marked decrease in growth rate in the NU-10, that is well vascularized, and has a very limited effect in the poorly vascularized NU-12. The combined treatment was synergistic in the NU-10 and had no potentiating effect in the NU-12. These experiments indicate that the synergistic antitumor effect of the combined treatment of shock waves and TNF-α is related to the vascularization of the tumor. Other characteristics of the tumor as type of cells, cell arrangement, grade of the tumor, number of mitosis per high power field seemed to be of less importance (Table 1).

We conclude that the anti-proliferative effects of the combined treatment of shock waves and BRM's depend on the tumor model and the BRM used. The sensitivity of a tumor for shock waves alone is closely related to its doubling time. When combined with BRM's, a synergistic anti-proliferative effect was seen only when TNF-α was used. This potentiating effect of the combined treatment on tumor growth is most likely related to the vascularization of the tumor.

Both TNF-α and shock waves probably act on the microcirculation of the tumor. The differential sensitivity of the various tumors for the combined treatment may thus be explained by the different degree in vascularization and doubling time. This, however, does not exclude that other factors such as size and ploidy of the cells or the portion of stromal cells and thickness of the septa are also of influence.

ACKNOWLEDGEMENTS

REFERENCES

Beniers A.J.M.C., van Moorselaar R.J.A., Peelen W.P., Debruyne F.M.J., Schalken J.A. Differential sensitivity of renal cell carcinoma xenografts towards therapy with Interferon-alpha, Interferon-gamma, Tumor Necrosis Factor and their combinations; possible implications for clinical studies. Urol. Res., 19, 91, 1991.

Brendel W., Delius M., Goetz A. Effects of shock waves on the microvasculature. Prog. appl. Microcirc. Karger, Basel. 12, 41, 1987.

Hoëhn W., Schröder F.H. Renal cell carcinoma: two new cell lines and a serially transplantable nude mouse tumor (NC 65). Invest. Urol., 16, 106, 1978.

Oosterhof, G.O.N., Smits G.A.H.J., de Ruyter J.E., Schalken J.A., Debruyne F.M.J. Effects of high energy shock waves combined with biological response modifiers or adriamycin on a human kidney cancer xenograft. Urol. Res., 18, 419, 1990a.

Oosterhof, G.O.N., Smits G.A.H.J., de Ruyter J.E., Schalken J.A., Debruyne F.M.J. In vivo effects of high energy shock waves on urological tumors; an evaluation of treatment modalities. J. Urol., 144, 785, 1990b.

Oosterhof G.O.N., Smits G.A.H.J., de Ruyter J.E., van Moorselaar R.J.A., Schalken J.A., Debruyne F.M.J. The in vitro effect of electromagnetically generated shock waves (Lithostar) on the Dunning R3327 PAT-2 rat prostatic cancer cell-line. Urol. Res., 17, 13, 1989.

Randazzo R.F., Chaussy C.G., Fuchs G.J., Bhuta S.M., Lovrekovich H., de Kernion J.B.: The in vitro and in vivo effects of extracorporal shock waves on malignant cells. Urol. Res., 16, 419, 1988.

Russo P., Stephenson R.A., Mies C., Huryk R., Heston W.D.W., Melamed M.R., Fair W.R. High en-energy shock waves suppress tumor growth in vitro and in vivo. J. Urol., 135, 626, 1986.

Russo P., Mies C., Huryk R., Heston W.D.W., Fair W.R. Histopathologic and ultrastructural correlates of tumor growth suppression by high energy shock waves. J. Urol., 137, 338, 1987.

Smits G.A.H.J., Oosterhof G.O.N., de Ruyter J.E., Schalken J.A., Debruyne F.M.J. Cytotoxic effects of high energy shock waves in different in vitro models: influence of the experimental set-up. J. Urol. 145, 171, 1991.

BIOLOGICAL EFFECTS OF HIGH ENERGY SHOCK WAVES
IN MOUSE SKELETAL MUSCLE:

correlation between ^{31}P nuclear magnetic resonance spectroscopic and microscopic alterations.

Geert A.H.J. Smits[1], Paul H.K. Jap[2], Arend Heerschap[3],
Gosse O.N. Oosterhof[1], Frans M.J. Debruyne[1], Jack A. Schalken[1].

Departments of Urology[1] and Radiology[3], University Hospital Nijmegen
Department of Cell Biology and Histology[2], Faculty of Medical Sciences, University Nijmegen

ABSTRACT

To investigate the in vivo effects of electromagnetically generated high energy shock waves (HESW) on skeletal muscle, we used in vivo ^{31}P nuclear magnetic resonance (NMR) spectroscopy (MRS) measurements and correlated the results with microscopical studies. Mouse skeletal muscle (calf muscle) was exposed to 200 or 800 HESW (P_{max}: 37.5 MPa, P_{min}: 5.2 MPa, t_r: 30-120 nsec, t_w: 340 nsec, frequency: 1.25 Hz). In the ^{31}P MRS spectra transient alterations were observed. A prominent increase of inorganic phosphate (Pi) peaks was found, as well as the appearance of Pi with different chemical shifts, reflecting the presence of different pH values (5.4-7.1) in cellular or tissue compartments. Within 20-96 hours after exposure, pH values and Pi levels returned to normal. The changes were more pronounced in the animals treated with 800 HESW as compared to 200 HESW.

Light- and electron microscopy demonstrated focal degenerations of muscle fibers. This process consisted of disorganization of myofilaments and structural changes in sarcoplasmic organelles and was progressive in time.

The (ultra-)structural changes were not present in all myofibers, i.e., between affected degenerating fibers unaffected intact fibers were seen. Several ultra-structural abnormalities were also found in capillaries even up to severe dilatation and disruption, as well as in the peripheral nerves. The degeneration of the pre-existing myofibers was predominantly confined to type 1 fibers and was followed by a regeneration of the muscle tissue by proliferation of myoblasts. A notable amount of myotubes still showed vacuolization.

We conclude that in vivo HESW exposure of skeletal muscle tissue results in a degeneration of myofibers. The cellular effects are present in foci and associated with changes in the ^{31}P NMR spectra. The NMR spectroscopy technique provides us with a non-invasive method to evaluate in a longitudinal way the biological effects of HESW.

INTRODUCTION

High energy shock waves (HESW) are used clinically in extracorporeal shock wave lithotripsy (ESWL), (Chaussy 1986, Sauerbruch 1986). More recently, this type of focussed acoustic energy is investigated for applications extending beyond that of stone fragmentation. Other in vivo biomedical applications, like treatment of pseudoarthrosis and experimental anti-tumor therapy have been studied (Debus 1991, Oosterhof 1991, Russo 1985, Weiss 1990). The knowledge of the biological effects resulting from HESW exposure may not only contribute to a better understanding of a safe operation with this type of ultrasound equipment for stone disintegration, but also to the use of HESW in new (experimental) applications on living tissue.

Acute and late side effects of HESW and various histopathological or pathophysiological effects of shock waves on organs or tissues have been described (review: Brümmer 1991). The majority of the data relates to effects on the vascular system. Little is known about the mechanisms of HESW action and induced biological effects at a cellular level in vivo. In vitro studies clearly reveal cytotoxic events due to HESW exposure. However, an extrapolation to the in vivo situation is difficult (Smits 1991a) and more detailed investigations are necessary to gain information on HESW induced cell-degeneration, cell-death and cell-regeneration in vivo.

In order to elucidate these effects in more detail, the in vivo biological effects of HESW were investigated on mouse skeletal muscle (calf muscles) by ^{31}P nuclear magnetic resonance spectroscopy (MRS). By use of surface coils ^{31}P MRS offers a non-invasive tool for measurements of high energy phosphate metabolism and estimation of tissue pH (Gadian 1982). We have shown that this technique provides an adequate method of establishing changes in tumor cell metabolism longitudinally, i.e., sequentially over time, in vivo after HESW treatment of experimental tumors (Smits 1991b).

In addition to MRS, extensive microscopic investigations (light- and electron microscopy) were carried out after HESW treatment.

This enabled us to correlate spectroscopically detected changes in myofiber metabolism with subsequent microscopic alterations.

With these methods, functional and structural cellular effects induced by HESW in vivo were assessed as a function of time.

MATERIALS AND METHODS

Animals

Twelve to sixteen week old male BALB/c athymic mice (Bornholtgård, Ry, Denmark) were used in each experiment. The mice were kept in groups of five fed ad libitum with irradiated SRM food (Hope Farms, Woerden, The Netherlands). Drinking water was acidified with 0.7 ml concentrated HCl/l.

HESW treatment

The shock waves were generated electromagnetically by a commercially available lithotriptor (Lithostar, Siemens) used in the treatment of urolithiasis.

The experimental set-up and administration of the shock waves were described earlier (Oosterhof 1990). The characteristics of the shock waves in the center of the focal area in water are as follows: maximum pressure (P_{max}) is 37.5 MPa and the negative pressure (P_{min}) is 5.0 MPa, pressure rise time (t_r), defined as the time for the pressure to rise from 10% to 90 % of the value of P_{max} is 30-120 nsec, the half width time (t_w) is defined as the half amplitude width of the initial positive pressure half cycle and is about 340 nsec, the pulse to pulse variation is about 3% and the pulse repetition frequency is 1.25 Hz. The focal area (area limited by pressures which are half of the maximum pressure ($P_{max}50$) is 6 mm in the lateral plane and approximately 8 cm in the transverse plane.

For HESW exposure the animals were placed in a water-filled container and kept in fixed position by a plastic cocoon in such a way that only calf muscles were exposed whereas the rest of the body was placed outside the focal area. The temperature of the water was maintained at 37°C. The nude mice were anaesthetized for a 15 minute period with ketamine hydrochloride (Ketalar, Parke-Davis) 125 mg/kg just before the HESW treatment.

In vivo ^{31}P NMR spectroscopic evaluation

The ^{31}P MRS experiments were performed as described earlier (Smits 1991b). In short, a Bruker WM-200 spectrometer equipped with a 4.7 T magnet and a home-built ^{1}H / ^{31}P double tunable two-turn surface coil with an inner diameter of 10 mm were used. The mice were anaesthetized during these NMR studies with a flow of 1.5% enflurane in a mixture of O_2 and N_2O. The HESW exposed part of the calf muscles was precisely positioned adjacent to the coil. The body temperature of the animals was maintained by a flow of warm air. The magnetic field homogeneity was optimized by observing the ^{1}H NMR signal from tumor H_2O. The H_2O line widths were 0.2 - 0.3 ppm. For the ^{31}P NMR Spectroscopy typical acquisition parameters were as follows; composite 90° excitation pulse with a nominal 90° pulse at about 1 mm from the coil center, 4 K data points/scan, 3.5 sec pulse repetition time.

The free induction decays (FID) were averaged for each spectrum and analyzed on an Aspect 3000 computer using standard Bruker software. Convolution difference was applied to remove broad spectral components using a line broadening of 300 Hz. In order to improve the signal to noise ratio the averaged FID was multiplied by an exponential function resulting in a linebroadening of 10 Hz. After Fourier transformation an automated baseline correction was used.

The pH was deduced from the inorganic phosphate (Pi) signal chemical shift with respect to the phosphocreatine (PCr) signal chemical shift. The following expression was used: $pH = pK + \log\{^{(shift - a)}/_{(shift - b)}\}$,

where pK = 6.75, a = 3.26, and b = 5.75 (Heerschap 1988, Radda 1986).

The $^{PCr+Pi}/_{Ptot}$, $^{Pi}/_{PCr}$, and $^{Pi}/_{Ptot}$ ratios were used to evaluate the ^{31}P data quantitatively (Ptot = PCr+ATP+Pi). The relative quantities of the detected phosphorous compounds were determined by computerized peak integration. Longitudinal in vivo ^{31}P MRS measurements were performed once before and, 4 to 6 times during at least 48 hours after HESW exposure, in the three different treatment groups (0 = sham-treated control, 200 and 800 HESW, each group n=3).

In vitro NMR measurements

In order to obtain calf muscles tissue for in vitro measurements, treated and sham-treated mice were anaesthetized. A few seconds after removal of the overlying skin, calf muscles were dissected, clamped, and stored in liquid nitrogen (within 5 sec. after start of dissection). Frozen tissue was pulverized and perchloric acid (PCA) extracted as described earlier (Smits 1991b).

^{31}P NMR spectra were acquired on the same 200 MHz spectrometer with a standard ^{31}P NMR high resolution probe employing a 60^0 flip angle (6 μsec.) and a 5 sec. pulse repetition time. WALTZ-16 low power ^{1}H decoupling was used.

Both for the in vivo and in vitro measurements the chemical shifts were referenced with respect to the chemical shift position of the PCr resonance.

Microscopic studies

Animals of both the treated (800 HESW) and untreated group were sacrificed at different time intervals after HESW exposure in three independent experiments (each experiment n=10). The skeletal muscle tissues (hind limb) were frozen in liquid nitrogen or fixed in 4% formalin for light microscopy (LM), as well as prefixed in 2% glutaraldehyde in 0.1 M cacodylate buffer containing 4% sucrose (pH 7.3, 4 °C) for at least 4 hours for electron microscopy (EM).

Paraffin embedded sections (4 μm) were stained with hematoxylin and eosin. For histochemistry frozen sections were stained for ATPase activity at pH 9.4 according to Round et al (1980). For EM the prefixed tissues were cut orientated in blocks, rinsed overnight (4°C) in 0.1 M cacodylate buffer and postfixation was effected in 1.5% osmic acid in the same buffer for 1 hour (20 °C). After rinsing, dehydration was performed in an ascending series of aqueous ethanol, and the tissues were subsequently transferred via a mixture of propylene oxide and Epon to pure Epon 812. After polymerization, semi-thin sections were cut and stained with toluidine blue. Appropriate areas were selected under the light microscope and ultrathin sections cut with a diamond knife on a Reichert OM U3 ultramicrotome. The silver sections were picked up on copper grids, double contrasted with uranyl acetate and lead citrate, and examined in a Philips EM 300 or 301 electron microscope.

RESULTS

^{31}P magnetic resonance spectroscopy in vivo

In this study ^{31}P MRS was used to get more insight in the duration and quality of effects induced by HESW on mouse calf muscle tissue. By using a specially designed probe equipped with a surface coil, this technique enables us to monitor metabolism of energy rich phosphor-containing bio-molecules and pH of exposed muscle tissue of the hind limb of the mice.

Two representative ^{31}P spectra, obtained before and after treatment with 800 HESW, are shown in Figures 1 and 2.
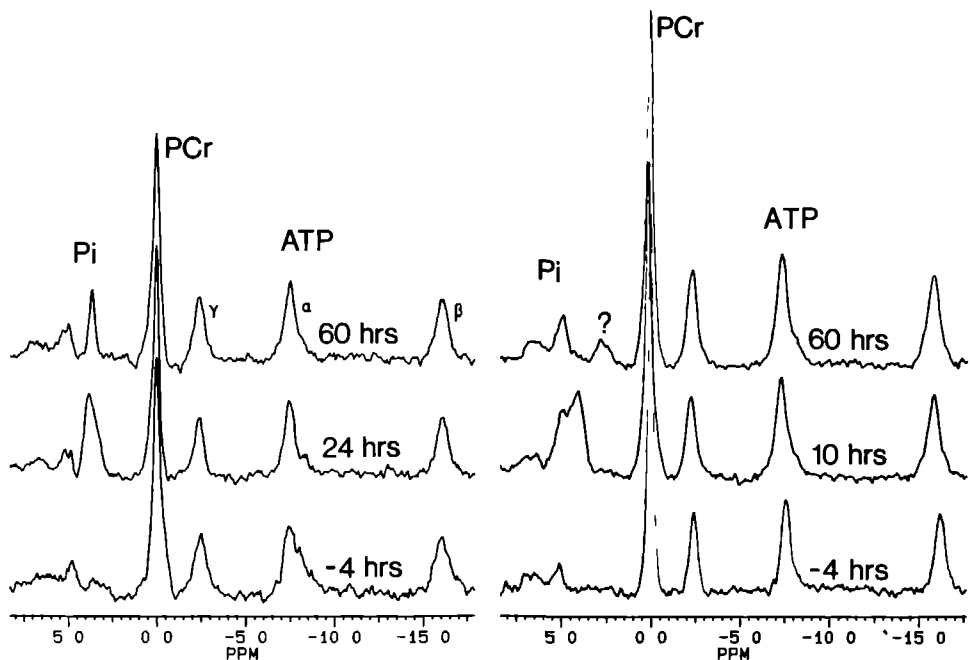

Fig. 1 and 2:

Two representative longitudinal in vivo 81 MHz ^{31}P MRS evaluations of skeletal calf muscle tissue, 4 hours before, and up to 60 hours after treatment with 800 HESW.

Note a temporary increase in resonances in the Pi region.

? refers to an increase of resonances in the phosphodiester region.

Abbreviations; Pi: inorganic phosphate, PCr: phosphocreatine, ATP: adenosine-triphosphate.
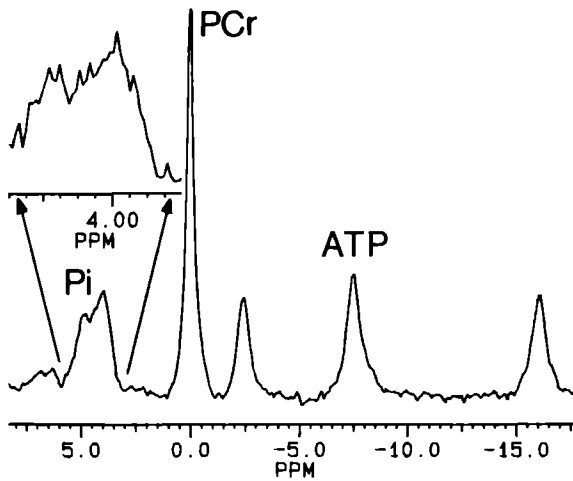
Fig. 3:
A detail of the Pi region 10 hours after treatment with 800 HESW. This region appears to consist of resonances with different chemical shifts (3.7 - 5.1 ppm, linebroadening of 2 Hz instead of 10 Hz). Abbreviations; Pi: inorganic phosphate, ATP: adenosine-triphosphate, PCr: phosphocreatine.

The control spectra of the muscle, taken 4 hours before HESW exposure, show specific patterns for muscle tissue with resonances for ATP, PCr and Pi. (Cady 1990).

Longitudinal evaluation of the spectra (starting 1 hour after the end of HESW treatment) showed a gradually increasing signal intensity between 3.5 and 5.1 ppm. This additional signal appeared to consist of distinct resonances with different chemical shifts. In the inset of Figure 3 a typical example of the composition of this signal is shown. Between 3.5 and 5.1 ppm resonances may occur of phosphodiesters, Pi, and sugar-1-phosphates. In order to characterize this complex of resonances more in detail, we performed in vitro ^{31}P MRS measurements (at a constant pH value) on PCA extracts obtained from calf muscles tissue 10 hours after HESW exposure.

In the chemical shift region of interest (3.5-5.1 ppm), both in vitro spectra showed the same peak pattern, i.e. in the in vitro spectrum of the treated muscle the same peaks specific for sugarphosphates, Pi, and glycerolphosphoethanolamine (GPE) were observed as compared to sham-treated muscle with no additional resonances (data not shown). Sugar-1-phosphates are present in low concentrations both in treated and untreated muscle tissue as deduced from the in vitro NMR spectra. The resonance position of GPE is not pH dependent over the pH range studied. This identifies the multiple resonance profile as originating from Pi in different environments (Gadian 1982).

Figure 2 shows an appearance of resonances 60 hours after treatment (marked by ?). This intensity might be assigned as an increase in phosphodiester (PDE) compounds and probably reflects an increased phospholipid breakdown in biomembranes. However, this phenomenon was only seen incidentally.

In an attempt to examine the temporary metabolic events after HESW exposure, we determined the $^{PCr+Pi}/_{Ptot}$, $^{Pi}/_{PCr}$, and $^{Pi}/_{Ptot}$ ratios by peak integration. The data for the two treatment groups (200 or 800 HESW) are presented as a function of time in Figures 4, 5 and 6 for each of three individual longitudinal evaluations. In general, treatment with 200 or 800 HESW resulted in qualitatively similar changes. Both, the $^{Pi}/_{PCr}$ as well as the $^{Pi}/_{Ptot}$ ratio's showed a temporary increase. In the $^{PCr}/_{ATP}$ ratio only slight variations were detected after HESW exposure. The $^{PCr+Pi}/_{Ptot}$ ratio remained constant in both treatment groups during the whole evaluation.

The changes in relative amount of Pi and chemical shift positions of Pi became evident only a few hours after treatment and reached their maximum after 8 to 24 hours. The increased relative intensities as well as the chemical shifts of the Pi signals were more pronounced after 800 HESW than after 200 HESW. The calculated pH ranged between 6.4 - 7.1 and 5.7 - 7.1 after 200 and 800 HESW, respectively. After a period of time the resonances in the spectra regained their original intensities as before HESW treatment and remained stable for the observation period (two months). The recovery of the spectrum was detected after 24 to 72 hours in the 200 HESW group, and after 48 to 120 hours in the 800 HESW group. Longitudinal spectroscopic evaluation of sham-treated muscle tissue showed no detectable changes in metabolism. Moreover, in muscle tissue of the non-exposed (i.e. outside the focal area) contralateral hind limb no spectral changes were observed either.
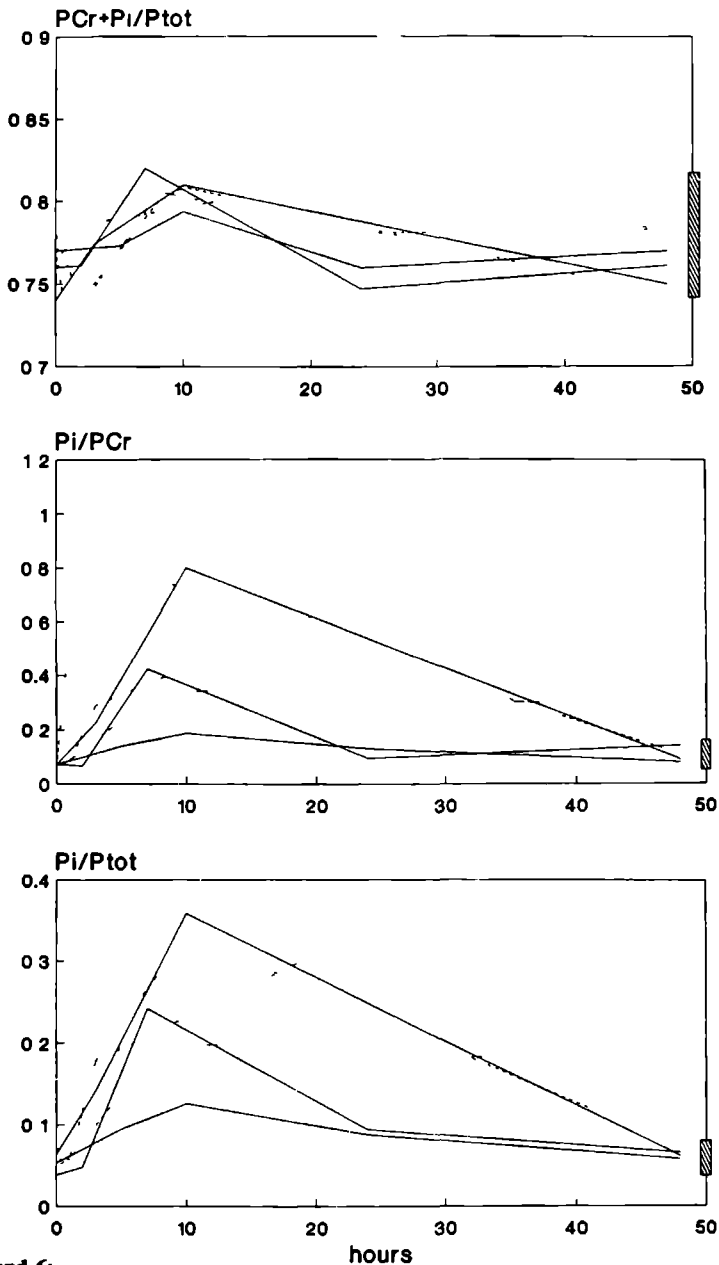
Fig. 4, 5, and 6:

$^{PCr+Pi}/_{Ptot}$, $^{Pi}/_{PCr}$, and $^{Pi}/_{Ptot}$ ratio's, calculated from the in vivo ^{31}P NMR spectra of calf skeletal muscles, after 200 or 800 HESW exposure depicted as a function of time (each group n=3). The dotted line represents 800 HESW. The vertical bar at the right represents the range in ratio's obtained in sham-treatment (n=6)

The normal appearance of the LM and EM detectable structures in muscle tissue is presented in the figures A, B and C. The LM and EM features of sham-treated muscle tissue showed intact capillaries lined with normal endothelial cells. The myofibers showed a normal sarcomeric pattern and distinct sarcoplasmic reticulum cisterns (SER). Subsarcolemmal and juxtanucleair accumulation of mitochondria were present.

Myofibers, degeneration

Generally, the LM of the treated tissues demonstrated structural changes of several myofibers located in between unaffected fibers (figures D, E, F). These alterations included vacuolization of various degrees and sarcoplasmatic edema. Hypercontraction or sarcoplasmic clumping and degeneration/necrosis as well as cellular ruptures were observed. These phenomena were confined to local areas in the muscle tissue and were either localized throughout the whole length of the myofiber or localized partly in the myofiber.

In the toluidine blue stained semi-thin sections the vacuoles demonstrated different coloring (not shown).

These vacuoles appeared to consist of different entities in the EM i.e. either swollen and dilated mitochondria or different-sized accumulations of small SER cisterns and aggregated lipidic vacuoles (figures G, H).

These ultra-structural changes of the myofibers were graded in stages 1 to 3. In stage 1 no ultra-structural changes are detectable except for some few changes in the mitochondrial appearance. In the swollen mitochondrial matrix numerous membranous components are evident. Stage 2 is characterized by an increasing amount of dramatic alterations in cellular constituents. The Z-bandings of the contractile apparatus gradually are irregular and myofilaments loose their symmetrical pattern and start to disrupt. Subsarcolemmally, areas of fine granular material (blebs) are seen (figure I). These regions represent partially ballooned or even focally disrupted parts in the myofiber. Stage 3 is characterized by more severe alterations of the contractile system. Fragmentation is replaced by condensation and complete disappearance of the banding patterns resulting to degeneration and necrosis. Vacuolization is present in a greater extent in the regions closely adjacent to areas of hypercondensed myofibers.
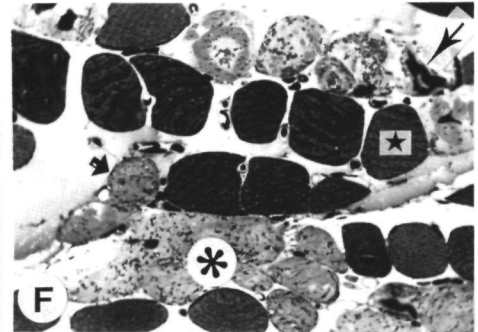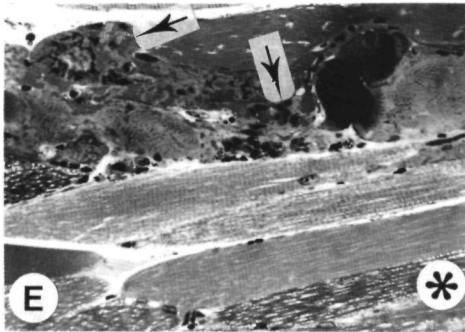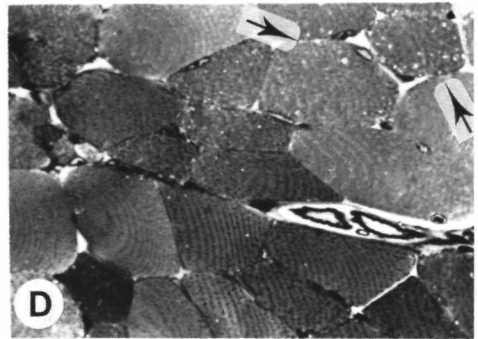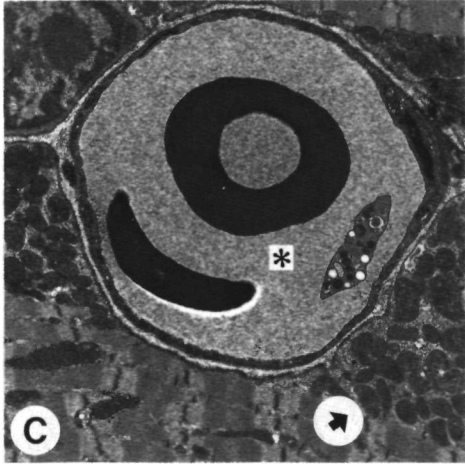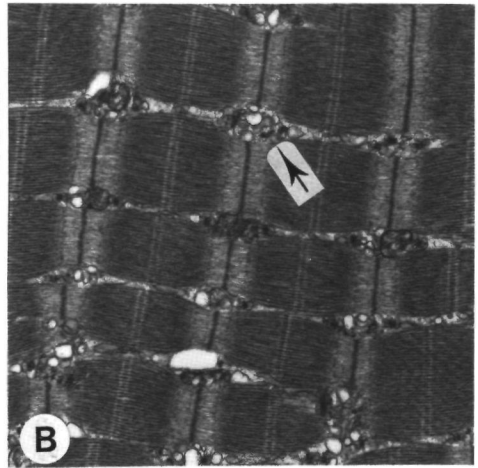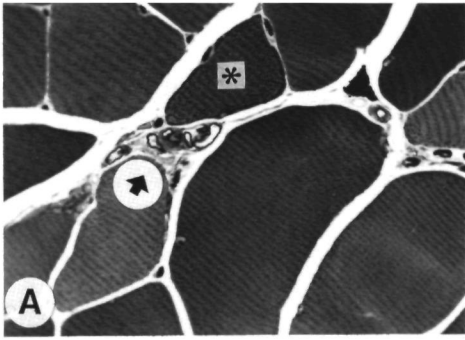
A:

Cross section of sham-treated muscle tissue. Intact myofibers with peripheral located nuclei. Striation depicts mitochondria and Z-discs.

Asterisk shows individual fiber with dense peripheral rim (subsarcolemmal mitochondria). In the interstitium capillaries and myelinated axons are present (thick arrow). (Magnification: x330).

B:

Part of a myofiber with normal contractile apparatus (sham-treated). In between the myofilaments organelles e.g. mitochondria and slightly swollen sarcoplasmic reticulum (SER) are regularly observed (thin arrow). (Magnification: x11,850).

C:

Parts of two adjacent myofibers (sham-treated) and an interstitial capillary (asterisk). Note subsarcolemmal localization of mitochondria (thick arrow). (Magnification: x6,350).

D:

Cross sectioned fibers show early events of injury e.g. small white vacuoles (arrows). Two normal appearing myelinated axons are present. (Magnification: x330).

E:

Increased vacuolization was observed in the entire length of the affected fibers (asterisk). Adjacent to these vacuolated fibers degeneration stages and distinct necrosis of the other fibers are evident. Within these areas of severe alterations neutrophilic granulocytes were even seen intrasarcoplasmatically (arrows). (Magnification: x200).

F:

Darker stained normal myofibers show unaffected, oblique cut contractile apparatus (star). Clusters of myofibers show granularity (thick arrow). Increased granularity exhibit dissolution of sarcoplasm (asterisk). Thick arrow points to hypercondensation of sarcoplasmic remnant. (Magnification: x200).
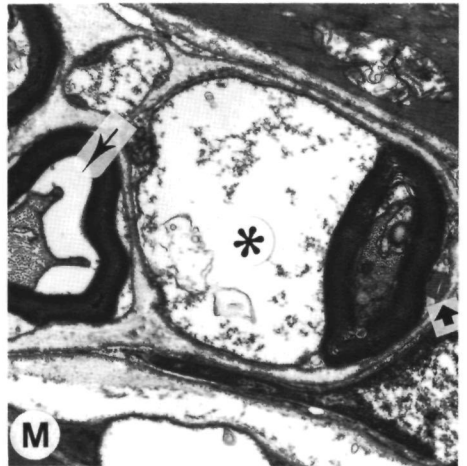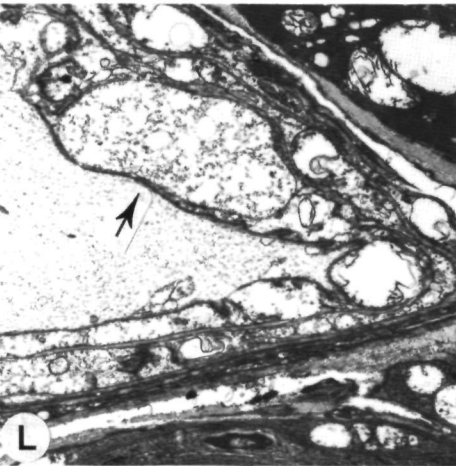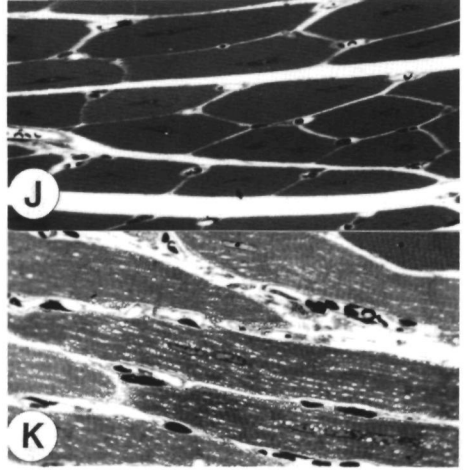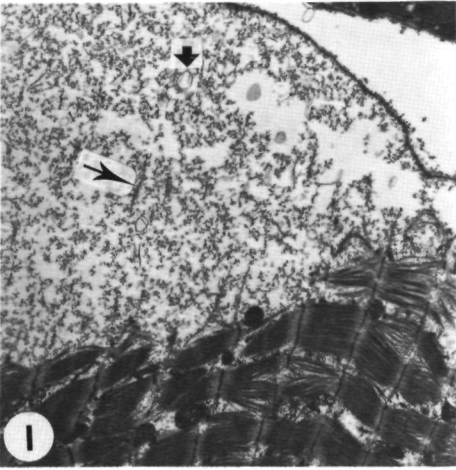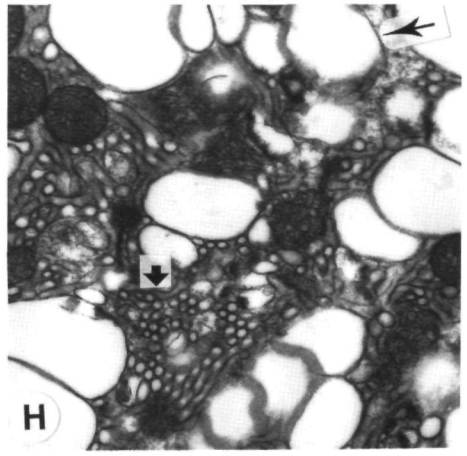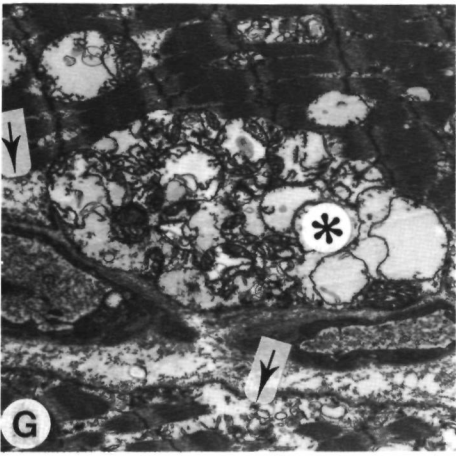
G:

Parts of two myofibers and in between a sectioned capillary. Vacuolization is largely due to swollen and disrupted mitochondria (asterisk). Locally, sarcoplasmic dissolution is present (arrows). Note intact myofilaments. (Magnification: x6,350).

H:

High magnification of vacuolated parts of sarcoplasm reveals accumulation of proliferated tubular SER (thick arrow) with lipid inclusions (thin arrow) with normal appearing mitochondria. (Magnification: x24,200).

I:

Bleb formation of the peripheral part of a myofiber with beginning disruption of myofilaments. The edematous sarcoplasm still contains remnants of filaments (thin arrow), vesicles (thick arrow) between proteinaceous precipitation. (Magnification: x7,700).

J:

Regeneration of myofibers. All fibers still exhibit centrally located nuclei (= internal nuclei). (Magnification: x200).

K:

Apart from normal appearing regenerated myofibers areas of vacuolated myofibers with internal nuclei are also observed. (Magnification: x330).

L:

Locally an extended arteriole shows severe ballooning of the endothelial cytoplasm (arrow). Most endothelial organelles as well as those of the smooth muscles are disrupted and not recognizable anymore. (Magnification: x330).

M:

Interstitial axons show several abnormalities: disruption and edema of the Schwann cytoplasm (asterisk) or retraction of the axoplasm from the myelin sheath (thin arrow). Thick arrow points to a phi-body. (Magnification: x6,350).

In the first hours after HESW most fibers are characterized by stage 1, whereas after 8 hours the changes are more dramatic and a gradual increasing number stage 2 and 3 fibers were seen.

To investigate a possible differential sensitivity between the myofibers for HESW, fiber type specific stainings were carried out in a series of HESW treated muscle tissue. It appeared that type 2 (fast twitch, glycolytic) fibers were seldomly affected by HESW. The relative amount of these fibers remained constant. In contrast, all structural changes were seen in the type 1 (slow twitch, oxidative) fibers. Also, in these series, a gradual increase in time, in amount and severity of affected fibers was seen (data not shown).

Myotubes, regeneration

After a few days, proliferation of myoblasts and eventually myotubes with their characteristic internal nuclei were observed (figure J). Apart from these immature myofibers distinct vacuolization of numerous pre-existing mature fibers was present. However, several immature fibers also showed vacuolization even 21 days after HESW exposure (figure K).

Capillaries - endothelial cells

Macroscopical examination after HESW exposure showed small petechial bleeding (even after a few HESW) and some haemorrhagic areas confined to the epimysium. The observed macroscopic bleedings were confirmed microscopically. Within the muscular tissue most of the capillary system appeared to be virtually intact. Only locally, extravasation of erythrocytes was observed but this was predominantly restricted to the perimysium.

Ultra-structurally, edematous and ballooned endothelial cells as well as swollen pericytes with deposition of fibrin on the damaged luminal endothelial surface was observed (figure L).

Nervous tissue

Striking structural abnormalities of the peripheral nervous tissue within the exposed area became evident. Whereas the axons showed no structural aberrations, the cytoplasm of the Schwann cells appeared to be severely affected. Apart from vacuolization and cytoplasmic edema of these Schwann cells, retraction of the axon of the myelin sheet was noted. Also, few so called phi-bodies were detected (fig. M)

DISCUSSION

To study the in vivo effects of HESW at a cellular level, we investigated exposed muscle tissue of the hind limb of nude mice. These animals are ideal for these experiments since the skin contains (few) hair follicles with a disturbed hair outgrowth thus limiting the source of interfering cavitation nuclei. Treatment of muscle tissue with HESW results in pronounced changes in the ^{31}P spectrum. A broad signal appears between 5.1 and 3.6 ppm and consists of distinct entities at different chemical shifts (Figure 3). in vitro characterization of exposed and non-exposed calf muscles reveal no spectral differences and hence we conclude that these changes in the in vivo spectrum are due to an increase of the inorganic phosphate signal concomitant with an acidification (decrease of the chemical shift position of Pi) in distinct compartments resulting in different shifts (Gadian 1982). In other words, Pi is present in different chemical environments with different pH values varying from 7.15 to 5.92. These compartments can be either intercellular (distinct cells), or intra-cellular.

In order to detect HESW induced (sub-)cellular alterations accompanying the observed transient changes in the ^{31}P NMR spectra, detailed light and electron microscopical studies were performed at different time intervals.

In general, the (ultra-)structural studies revealed, besides some small bleedings in the perimysium (the most peripheral zone of skeletal muscular tissue), focally severe alterations within the myofibers consisting of disarrangement and disorganization of myofilaments and structural changes in the sarcoplasmic organelles. These alterations became evident directly after exposure (within 1 hour) and are described as myofiber degeneration (Ischikawa 1986). By defining different stages of degeneration it appeared that this proces developed progressively in time and was maximal after about 24 hours.

It is most likely that the ^{31}P spectral changes in Pi represent this degenerative process. The increase of Pi and the acidification (shift of Pi) can be interpreted as a metabolic event in the (non-synchronous) process of degenerating myofibers. In this way the affected myofibers reflect a pool of cellular entities with distinct chemical contents (cellular compartmentation). The toluidine blue stained sections showed vacuoles in the degenerating myofibers that colored differently due to metachromatic staining at different pH. These intra-cellular compartments could also contribute to the different chemical shift positions of the Pi resonances.

The HESW induced degeneration of the myofibers can be explained by direct effects at the cellular level. In vitro studies have revealed direct membrane damage and cell disruption depending on the microenvironment of the model used (Smits 1991a). To what extent this immediate cellular injury is present in the vivo situation is not known. In this in vivo study only few effects were detectable by microscopy or spectroscopy immediately after HESW exposure. The (ultra)structural and metabolic changes are progressive in time and thus direct HESW induced effects represent only a minority of the total impact of HESW on (muscle) tissue in vivo. This strongly indicates that (additional) cytotoxic events are initiated in vivo during a certain period of time (hours) after the application of HESW.

Several observations are in favor of an induction of partial ischemia. HESW clearly cause (micro)vascular disruptions (even after one shock wave) and ischemia may be the result. In addition, the MRS studies show ischemic patterns by the increase in Pi concomitant with acidification. The $PCr+Pi/P_{tot}$ ratio doesn't change after HESW exposure and thus the Pi-increase is the result of the decrease of PCr at constant ATP levels (Veech 1982). During complete ischemic periods of rat muscle for more than 3 hours, the PCr and ATP resonances completely disappear (Newman 1984).

An apparent differential sensitivity between individual myofibers towards shock waves became evident. Staining for ATP-ase reactivity revealed that the degenerative proces was almost completely confined to type-1 myofibers (slow-twitch fibers). These fibers are oxidative and therefore presumed to be more sensitive towards ischemia than their type-2 counterparts which are glycolytic (Meyer 1985). Thus, one can assume that the cytotoxic events in time are due to an ischemia leading to a degeneration of preferentially type 1 fibers.

However, several observations are not in concordance with this assumption and suggest the existence of other cytotoxic phenomena. Although some arteriols show severe alterations, the majority of degenerating myofibers are surrounded by a structurally intact microvascular system without thrombus formation. Since muscle tissue is well perfused due to extensive capillarization it is not likely that these areas are less perfused. In addition, most ultra-structural characteristics of these affected fibers are not suspect for hypoxia (Makitie 1977, Sjöstrom 1982). Only a few of the affected fibers contained mitochondria with a characteristic ischemic pattern. The formation of different sized SER cisterns is formed under distinct toxic conditions. Thus, the myofiber degeneration can only partially be explained by a HESW induced ischemia.

At present, it is unclear how HESW induced biological effects are mediated. Besides possible intrinsic effects of the pressure (changes) during the shock wave (Carstensen 1990), acoustic cavitation has been shown to play a key role in the biological effects (Crum 1986, Delius 1990, Gahmbiler 1990, Miller 1987, Smits 1991a). The lithotriptor provides an ideal system to study the effects of acoustic cavitation (Coleman 1987). Cavitation in vitro is a complicated and typically uncontrolled process which is very difficult to characterize in a manner amenable to detailed analysis of biological effects (Miller 1987) and several critical factors should be considered in the assessment of the effects of cavitation in vitro (Bräuner 1989, Smits 1991a). A number of cavitation related phenomena have been described (Miller 1987). These include the formation of radicals with concomitant chemical activity (Coackley 1978, Crum 1986, Morgan 1989), induction of the degradation of polymer macromolecular structures (Kost 1989), and induction of hydrodynamic shear stresses and intra-cellular microstreaming resulting in viscous shearing stress. To what extent these phenomena are responsible for the myofiber degeneration is speculative.

Irrespective of the mechanism of action, the observed effects represent a spectrum of injuries which are confined to the lithotriptor field. Outside the focus no significant abnormalities were observed. The local injury caused by HESW resulted in a regenerative response with common characteristics like an induction of activation and proliferation of satellite cells, and eventually their fusion to myotubes (Weller 1991, Grounds 1991). However, several immature fibers still showed vacuolization 21 days after HESW exposure, suggesting a disturbed regeneration.

Overall, it has become evident that shock waves have an impact at the cellular level in skeletal muscle tissue and lead to degeneration of numerous myofibers. This biological effect can be indirectly mediated by ischemia but other cytotoxic events at a subcellular and (macro)molecular level most likely occur as well. ^{31}P MRS is able to monitor accompanying metabolic alterations of these degenerating myofibers. Until now, the studies of side effects in parenchymatous organs like kidney and liver reveal pathological changes related to wound healing, scar formation and fibrosis due to direct tissue damage and vascular injury. For several reasons, it is difficult to extrapolate the data presented here to these organs, but we present evidence for cytotoxic effects which might be of importance in the development of functional and structural abnormalities in these organs due to HESW treatment.

Further research in HESW cytotoxicity in vivo is necessary and will be crucial to increase our knowledge of the mechanism of action and the effects in other biomedical applications (especially on tumor tissue) of this form of focussed energy.

ACKNOWLEDGEMENTS

REFERENCES

Bräuner T., Brümmer F., Hülser D.F. Histopathology of shock wave treated tumor cell suspensions and multicell tumor spheroids. Ultrasound in Med. & Biol., 15, 451, 1989.

Brümmer F., Bräuner T., Hülser D.F. Biological effects of shock waves.
World J. Urol., 8, 224, 1990.

Cady E.B. Clincal magnetic resonance spectroscopy. New York and Londen: Plenum Press, 1990.

Carstensen E.L., Campbell D.S., Hoffman D., Child S.Z., Aymé-Bellegarda E.J. Killing of Drosophila larvae by the fields of an electrohydrolic lithotrypter.
Ultrasound in Med. & Biol., 16, 687, 1990.

Chaussy C. Extracorporeal shock wave lithotripsy. New York: Karger 1986.

Coackley W.T., Nyborg W.L. Ultrasound: Its applications in Medicin and Biology, ed. Fry F.J. Elsevier Amsterdam, 77-159, 1978.

Coleman A.J., Saunders J.E., Crum L.A., Dyson M. Acoustic cavitation generated by an extracorporeal shockwave lithotripter. Ultrasound in Med. & Biol., 13, 69, 1987.

Crum L.A., Fowlkes J.B. Acoustic cavitation generated by microsecond pulses of ultrasound.
Nature, 319, 52, 1986.

Debus J., Peschke P., Hahn E.W., Lorenz W.J., Lorenz A., Iffländer H., Zabel H.J., van Kaick G., and Pfeiler M. Treatment of the Dunning tumor R3327-AT1 with pulsed high energy ultrasound shock waves (PHEUS): growth delay and histomorphologic changes.
J. Urol., 146, 1143, 1991.

Delius M., Jordan M., Liebich H-G., Brendel W. Biological effects of shock waves on the liver and gall-bladder wall of dogs - administration rate dependece.
Ultrasound in Med. & Biol., 16, 459, 1990.

Gadian D.G. Nuclear magnetic resonance and its applications to living systems.
Oxford: Clarendon Press, 1982.

Gahmbiler S., Delius M., Brendel W. Biological effects of shock waves: cell disruption, viability, and proliferation of L1210 cells exposed to shock waves in vitro. Ultrasound in Med. & Biol., 16, 587, 1990.

Grounds M.D.: Towards understanding skeletal muscle regeneration. Path. Res. Pract., 187, 1, 1991.

Heerschap A., Bergman A.H., Vaals J.J., Wirtz P., Loermans H.M.Th., Veerkamp J.H. Alterations in relative phosphocreatinine concentrations in preclinical muscular dystrophy revealed by in vivo NMR. NMR in Biomedicine, 1, 1, 27, 1989.

Kost J., Leong K., Langer R. Ultrasound enhanced polymer degradation and release of incorporated substances. Proc. Natl. Acad. Sci., 86, 7663, 1989.

Makitie J., Teravainen H. Histochemical studies of striated muscle after temporary ischemia in the rat. Acta Neuropath., 37, 101, 1977.

Meyer R.A., Brown T.R., Kushmerick M.J. Phosphorus nuclear magnetic resonance of fast- and slow-twitch muscle. Am. J. Physiol., 248, c279, 1985.

Miller D. L. A review of the ultrasonic bioeffects of microsonation, gas-body activation, and related cavitation-like phenomena. Ultrasound in Med. & Biol., 13, 443, 1987.

Morgan T.R., Laudone V.P., Heston W.D.W., Zeitz L. and Fair W.R. Free radical production by high energy shock waves - comparison with ionizing irradiation. J. Urol., 139, 18, 1988.

Newman R.J. Metabolic effects of tourniquet ischemia studied by nuclear magnetic resonance spectroscopy. Journal of bone and joint surgery, 66-B, 434, 1984.

Oosterhof G.O.N., Smits G.A.H.J., de Ruyter J.E., Schalken J.A., Debruyne F.M.J. In vivo effects of high energy shock waves on urological tumors, an evaluation of treatment modalities. J. Urol., 144, 785, 1990.

Oosterhof G.O.N., Smits G.A.H.J., de Ruyter J.E., Schalken J.A., Debruyne F.M.J. Effects of high energy shock waves combined with biological response modifiers in different human kidney cancer xenografts. Ultrasound in Med. & Biol., 17, 391, 1991.

Radda. The use of NMR spectroscopy for the understanding of disease. Science, 233, 640, 1986.

Round J.M., Matthews Y., Jones D.A. A quick simple and reliable method for ATPase in human muscle preparation. Histochem. J., 12, 707, 1980.

Russo P., Heston W.D.W., Fair W.R. Suppression of in vitro and in vivo tumor growth by high energy shock waves. Surg. Forum, 36, 645, 1985.

Sauerbruch T., Delius M., Paumgartner G., Holl J., Wess O., Weber W., Hepp W., Brendel W. Fragmentation of gallstones by extracorporeal shock waves. N. Engl. J. Med., 314, 818, 1986.

Sjöstrom M., Neglen P., Friden J., Eklof B. Human skeletal muscle metabolism and morphology after temporary incomplete ischemia. European Journal of Clinical Investigation, 12, 69, 1982.

Smits G.A.H.J., Oosterhof G.O.N., de Ruyter J.E., Schalken J.A., Debruyne F.M.J. Cytotoxic effects of high energy shock waves in different in vitro models: influence of the experimental set-up. J. Urol., 145, 171, 1991a.

Smits G.A.H.J., Heerschap A., Oosterhof G.O.N., Ruys J.H.J., Hilbers C.W., Debruyne F.M.J., Schalken J.A. Early metabolic response to high energy shock waves in a human tumor kidney xenograft monitored by ^{31}P magnetic resonance spectroscopy. Ultrasound in Med. & Biol., 17, 791, 1991b.

Veech R.L., Lawson J.W., Cornell N.W., Krebs H.A. Cytosolic phosphorylation potential. J. Biol. Chem., 254, 6538, 1979.

Weiss N., Delius M., Gambihler S., Dirschedl P., Goetz A., Brendel W. Influence of the shock wave application mode on the growth of A-MEL 3 and SSK2 tumors in vivo. Ultrasound in Med. & Biol., 16, 595, 1990.

Weller B., Karpati G., Lehnert S., Carpenter S. Major alteration of the pathological phenotype in gamma irradiated mdx soleus muscle. Journal of neuropathology and experimental neurology, 50, 419, 1991.

EARLY METABOLIC RESPONSE TO HIGH ENERGY SHOCK WAVES IN A HUMAN TUMOR KIDNEY XENOGRAFT MONITORED BY ^{31}P MAGNETIC RESONANCE SPECTROSCOPY.

G.A.H.J. Smits[1], A. Heerschap[2], G.O.N. Oosterhof[1], J.H.J. Ruys[2], C.W. Hilbers[3], F.M.J.Debruyne[1], J.A. Schalken[1]

Department of Urology[1] and Radiology[2], University Hospital Nijmegen
Department of Biophysical Chemistry[3], University Nijmegen, The Netherlands

ABSTRACT

The effects of electromagnetically generated High Energy Shock Waves (HESW, Siemens Lithostar) on the phosphate metabolite levels of the NU-1 human kidney cancer xenograft implanted under the skin of the hind limb of nude mice were monitored by ^{31}P Magnetic Resonance Spectroscopy (MRS).

Administration of 200 and 800 HESW (18.1 kV, P+ =37.5 MPa, P-=5.2 MPa, t_r=30-120 nsec, t_w=340 nsec, freq.=1.25 Hz), focussed on the tumor centre, resulted in an immediate tumor decline; 2 hours after exposition to the HESW, the high energy phosphate resonances had decreased drastically. This decline in energy rich molecules was accompanied by a concomitant increase in the inorganic phosphate resonance and a decrease in pH of the tumor. During the following period a dose-time dependent recovery of the original high energy phosphate resonance intensities was observed. These changes are qualitatively similar to those produced by ischemic inhibition of energy metabolism and are correlated with early histological features like vascular disruption, stasis within capillaries and focal thrombosis.

These results demonstrate that experimental HESW treatment of the NU-1 kidney tumor is effective in provoking a temporary reduction of both high energy phosphate metabolism and tissue pH of the tumor. The data presented here strongly suggest that these effects are predominantly indirect by affecting tumor vascularity. Overall, this study shows that MRS is a powerful technique for longitudinal investigations of HESW induced effects, and can provide information about its mode of action.

INTRODUCTION

Recently High Energy Shock Waves (HESW) have been point of interest in the development of a new experimental form of antitumor therapy. In most studies a shock wave induced suppression of tumor growth in murine transplantable solid tumors has been described (Russo 1985, 1986, 1987, Randazzo 1986, Holmes 1990, 1991, Weiss 1990). Experiments with different animal tumor models performed in our laboratory, confirmed that HESW can provoke a temporary suppression of tumor growth. In an evaluation of different treatment modalities we found that the in vivo antitumor effect of HESW depended on the number of shock waves, the number of shock wave sessions, the tumor volume at start the of treatment, and the tumor model used (Oosterhof 1990a). Furthermore, combining HESW with other treatment modalities, e.g. combination with chemotherapeutic drugs or cytokines, resulted in more pronounced effects (Oosterhof 1990b). Especially, the potentiating effect of TNF on HESW indicates that combined therapy is potentially useful as a new cancer treatment modality (Oosterhof 1991).

Despite these hopeful experimental efforts, only limited data with respect to the mechanisms of action and bio-effects of HESW in vivo are available. In vitro experiments with (tumor-) cells can be useful to study shock wave induced bioeffects at the cellular level and reveal a dose dependent direct cytotoxicity and diminished proliferative capacity (Randazzo 1988, Berens 1989, Oosterhof 1989). However, these effects depend on the way cells are exposed to the shock waves and can be greatly influenced by changing the micro-environment (Brummer 1989, Brauner 1989, Laudone 1989, Gambihler 1990, Smits 1991). Therefore, interpretations of in vitro experiments are restricted to the particular model used, and the relevance for in vivo effects of HESW remains questionable. Moreover, HESW can exert their effects indirectly, e.g (tumor) vasculature can be affected significantly (Goetz 1988, Delius 1990). Functional and structural changes have been observed after HESW treatment and presumably have a great impact on (tumor-) cell metabolism.

Considering that the indirect effects of HESW at the vascular level may change tumor cell metabolism and that these changes are reversible, we sought to evaluate the effects in a longitudinal setting which requires the use of a non-invasive method. [31]Phosphorus Magnetic Resonance Spectroscopy (^{31}P MRS) provides us with such a technique.

This technique has proven to be a sensitive method to monitor changes in metabolites involved in high energy metabolism, tissue pH, and levels of cellular phospholipids (Pettegrew 1990). In particular, this method has a great potential for studies of progressive metabolic changes that accompany (tumor-) response to different kinds of therapy (Ng 1982, Steen 1989, Glickson 1990).

The purpose of this study was to examine alterations in the ^{31}P NMR spectrum, in order to get more insight in the duration and quality of the HESW induced effects on in vivo growing tumors and to come to a better insight and rational for improving HESW effectiveness as a monotherapy or in a combined treatment modality.

MATERIALS AND METHODS

Animals

Xenografts were transplanted in six-eight week old male Balb/c athymic mice (Bornholt Gård, Rye, Denmark). The mice were kept in groups of five in PAG type 2 cages (IFFA Credo) covered with an iso cap for sterile conditions. The mice were fed ad libitum with irradiated SRM food (Hope Farms, Woerden, The Netherlands) and drinking water was acidified with 0.7 ml concentrated HCl/l.

Tumors

The human renal cell carcinoma NU-1 xenograft was established in our laboratory by serial subcutaneous transplantation of tumor pieces after original subcutaneous transplantation of small primary tumor pieces direct after nephrectomy. The tumors were transplanted subcutaneously as trocar pieces in the hind limb of the animals, under ether anaesthesia. For the HESW studies, passage 30-40 in vivo were used. Tumors were allowed to grow to a size of 250 ± 25 mm^3. After reaching this tumor volume the animals were randomly divided in a sham treated control group, and two groups receiving 200 and 800 HESW respectively.

The shock waves were generated electromagnetically by the commercially available lithotriptor (Lithostar, Siemens) which is used clinically in the treatment of urolithiasis. The experimental set-up and way of administration of the shock waves were described earlier in detail (Oosterhof 1990). In short, the shock wave tube of the lithotriptor was in contact with a water filled plexiglass container over a silicon membrane in its lateral side. Optimal contact was ensured by a gel placket and lubricating gel. The characteristics of the shock waves and the focal area (area limited by pressures which are half of the maximum pressure (P_{max} 50)) in our experimental set-up were determined, at an 18.4 kV energy level as used in all experiments, with a polyvinylidene difluoride (PVDF) needle hydrophone (Imotec) connected with an oscilloscope (Gould, DSO, 4072). This needle transducer has a broad spectrum and an effective area of 0.5 mm^2 with a constant sensitivity of up to 5 MHz. Measurements are possible up to the focal point with a measuring range from 0 to 200 MPa. The focal area is 6 mm in the lateral plane and approximately 8 cm in the transverse plane. The maximum pressure (P_{max}) is 37.5 MPa and the negative pressure (P_{min}) 5.0 MPa. Pressure rise time (t_r) is defined as the time for the pressure to rise from 10% to 90 % of the value of P_{max} and is 30-120 nsec. The half width time (t_w) is defined as the half amplitude width of the initial positive pressure half cycle and is about 340 nsec. The pulse to pulse variation is about 3%. The shock waves were applied with a frequency of 1.25 Hz.
For HESW exposure the animals were placed in the water-filled container and kept in fixed position by a plastic cocoon. The temperature of the water was maintained at 37°C. At the site of the limb of the animal a 1.5 x 1.5 cm hole in the tube allows the shock waves to reach the tumor while the animal is protected by the tube against shock wave exposure at other sites. The tumors were positioned in the center of the focal area (fluoroscopically controlled).
The nude mice were anaesthetized for a 15 minute period with ketamine hydrochloride (Ketalar, Parke-Davis) 100 mg/kg just before the HESW treatment.

In vivo ^{31}P NMR spectroscopic evaluation

NMR experiments were performed on a Bruker WM-200 spectrometer equipped with a 4.7 T magnet employing a home-built ^{1}H / ^{31} P double tunable two-turn surface coil with an inner diameter of 10 mm. The mice were anaesthetized during these NMR

studies with a flow of 1.5% enflurane in a mixture of O_2 and N_2O. The tumors were led through a matched hole in a Faraday shield and positioned adjacent to the coil. In this way only signals confined to the tumor were detected and signal contamination from adjacent non-malignant tissue was avoided. The body temperature of the animals was maintained by a flow of warm air. The mice were fed parenterally when measurements lasted more then 8 hours.

The magnetic field homogeneity was optimised by observing the ^1H NMR signal from tumor H_2O. Typical H_2O line widths were 0.1 - 0.2 ppm. Typical acquisition parameters were as follows; composite 90° excitation pulse with a nominal 90° pulse at about 1 mm from the coil center, 4 K data points, 3.5 sec pulse repetition time, 1280 scans (40 min. total measurement time). From spectra obtained at a repetition time of 9.5 sec. the saturation of spinsystems was estimated to be less than 20% for Pi and PCr at this pulse repetition time. Free induction decays were analyzed on a Aspect 3000 computer. Convolution difference was applied to remove broad spectral components using a line broadening of 300 Hz. In order to improve the signal to noise ratio an exponential multiplication was used resulting in a linebroadening between 20 and 30 Hz. After Fourrier transformation an automated baseline correction was used (all standard Bruker software).

Peak intensities were evaluated by peak height measurements. Because no attempt was made for absolute quantification of metabolite concentrations the data in this paper are all expressed as ratio's of peak heights.

The pH was deduced from the Pi signal chemical shift with respect to the PCr signal chemical shift, or to the α-ATP signal chemical shift in the absence of a PCr resonance. The Henderson-Hesselbach equation modified for this purpose was used: pH = pK + log{(shift - a)/(b - shift)} (pK = 6.75, a = 3.29, b = 5.70 (Moon 1973, Seo 1983).

In vitro NMR measurements

A perchloric acid (PCA) extraction procedure was used (Barany 1982). In short, mice were anesthetized and the overlying skin was removed. Liquid nitrogen was poured into a funnel placed over the tumor during several minutes. The mice were then sacrificed by cervical dislocation and the frozen tumor was removed without surrounding tissue and stored in liquid nitrogen. Frozen tissue was pulverized and transferred in a glass tissue grinder. While adding dropwise 0.9 M PCA complete tissue homogenation was achieved.

The total volume of PCA equalled 5-times the weight of the tumor (in g.). After centrifugation (30,000g, 15', 4°C) the supernatant is transferred immediately into 9 M potassiumhydroxide and the pH was adjusted to 7.5. The potassium perchlorate precipitate was spun down and the supernatant was passed through a Chelex sample preparation disc (Bio-Rad Laboratories) and lyophilized. Just before the MRS measurements the lyophilizate was dissolved in 450 μl. containing 7.5 mM dimethylphosphate, 20 mM EDTA and 10 mM Tris, 30% D_2O at pH=7.8. ^{31}P NMR spectra were acquired on the same 200 MHz spectrometer with a standard ^{31}P NMR high resolution probe employing a 60^θ flip angle (6 μsec.) and a 3 sec. pulse repetition time. WALTZ-16 low power ^{1}H decoupling was used during acquisition. Exponential multiplication before Fourier transformation resulted in a linebroadening of 2 Hz.
Both for the in vivo and in vitro measurements the chemical shifts were referenced with respect to the chemical shift position of the PCr resonance.

Histology

Treated and untreated animals were sacrificed at different intervals after HESW exposure. The tumors were fixed in formalin 4%, embedded in paraffin and 4 μm sections were stained with hematoxylin and eosin.

^{31}P Magnetic Resonance Spectroscopy

In order to monitor shock wave induced effects on tumor cell metabolism we used ^{31}P MRS. Both during the shock wave treatment as well as during the MRS measurements the animals require mild anaesthesia in order to remain sufficiently immobilized. The Ketamine anaesthesia used during shock wave treatment did not interfere with the MRS measurements i.e. comparison of spectra of control animals with those anaesthetized 2-8 hours before MRS measurements revealed no differences. It should be noted that MRS measurements were performed under N_2O/Enflurane anaesthesia which virtually have no effect on ^{31}P NMR spectra for measurements lasting several hours. We therefore conclude that, even though Ketamine can influence MRS results when given during the measurements (Wehrle 1988), it has no effects detectable by ^{31}P NMR spectroscopy for periods longer than 2 hours.

A representative in vitro ^{31}P NMR spectrum of a PCA extract of 2 tumors (500 and 650 mm^3 respectively) of the NU-1 xenograft is shown in Fig.1. The resonances were assigned on the basis of literature data (Evanochko 1984, Corbett 1987). Apart from ATP other nucleotide triphosphates also contribute to the NTP labelled resonances. This is evident from the presence of multiple ß-NTP triplets in the spectrum.

Each subcutaneous growing tumor was evaluated just before (once) and after HESW treatment (4 - 6 times) until no changes in the ^{31}P NMR spectra were noted anymore (24 -72 hours after HESW treatment).

Two representative pre-treatment in vivo spectra are shown in the inset to Fig.1. For in vivo spectra much broader lines are observed compared with the in vitro spectra which can be ascribed to magnetic field susceptibility variations within the tumor, cation and macromolecular binding as well as chemical exchange.

Despite this broadening the resolution of the in vivo spectrum is sufficient to assign resonances according to the in vitro spectrum. Taking the linebroadening into account the peak distribution of the in vivo spectrum is similar to that of the in vitro spectrum. For the in vivo growing tumors (250 mm3 ± 25), slight differences in the height of the PCr and Pi peaks were detected. This probably reflects tumor heterogeneity in the metabolic state due to differences in the amount of pre-necrosis and tumor perfusion.

In the evaluation of the HESW induced effects we therefore expressed peak height ratio's as a percentage of the pre-HESW values. The spectrum of each individual tumor was highly reproducible and during 70 hours of untreated growth no significant spectral changes occurred.
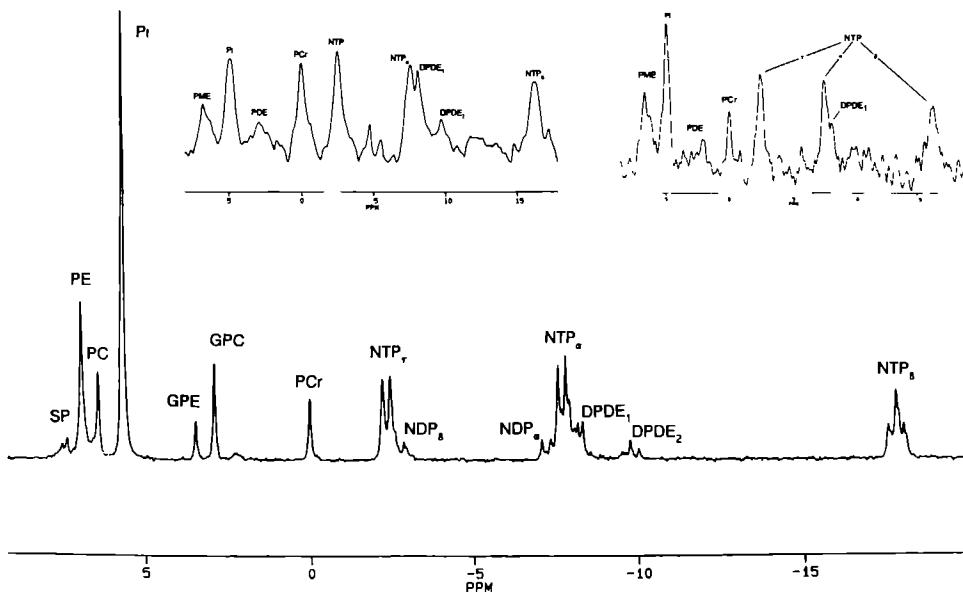
Figure 1:
In vitro and in vivo 81 MHz ^{31}P NMR spectra of a control (untreated) NU-1 human kidney cancer xenograft. The major peaks in the in vitro spectrum (below) are attributed as follows; SP: sugarphosphates, PME: phosphomonoesters; PE: phosphoethanolamine and PC: phosphocholine, Pi: inorganic phosphate, PDE: phosphodiesters; GPE: glycerophosphoethanolamine and GPC: glycerophosphoethanolamine, PCr: phosphocreatine, NTP: nucleoside triphosphate, NDP: nucleoside diphosphate, DPDE: diphosphodiester, DPDE$_1$: NAD, oxidized nicotinamide adenine dinucleotide, DPDE$_2$: nucleosidediphosphorylsugars.
Above two representative in vivo spectra are shown.

A representative qualitative ^{31}P MRS evaluation before and after HESW treatment is shown in Fig 2. During the first hours after HESW treatment the NTP and PCr resonances are decreasing concomitant with an increase of the Pi resonance. In the following period a recovery of the original intensities is observed. It appeared that these temporary changes were more intense and lasted longer for the 800 HESW treated tumors as compared to the 200 HESW treated animals, whereas the sham treated tumors showed no differences in their ^{31}P NMR spectra during the complete follow-up time of 72 hours. No persistent changes in PME and PDE resonances were detectable, neither for the 200 HESW nor for the 800 HESW treated tumors.
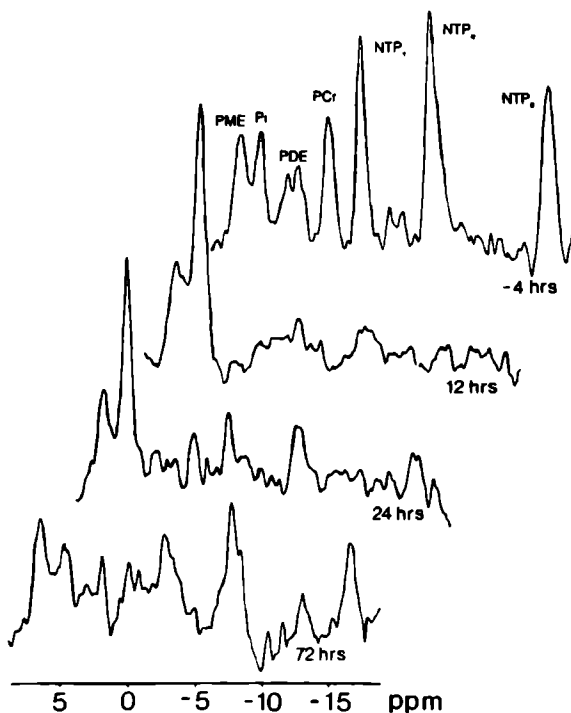
Figure 2:
Longitudinal in vivo 81 MHz ^{31}P MRS evaluation of a NU-1 human kidney cancer xenograft implanted in a nude mouse during 4 hours before and 72 hours after treatment of the tumor with 800 HESW. Note the temporary depletion of nucleoside triphosphates in the tumor along with a concomitant increase in inorganic phosphate. The abbreviations used are; PME: phosphomonoesters, Pi: inorganic phosphate, PDE: phosphodiesters, PCr: phosphocreatine, NTP: nucleoside triphosphate.

In order to quantify these temporary metabolic events, we evaluated the changes in mean NTP/Pi ratio (as a suitable indicator of energy metabolism) and pH in time in the three different treatment groups (0 = sham treated control, 200 and 800 HESW, each group n=4). Analysis of the variance of these parameters before the shock wave treatment showed no significant differences between these three treatment groups, (NTP/Pi ratio; p=0.33 and pH; p=0.74).

NTP/Pi ratio

In Figure 3 the NTP/Pi ratio is presented as a percentage of the value before treatment and plotted against time. In general HESW exposure of the tumor resulted in a temporary decrease of the NTP/Pi ratio. After an initial decrease, the ratio is restored to its pre-shock wave value. After 800 HESW the maximum decrease in the NTP/Pi ratio's was significantly more pronounced as compared with 200 HESW (Wilcoxon, p < 0.0001). The lowest mean ratios were 0.09 (range 0 - 0.28) for the 800 HESW group and 0.47 (0.39 - 0.67) for the 200 HESW group. This minimum was reached after 6.5 hours (3 - 15) and 8 hours (7 - 8) respectively. The original NTP/Pi ratio was reached again after 26 hours (range 19 - 38) and after 52 hours (range 38 - 72 hours) for the 200 and 800 HESW groups respectively.
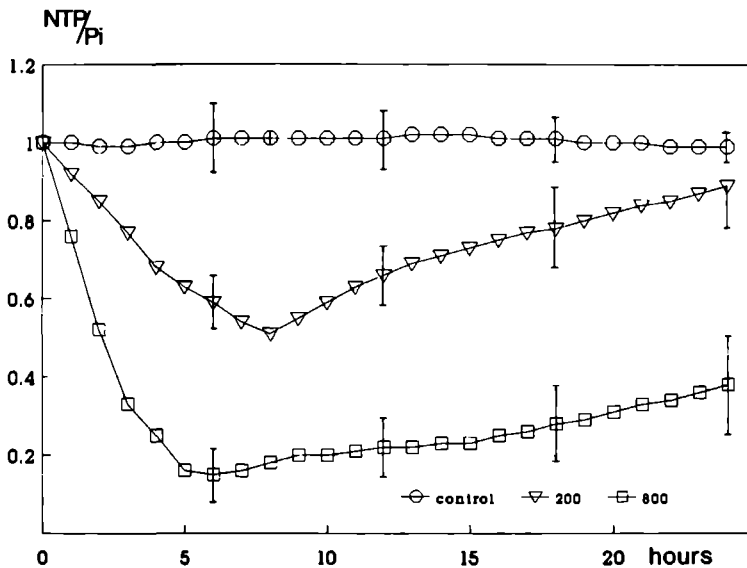

Figure 3:

Time and dose dependence of the effect of HESW on the NTP/Pi peak height ratio observed in the ^{31}P MRS spectra of NU-1 tumors. Data are presented as mean ± standard error (bars) and expressed as a percentage of control (before HESW treatment). Each group consisted of 4 mice.

pH

In all animals treated with 200 and 800 HESW, the exposure induced a significant tumor tissue acidification. After 800 HESW, the mean tumor pH decreased from 7.09 (range; 7.04-7.14) to 6.67 (6.50-6.87) and recovered to 7.06 within the following 20 hours (Fig. 4). The time period to reach the minimum pH was 4 hours (range 3-7 hours). After 200 HESW group the mean pH decreased from 7.07 (range 7.00-7.12) to 6.87 (6.79-6.91) after 6 hours (4-8). Unlike the dose dependent reduction of the NTP/Pi ratio, the maximum decrease in pH was not significantly different in the 800 HESW group versus the group treated with 200 HESW. In contrast to a significant difference after treatment with 200 or 800 HESW in decrease of the mean NTP/Pi ratio, the maximum decrease in pH appeared to be not significantly different in the two HESW treatment groups (Wilcoxon, p=0.73). Also the original (pretreatment) pH was reached in a similar way in a similar time period (20-24 hours).
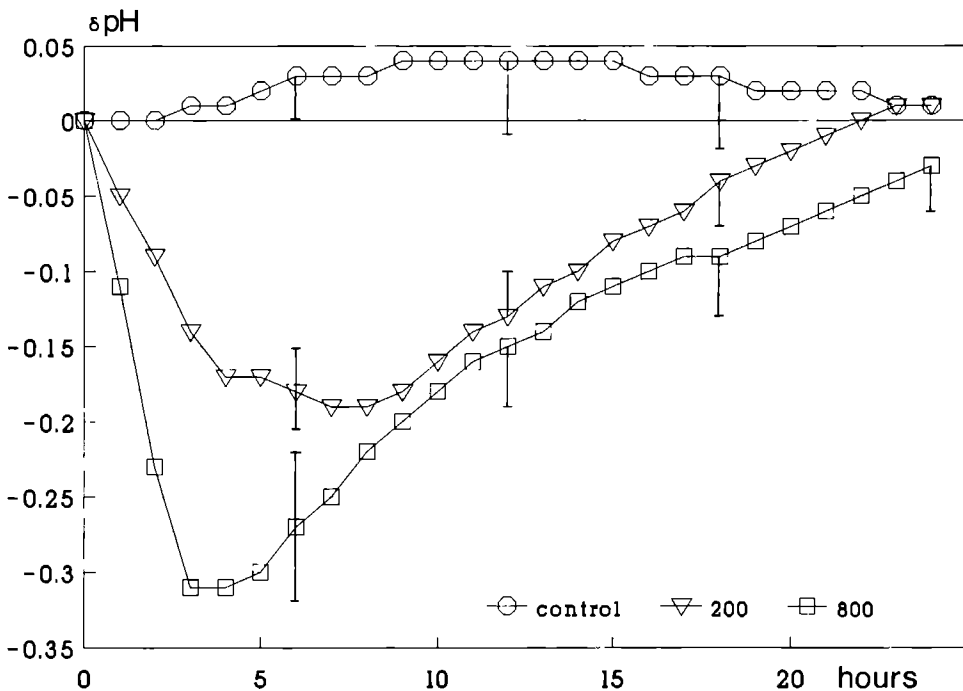

Figure 4:

Time and dose dependence of the effect of HESW on the tissue pH (as determined by ^{31}P MRS) of NU-1 tumors. Data are presented as mean ± standard error (bars) and expressed as a change in pH units of the original pH (before HESW treatment). Each group consisted of 4 mice.

Histology

Histological examinations of implanted NU-1 kidney cancer xenograft were performed at various time points. This human renal adenocarcinoma is well vascularized and grows with a doubling time of 3-4 days. Histologically the tumor consists of spindle cells of different size arranged in an anarchistic sarcomatous pattern and shows spontaneous haemorrhagic necrosis (Photo 1). Changes were detected immediately after HESW treatment.

Small peritumoral bleedings were noted and within the tumor petechial bleedings were seen due to broken capillary walls with extravasation of erythrocytes into the surrounding peri-vascular tumor stroma. Also intact capillaries became distended and were occluded with tightly packed erythrocytes (Photo 2). 8 Hours after exposure, focal thrombosis was seen followed by evidence of beginning focal necrosis.
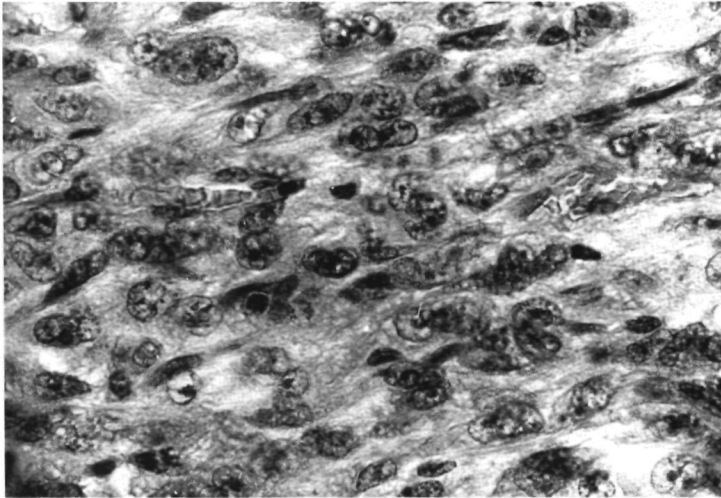

Photo 1:
Light microscopy of the NU-1 human renal adenocarcinoma xenograft transplanted in the nude mouse. The tumor is well vascularized and consists of spindle cells of different size arranged in an anarchistic sarcomatous pattern. (HE-staining, magnification 600X).
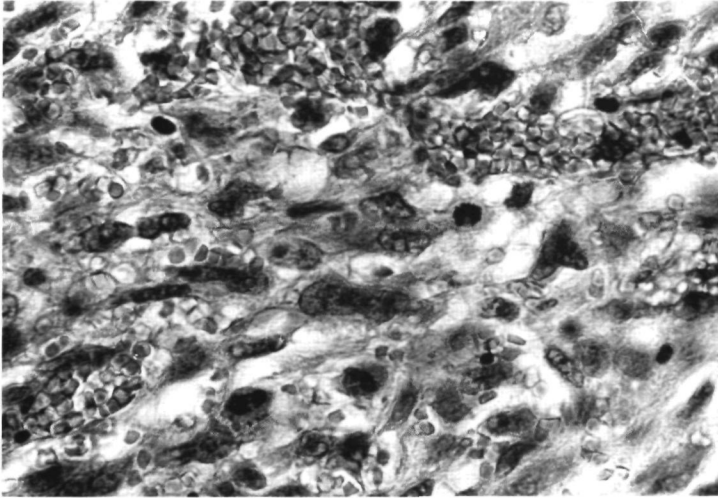
Photo 2:

Histology after HESW treatment. Small peritumoral bleedings were noted and within the tumor petechial bleedings were seen due to broken capillary walls with extravasation of erythrocytes into the surrounding peri-vascular tumor stroma. Also intact capillaries became distended and were occluded with tightly packed erythrocytes. (HE-staining, magnification 600X).

DISCUSSION

The primary aim of this study was to examine the short term effects of HESW on tumor cell metabolism in vivo in order to get a better insight in the qualitative and quantitative effects of this experimental treatment. We, therefore employed ^{31}P MRS that enables a dynamic evaluation of biochemical changes in vivo, and combined it with microscopic studies. ^{31}P NMR spectra give information about the metabolic changes that occur in viable cells and thus in cells that may be the target for HESW therapy (Stubbs 1989).

Exposure of the NU-1 kidney tumor xenograft, implanted subcutaneously at the hind limb, to unifocal HESW treatment results in an immediate dose dependent reduction in concentration of energy rich molecules PCr and NTP's, concomitant with an increase of Pi. At the same time, an immediate decrease in the pH of the tumor is induced.

These events are defined as a tumor decline (Steen 1989) and can be seen in acute ischemia (ligation of tumor blood flow) and several antitumor therapies (like hyperthermia, photodynamic therapy, treatment with TNF) with a direct major impact on tumor vascularity (Ng 1982, Lilly 1985, Gibson 1989, Wehrle 1987, Evelhoch 1988, Shine 1989). The histological studies of this kidney tumor xenograft show mainly changes in tumor vasculature due to HESW exposure i.e. disrupted capillaries, extravasation of erythrocytes, distended microvessels with tightly packed erythrocytes and thrombi formation (Photo 2), and these findings clearly represent (micro)-vascular obstruction. It is known that shock waves can have a major impact on blood vessels (Goetz 1988, Delius 1989, 1990). In addition, vascularization of a tumor plays a role in sensitivity towards HESW; tumors that are well vascularized appeared to be more susceptible towards HESW (Oosterhof 1991). Thus, the metabolic inactivation and acidification after HESW treatment are most likely to be the result of an impairment of oxygenation status by decreased tumor blood flow due to structural and functional disturbances in the vascular component.

It is not clear to what extent these initial spectral changes are due to cell death or sublethal damage. The latter seems to be the major event but cell death will certainly be induced since focal necrosis becomes apparent within a few days following HESW treatment.

The HESW induced tumor decline is only temporary, the NTP/Pi ratio (representing the metabolic state of the tumor) and tumor pH reach their original pretreatment levels (Fig. 3 and 4). The duration of the acidotic period appears to be relatively independent of the number of HESW (200 vs. 800). In the 200 HESW group the time span needed to regain the original treatment levels is the same for both NTP/Pi and pH. However, after 800 HESW, metabolic activity of the tumor is returned to the original state only about 24 hours after recovery of the acidification.

This observation suggests besides indirect (vascular induced) effects also direct cytotoxic effect of HESW and one could speculate that dose dependency of vascular and direct tumor cellular effects are not necessarily similar. Further studies are needed to elucidate more in detail to what extent the acute effects of HESW on tumor metabolism reflect vascular damage and subsequent ischemia or direct metabolic effects.

Irrespective of the mechanism(s) of action, how do these observations fit into earlier experiments showing a HESW induced tumor growth suppression?

a/ HESW as a monotherapy.

In earlier studies in different animal tumor models we found that the number of shock waves, serial exposure (shock wave exposure in different sessions) and time interval between each session influence the outcome of the experiments (Oosterhof 1990a). These studies revealed a dose dependent anti-tumor effect and showed the importance of repeated HESW sessions to provoke a more prolonged tumor growth suppression. From these observations we concluded that since HESW treatment alone only resulted in temporary antiproliferative effects, this treatment would not be beneficial as a monotherapy.

The data shown here are in agreement with the outcome of the experiments mentioned above. Indeed, administration of HESW results in a dose dependent inhibition of high energy phosphate metabolism and (as stated before) this reflects a decrease in the viable tumor population resulting in a tumor growth delay.

In our former studies using 12 or 24 hours time intervals between each 800 HESW session no permanent anti-tumor effect could be established. The tumor volume at start of these treatment regimens was about 80 mm^3 and therefore the results of both studies are not fully comparable. Nevertheless the results presented in this paper suggest that these regimens are not sufficient in obtaining a permanent tumor growth suppression since apparently tumor cell reactivation and/or repopulation takes place before the second treatment (Fig. 3). More recently, successful efforts are made to improve the 'debulking' of viable tumor load by shortening the interval between two subsequent sessions to 6 hours or less (Weiss 1990).

b/ HESW in a combined treatment modality.

Several attempts were made to improve the effectiveness of the HESW treatment and therefore combined with other systemic treatment modalities like chemotherapy (Randazzo 1989, Holmes 1990) and immunotherapy . Since we could not produce a complete destruction of even a small tumor with the serial exposure of shock waves every 24 hours, we studied the combination of these two treatment modalities that might have a potentiating antitumor effect (Oosterhof 1990b, 1991). In most studies it appeared that treatment with HESW and several chemotherapeutic drugs were more effective in establishing anti-proliferative effects.

The enhanced therapeutic efficacy of these combined treatment modalities in vivo can be explained in several ways.

First of all, since the effectiveness of chemotherapy depends to a great extent on tumor load, the HESW induced reduction of viable tumor cells may in fact explain the additive value of combination therapy. Secondly, the impaired metabolic state of the tumor cells may render them more susceptible to chemotherapy. In vitro studies show that HESW can cause a dose dependent direct cytotoxicity, impairment of the proliferative capacity and an increased drug cytotoxicity (Oosterhof 1989, Berens 1990). However, implications from these in vitro studies for the in vivo situation are difficult to make since the outcome of in vitro studies is dramatically influenced by micro-environmental conditions and it is not known to what extent HESW induced phenomena in vitro (like enhancement of direct cytotoxicity of chemotherapeutic drugs) can be extrapolated to the in vivo situation. Finally, since HESW have a major impact on tumor vasculature, changes in tumor perfusion can lead to altered local concentrations of drugs. In vivo studies on a rabbit liver did show a tremendous increase of local Methotrexate concentrations as a result of high frequency HESW exposure (Jones 1990). In addition, since HESW exposure induces an acidification of the tumor, drugs with a more selective activity at a lower pH become more effective. The observed effects can be considered also in the timing of application of HESW in other therapeutic modalities. For instance, HESW treatment could limit the effectiveness of subsequent radiotherapy since it (temporary) increases the hypoxic fraction of the tumor. Alternatively, the combination with hyperthermia could be synergistic because of enhanced thermal sensitivity, due to reduced perfusion (and therefore reduced convective heat dissipation) concomitant with acidosis which also reduces cellular thermal resistance. In this way a more selective heating of the malignant tissue could be established.

Overall, it becomes clear that HESW, generated outside a target location and focussed onto a limited area, can be used to alter tumor growth and response to therapy in vivo. This study shows that (^{31}P) MRS is a powerful method for longitudinal investigation of HESW induced anti tumor effects. It can provide information about causative mechanism(s) responsible for anti-tumor effects and give insight in the development of new, more effective HESW (combined) treatment modalities.

ACKNOWLEDGEMENTS

REFERENCES

Barany M., Glonek T. Methods Enzym., 85, 624-676, 1982.

Berens M.E., Welander C.E., Griffin A.S., McCullough D.L. Effect of acoustic shock waves on clonogenic growth and drug sensitivity of human tumor cells in vitro. J. Urol., 142, 1090, 1989.

Brümmer F., Brenner J., Bräuner T., Hülser D.F. Effects of shock waves on suspended and immobilized L1210 cells. Ultrasound Med. Biol., 15, 229, 1989.

Bräuner T., Brümmer F., Hülser D.F. Histopathology of shock wave treated tumor cell suspensions and multicell tumor spheroids. Ultrasound Med. Biol., 15, 451, 1989.

Coleman A.J., Saunders J.E. A survey of the acoustic output of commercial extracorporal shock wave lithotryptors. Ultrasound Med. Biol., 15, 213, 1989.

Corbett R.J.T., Nunnaly R.L., Giovanella B.C., Antich P.P. Characterization of the ^{31}P nuclear magnetic resonance spectrum from human melanoma tumors implanted in nude mice.
Cancer Res., 47, 5065, 1987.

Delius M., Jordan M., Liebich H.G., Brendel W. Biological effects of shock waves on the liver and gall-bladder wall of dogs - administration rate dependence. Ultrasound Med. Biol., 16, 459, 1990.

Evanochko W.T., Sakai T.T., Ng T.C., Krishna N.R., Kim H.D., Zeidler R.B., Ghanta V.K., Brockman R.W., Schiffer L.M., Braunschweiger P.G., Glickson J.D. NMR study of in vivo RIF-1 tumors; analysis of perchloric acid extracts and identification of ^{1}H, ^{31}P and ^{13}C resonances. Biochem. et Biophys. Acta, 805, 104, 1984.

Evelhoch J.L., Bissery M., Chabot G.G., Simpson N.E., McCoy C.L., Heilbrunn L.K., Corbett T.H. Flavone acetic acid induced modulation of murine tumor physiology monitored by in vivo nuclear magnetic resonance spectroscopy. Cancer Res., 48, 4749, 1988.

Gambihler S., Delius M., Brendel W. Biological effects of shock waves: cell disruption, viability, and proliferation of L1210 cells exposed to shock waves in vitro. Ultrasound Med. Biol., 16, 587, 1990.

Gibson S.L., Ceckler T.L., Bryant R.G., Hilf R. Effects of laser photodynamic therapy on tumor phosphate levels and pH assessed by ^{31}P-NMR spectroscopy. Cancer Biochem. Biophys., 10, 319, 1989.

Goetz A.E., Konigsberger R., Hammersen F., Conzen P., Delius M., Brendel W. Acute shock wave in duced effects on the microcirculation. In: Steiner R. (ed.) Laser Lithotripsy, Springer-Verlag Berlin.

Holmes R.P., Yeaman L.I., Li W., Hart L.J., Wallen C.A., Woodruff R.D., McCullough D.L. The combined effects of shock waves and cisplatin therapy on rat prostate tumors. J. Urol., 144, 159, 1990.

Jones B.J., McHale A.P., Butler M.R. Oncological applications for High Energy Shock Waves. Eur. Urol., 18, 285, 1990.

Laudone V.P., Morgan T.R., Huryk R.F., Heston W.D.W., Fair W.R. Cytotoxicity of high energy shock waves: methodologic considerations. J. Urol., 141, 965, 1989.

Lilly M.B., Katholi C.R., Ng T.C. Direct relationship between high energy phosphate content and bloodflow in thermally treated murine tumors. J. Natl. Cancer Inst., 75, 885, 1985.

Moon R.B., Richards J.H. Determination of intracellular pH by ^{31}P magnetic resonance. J. Biol. Chem., 248, 7276, 1973.

Ng T.C., Evanochko W.T., Hiramoto R.N., Ghanta V.K., Lilly M.B., Lawson A.J., Corbett T.H., Durant J.R., Glickson J.D. ^{31}P NMR Spectroscopy of in vivo tumors. J. Magn. Res., 49, 271, 1982.

Oosterhof G.O.N., Smits G.A.H.J., de Ruyter J.E., v. Moorselaar R.J.A., Schalken J.A., Debruyne F.M.J. In vitro effect of high energy shock waves in the Dunning PAT-2 rat prostatic cancer cell line. Urol. Res., 17, 13, 1989.

Oosterhof G.O.N., Smits G.A.H.J., de Ruyter J.E., Schalken, J.A., Debruyne F.M.J. In vivo effects of high energy shock waves on urological tumors, an evaluation of treatment modalities. J. Urol., 144, 785, 1990a.

Oosterhof G.O.N., Smits G.A.H.J., de Ruyter J.E., Schalken J.A., Debruyne F.M.J. Effects of high energy shock waves combined with biological response modifiers or adriamycin on a human kidney cancer xenograft. Urol. Res., 18, 419, 1990b.

Oosterhof G.O.N., Smits G.A.H.J., de Ruyter J.E., Schalken J.A., Debruyne F.M.J. Effects of high energy shock waves combined with biological response modifiers in different human kidney cancer xenografts. Ultrasound Med. Biol., 17, 391, 1991.

Pettegrew J.W. NMR, principles and applications to biomedical research. Springer-Verlag New York, 1990.

Randazzo R.F., Chaussy C.G., Fuchs G.J., Bhuta S.M., Lovrekovich H., de Kernion, J.B. The in vitro and in vivo effects of extracorporal shock waves on malignant cells. Urol. Res., 16, 419, 1988.

Russo P., Heston W.D.W., Fair W.R. Suppression of in vitro and in vivo tumor growth by high energy shock waves. Surg. Forum, 36, 645, 1985.

Russo P., Stephenson R.A., Mies C., Huryk R., Heston W.D.W., Melamed M.R., Fair, W.R. High energy shock waves suppress tumor growth in vitro and in vivo. J. Urol., 135, 626, 1986.

Russo P., Mies C., Huryk R., Heston, W.D.W., Fair W.R. Histopathologic and ultrastructural correlates of tumor growth suppression by high energy shock waves. J. Urol., 137, 338, 1987.

Seo Y., Murakami M., Watari H., Imai L.Y., Yoshizaki K., Nishikawa H., Morimoto, T. Intracellular pH determination by ^{31}P NMR technique. J. Biochem., 94, 729, 1983.

Shine N., Palladino M.A., Patton J.S., Deisseroth A., Karczmar G.S., Matson G.B., Weiner M.W. Early metabolic response to tumor necrosis factor in mouse sarcoma: a phosphorus-31 nuclear magnetic resonance study. Cancer Res., 49, 2123, 1989.

Smits G.A.H.J., Oosterhof G.O.N., de Ruyter J.E., Schalken J.A., Debruyne F.M.J. Cytotoxic effects of high energy shock waves in different in vitro models: influence of the experimental set-up. J. Urol., 145, 171, 1991.

Steen R.G., Response of solid tumors to chemotherapy monitored by in vivo ^{31}P nuclear magnetic resonance spectroscopy: a review. Cancer Res., 49, 4075, 1989.

Stubbs M., Rodrigues L.M., Griffiths J.R. Growth studies of subcutaneous rat tumors: comparison of ^{31}P-NMR spectroscopy, acid extracts and histology. Br. J. Cancer, 701, 1989.

Weiss N., Delius M., Gambihler S., Dirschedl P., Goetz A., Brendel W. Influence of the shock wave application mode on the growth of A-MEL 3 and SSK2 tumors in vivo. Ultrasound Med. Biol., 16, 595, 1990.

Wehrle J.P., Li S.J., Rajan S.S., Steen R.G., Glickson J.D. ^{31}P and ^{1}H NMR Spectroscopy of tumors in vivo; untreated growth and response to chemotherapy. Ann. NY. Acad. Sciences., 508, 200, 1987.

EFFECTS OF HIGH ENERGY SHOCK WAVES
ON TUMOR BLOOD FLOW AND METABOLISM;
^{31}P/^{1}H/^{2}H nuclear magnetic resonance spectroscopic studies.

Geert A.H.J. Smits[1], Erik B. Cornel[1], Erik v.d. Boogert[2], Gosse O.N. Oosterhof[1],
Frans M.J. Debruyne[1], Jack A. Schalken[1], Arend Heerschap[2]

Departments of Urology[1] and Radiology[2], University Hospital Nijmegen, The Netherlands

ABSTRACT

The effects of high energy shock waves (HESW) on tumor cell metabolism and tumor blood flow were studied in NU-1 kidney cancer xenografts by multi-nuclear ^{1}H/^{2}H/^{31}P magnetic resonance spectroscopy (MRS). The tumor xenografts were exposed to 800 HESW using an experimental electromagnetic shock wave emitter based on the Siemens Lithostar Plus which is used for clinical lithotripsy.

Exposure of the tumor to 800 HESW resulted in a dramatic, but temporary decrease of tumor blood flow (TBF) determined by the ^{2}H MRS monitoring of the ^{2}HO^{1}H wash-out after intra-tumoral injection. Concomitant monitoring of ^{1}H and ^{31}P MR spectra, enabled us to measure tumor pH and lactate concentration simultaneously. Treatment with HESW resulted in a transient acidification of the tumor. Also, in the same time interval the lactate concentration increased and subsequently decreased to pretreatment levels. In contrast, HESW sham treatment (i.e., administration of shock waves adjacent to the tumor) did not significantly influence TBF, tumor pH or lactate concentration, showing that the alterations of these parameters are caused by a interaction of HESW and tumor tissue.

This study supports the hypothesis that the vascular functionality of the tumor is the primary target of HESW. The effects of HESW cause a reduction in oxygen and nutrient supply of the tumor, leading to a decreased aerobic energy metabolism. These results provide an appropriate rational to design HESW combination therapy regimens, in which temporal impairment of vascular function and acidification of the tumor may be of importance in adjuvant therapy regimens.

INTRODUCTION

High energy shock waves (HESW) are of interest in the development of new experimental tumor treatment modalities. Generated extracorporally and focussed on a well-defined limited volume in the body, HESW can be used to influence tumor growth and response to therapy in vivo (Debus 1991, Delius 1989, Hoshi 1991, Randazzo 1988, Russo 1985). Studies using tumor models in animals have shown that, at a constant acoustic energy output, HESW have a dose dependent tumor growth suppressive effect, whereas treatment with a higher number of HESW or with the same number at different time intervals results in a more prolonged tumor growth inhibition (Oosterhof 1990a, Weiss 1990). In addition, combination with chemo- or cytokine-therapy resulted in more pronounced and even synergistic anti-tumor effects (Oosterhof 1990b, 1991).

Nuclear magnetic resonance spectroscopy (MRS) is a non-invasive technique to monitor changes in (tumor) cell metabolism in a longitudinal way and enables the evaluation of tumor therapies (Glickson 1990). Recently, using in vivo ^{31}P MRS, we have shown that the administration of HESW, focussed on the center of NU-1 human kidney cancer xenografts resulted in a significant, dose dependent, temporary reduction in high-energy phosphates, concomitant with an increase in inorganic phosphate (Pi) levels and a decrease in intra-cellular pH. These changes occurred immediately after HESW exposure and preceded the suppression of tumor growth (Smits 1991). These metabolic changes are qualitatively similar to those produced by ischemic inhibition of energy metabolism and suggest functional vascular changes following HESW exposure. Histological examinations in various tumor models clearly reveal structural abnormalities at a vascular level after HESW treatment and suggest that vascular damage in the tumor may be the primary cause in promoting tumor necrosis (Debus 1991, Hoshi 1991, Oosterhof 1990a). Thus, it is likely that the effects of HESW at the vascular level impair tumor cell metabolism.

In this study we tried to confirm the hypothesis that an important target of HESW involves the functionality of the vascular component of tumors. Tumor blood flow (TBF) and perfusion can be measured directly by ^{2}H NMR monitoring of ^{2}H$_2$O (D$_2$O) applied to the tumor (Evelhoch 1989, Kim 1988a,b). We have used this method to investigate the extent and duration of the effect of HESW on TBF. After intra-tumoral injection of D$_2$O as a freely diffusible tracer, the clearance of DOH was monitored. By using mathematical (multi-)compartment models, this technique

has shown to be a sensitive and reproducible method in the determination of TBF and perfusion (Evelhoch 1988, Kim 1988 a,b).

As a direct metabolic consequence of the reduced TBF and oxygenation an increase in anaerobic metabolism and lactate production is expected. Therefore, we also measured the tumor lactate concentrations with ^{1}H NMR before and after HESW treatment. In addition, the ^{1}H NMR measurements were combined with ^{31}P NMR measurements in order to investigate the relation between lactate levels and pH as a function of time.

MATERIALS and METHODS

Animals

Xenografts were transplanted in six to eight week old male BALB/c athymic mice (Bornholtgårt, Ry, Denmark). The mice were kept in groups of five in PAG type 2 cages covered with an iso cap (Iffa Credo, France) for sterile conditions. The mice were fed ad libitum with irradiated SRM-A MM food (Hope Farms, Woerden, The Netherlands) and drinking water was acidified with 0.7 ml concentrated HCl/l.

Tumors

The human renal cell carcinoma NU-1 xenograft was established in our laboratory by subcutaneous implantation of small tumor pieces derived from a tumor nephrectomy specimen. Histologically the tumor is characterized as sarcomatous (Oosterhof 1990b). For the HESW studies, tumors were implanted subcutaneously as trocar pieces at the hind limb. Passages 40-48 in vivo were used. The three dimensions of the tumor were determined with a precision sliding caliper by measuring the maximum diameter and the diameters perpendicular to it. The tumor volume was calculated by the equation (LxWxH) x ($\pi/6$). As in our earlier MRS experiments, tumors were allowed to grow to a volume of 250-300 mm^3 (mean 275 mm^3).

HESW treatment

The studies presented here were performed on a shock wave generator specially designed for experimental animal and in vitro studies. The principles of the experimental set-up, the way of administration of the shock waves, and the positioning of the tumors in the focal area were described earlier in detail (Oosterhof 1990a). In contrast to those experiments, we now used an electromagnetic HESW generator modified from the clinical available Lithostar *plus* (Siemens). With this experimental generator higher pressure amplitudes can be obtained in a smaller focal area. The physical principles and the definition of the parameters of its acoustic field were described elsewhere (Pfeiler 1989, Vergunst 1989). Standardization and control of the acoustic field was assured by pressure measurements performed before each experiment. Although the focus (defined by isobar lines representing 50% of the P_{max}) is somewhat smaller, the total acoustic energy is equivalent to that of the Lithostar and, assuming that the pressure profile and energy are the main determining factors, we compared the outcome of the experiments with our previous results. Tumors were treated with 800 HESW focussed centrally on the tumor or at 7 mm from the tumor (sham-treatment). Just before HESW exposure, mice were anaesthetized with ketamine hydrochloride (Ketalar, Parke-Davis) 100 mg/kg for a 15 minute period.

NMR Spectroscopy

In vivo NMR spectroscopy was performed on a 4.7 tesla Bruker WM-200 spectrometer as described previously (Smits 1991). The mice were anaesthetized by means of a gas flow of 1.5% enflurane in a O_2/N_2O mixture applied through a nosecone and the body temperature was maintained by a flow of humidified warm air. The tumors were exposed through a matched hole in a Faraday shield and positioned partly inside the radio-frequency (RF) coil to prevent any contribution of signals from surrounding tissue. The magnetic field homogeneity was optimized by using the ^{1}H NMR signal from tumor H_2O. Typical linewidths of this signal were 0.1 - 0.2 ppm. The animals were spectroscopically examined before and 4 to 6 times after administration of HESW.

^{2}H NMR.

The deuterium measurements were performed at a resonance frequency of 31 MHz, employing a home-built probe with a 1H / 2H double tunable three-turn solenoidal coil with an inner diameter of 13 mm. After optimizing the field homogeneity the RF probe was removed from the magnet and the tumors were injected outside the magnet with 10-20 μl PBS ^{2}H$_2$O solution at a single site (tumor center) or at three sites (concentric) using a micro-syringe. During this procedure the tumors remained in their original position in the RF coil. The probe was repositioned in the magnet and serial ^{2}H NMR measurements were started 90 seconds after injection.

Deuterium spectra were collected in 45 second time blocks with 64 scans/block using a 10 μs RF pulse, 2K data points and a spectral width of 5000 Hz.

^{1}H/^{31}P NMR.

Lactate detection by ^{1}H NMR and pH measurement by ^{31}P NMR were performed at 200 and 80 MHz respectively, employing a home-built ^{1}H / ^{31}P double tunable two-turn surface coil with an inner diameter of 10 mm.

The ^{1}H methyl signal of lactic acid has to be resolved from the co-resonating methyl signals of triglycerides from subcutaneous adipose tissue. For spectral editing of the methyl signal of lactate the spin-echo difference spectroscopy method was used (Hetherington 1985). The spin-echo RF pulse sequence was preceded by a CHESS sequence to reduce the H$_2$O signal (Haase 1985) and RF pre-pulses to reduce high flux signals (Bendall 1985, Shaka 1985). The prepulses and excitation pulse were all hard pulses (Bourgeois 1989). Further H$_2$O suppression was provided by the use of a 1-1 refocussing pulse (Hore 1983). Selective inversion of the methine (α) protons for lactate editing was achieved with a rotating-phase DANTE (Blondet 1987). In this way, on and off resonance inversion is realized by clock- and counter-clockwise phase rotation. During the experiment the RF carrier frequency was set at 3.75 ppm upfield from the water signal. The spin-echo time was 152 msec and the scan repetition time was 2.5 seconds. This way of lactate editing was found to be highly effective in the selection of the CH$_3$ signal of lactate from the dominating methylene proton signals of triglycerides. In all cases the reliability of the sequence to detect the lactate methyl protons was tested by shifting the DANTE excitation band away from the 4.1 ppm position of the α lactate proton.

To estimate the absolute concentration of lactate, a ^{1}H NMR spectrum without H$_2$O suppression was also recorded with the same spin-echo sequence to obtain the

tissue H_2O resonance. To avoid interference of H_2O spin relaxation with the quantification of lactate a short echotime (1 msec) and a long scan repetition time (7 seconds) were chosen.

[31]P spectra were obtained as previously described (Smits 1991) with a composite 90° pulse with a nominal 90° pulse at about 1 mm from the coil center. The pulse repetition time was 3.5 seconds and the spectral width was 5000 Hz acquired with 4K data points. Typically 256 or 512 scans were acquired.

Data Analysis

The free induction decays (FID) were analyzed on an Aspect 3000 computer using the standard Bruker software. If necessary, the convolution difference method (for removing broad spectral components) and multiplication of the averaged FID by an exponential function (for improving the signal to noise ratio) were carried out.

DOH wash-out and TBF

After Fourier transformation of the free induction decays, the deuterium resonances were quantified by interactive computerized integration over the spectral peaks considered (all standard Bruker software). The deuterium resonance integrals were plotted as a function of time.

Tumor blood flow was determined using compartment kinetic models as described by Kim and Ackerman (1988 a,b). In all cases the tumor deuterium residue wash-out could accurately be described by:

$Q(t) = a.e^{-\alpha t} + b.e^{-\beta t}$ (and $\alpha > \beta > 0$).

This equation describes a flow model which represents (non-communicating) fast and slow flow compartments in the tumor, where $Q(t)$ is the quantified deuterium residue at time t, and the half-life times of the tracer in the fast and slow flow compartment are $Tf = \frac{ln2}{\alpha}$ and $Ts = \frac{ln2}{\beta}$ respectively.

The (volume) fractions of the fast and slow components can be expressed as $\frac{a}{a+b}$ and $\frac{b}{a+b}$.

The initial half life (t = 0) is defined by $\frac{ln2}{\tau}$ where τ is the weighed average ($\frac{a\alpha+b\beta}{a+b}$) of α and β.

The formula TBF = 100 x lambda x τ is then an estimate of the initial tumor blood flow (in units of $\frac{ml}{100g\times min}$).

111

Here lambda is the tumor-to-blood partition coefficient (ratio of the water weight of a unit mass of tumor to the water weight of a volume of blood) which was determined by measuring wet and dry weights of tumor and blood. Dry weights were achieved by drying in an oven at a temperature of 90°C. Lambda was calculated to be 0.906 ± 0.019 (in units of ml/g (n=5). Per animal, the half lifes were calculated using (nonlinear) least squares regression.

Tumor lactate quantification

In order to estimate the absolute lactate concentration in the tumor, the resonance intensity of the lactate signal was related to the intensity of the water resonance.

The lactate concentration, expressed per tumor volume, was calculated by the following formula:

[lactate] = IF x $e^{te/T2lact}$ x F_c x $^2/_3$ x {RV_l/RV_w} x [H_2O].

T_{2lact} is the spin-spin relaxation time of the methyl proton spins of lactate; t_e is the echo time. The lactate signal is recorded with a spin echo sequence having a t_e of 152 msec and hence T_2 weighted. Corrections can be made if the T_2 value is known. T_2 relaxation time measurements of the methyl signal of lactate which is obscured by triglyceride signals is not trivial. We used a T_2 value of 150 msec which is close to the values as determined for the methyl signal of lactate in the rat brain at 4.7 T (Williams 1988).

The inversion factor (IF) was set at 0.8. In control experiments with lactate solutions we observed that complete inversion of the methyl resonance of lactate by the application of the DANTE sequence could not be achieved. About 80% of the original lactate signal intensity was recovered after editing. This result is similar to experiments of Hanstock (1987) who also used a DANTE sequence for inversion with a surface coil.

F_c is the excitation profile correction due to the 1-1 pulse which is necessary because the RF carrier was not exactly at the resonance position of the methyl protons of lactate. The factor $^2/_3$ corrects for the fact that water has 2 protons and the lactate methyl group 3. RV_l and RV_w are the resonance integral values of the methyl group of lactate and water respectively.

[H_2O] is the concentration of water per tumor volume.

<u>Phosphate energy metabolism and pH.</u>

The assignments of the resonances and the calculation of the tissue pH from the inorganic phosphate (Pi) signal chemical shift in the ^{31}P NMR spectra were performed as described before (Smits 1991).

<u>Statistics</u>

Due to the nonnormality of the statistical distribution, Wilcoxon's test was used to compare the DOH wash-out parameters in both groups. For the same reason the lactate concentration and pH data were analyzed using the Koziol test.

Statistical significance was set at p < 0.05.

RESULTS

Effects of HESW on TBF

To determine the reproducibility of the DOH wash-out method after intra-tumoral injection of the tracer, D_2O was injected into the tumor at subsequent time intervals (3 hours). We observed no difference in DOH wash-out curves (data not shown). The DOH profiles were best fitted using the expression describing two components in the wash-out. In this model a fast flow and slow flow component are characterized by their half life times (expressed as Tf and Ts of the tracer) and their (volume) fraction. In each individual tumor a similar wash-out was found either using single or multiple site injections. In the following experiments DOH was injected at three sites in the tumor.

Figure 1 shows representative data of two individual tumors, obtained before and after treatment with 800 HESW focussed adjacent to the tumor (sham) or central on the tumor (treated). No significant differences in DOH decay (fitted curves) before and after sham-treatment were detected (figure 1a). In contrast, after the application of 800 HESW at the center of the tumor, a significant decrease in wash-out was observed during the first 24 hours after treatment. After 48 hours the wash-out curves showed pretreatment values (figure 1b).

Fig. 1a

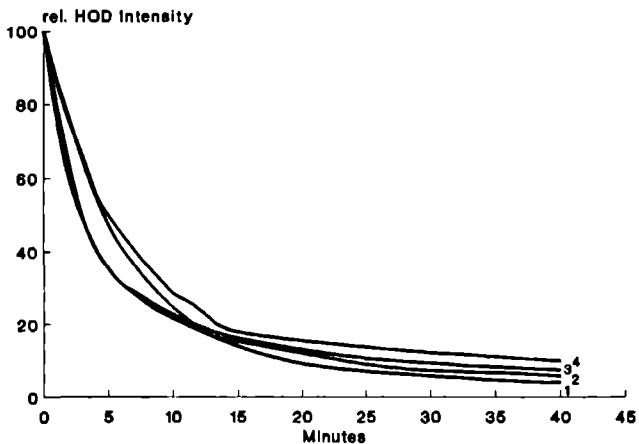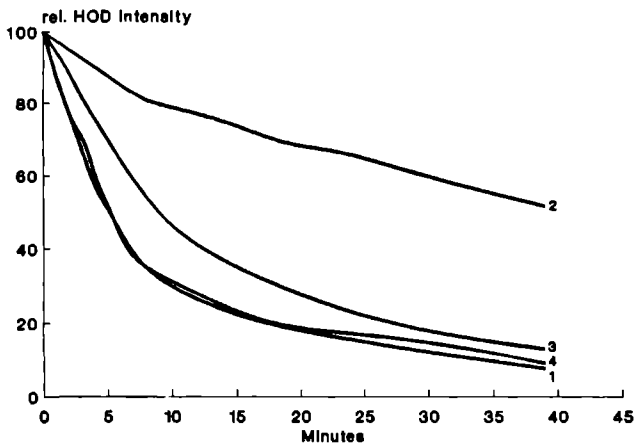rel. HOD Intensity

Fig. 1b

rel. HOD Intensity

Fig. 1

Representative figures of relative HOD intensity in time detected by ^{2}H NMR spectroscopy after intra-tumoral injection of an isotonic D_2O solution before (1), as well as at two (2), twenty-four (3), and forty-eight (4) hours after HESW exposure adjacent to the tumor (fig. 1a, sham-treatment) or central on the tumor (fig. 1b, treated).

Figure 2 shows the mean calculated tumor blood flow (ml/100g.min) before and after exposure (n=5 for each group). The mean pretreatment TBF value of the sham and of the treated group were slightly different but this was not significant (Wilcoxon; p=0.89).

Treatment with 800 HESW adjacent to the tumor resulted in an increase in mean TBF. However, these changes were not significant. After shock wave exposure to the center of the tumor, the mean TBF decreased with approximately 75% after 2 hours and afterwards increased to 50% after 24 hours as compared to the mean pretreatment TBF. As a result, TBF levels in the treatment group were significant lower than in the control group (Wilcoxon; p<0.005 and p<0.05 respectively). In order to detect a possible differential impact on the fast and slow component of the DOH wash-out we evaluated the bi-exponential wash-out in more detail.
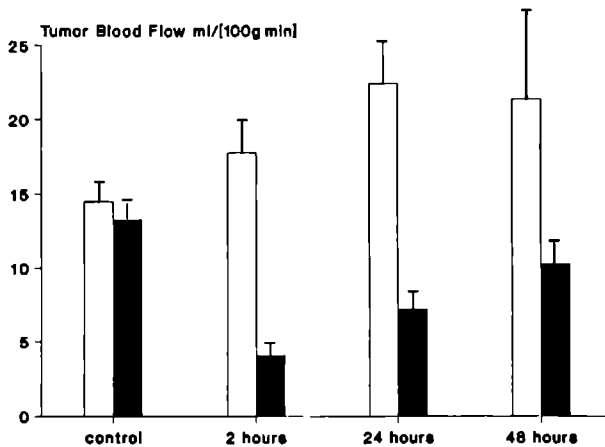
Fig. 2:
NU-1 kidney cancer xenograft tumor blood flow (in units of $ml/100gxmin$) before (control) and after treatment with 800 HESW (white bars: sham-treated group; black bars: treated group). D_2O was injected at three sites intra-tumorally and TBF was calculated from the fitted bi-exponential wash-out curves. Values are mean ± standard error of the mean (each group n=5).

In Table 1 the half life times of the tracer in the fast and slow compartment (Tf respectively Ts) as well as the volume fraction of the fast component before and two hours after treatment are presented. Two hours after exposure to 800 HESW a significant higher Ts and smaller volume fraction of the fast flow component

(Wilcoxon; p=0.01 and 0.02 respectively) were seen. The remaining fast fraction showed no significant differences in Tf. Similar analysis of these parameters for the subsequent period (10 hours or more) revealed no clear patterns.

Table 1: Median half life times of the tracer (DOH) in the fast and slow compartment (Tf resp. Ts) as well as the volume fraction of the fast component before and two hours after treatment

| | PRE-TREATMENT | | | +2 HRS | | |
	Tf	Ts	fraction	Tf	Ts	fraction
Sham (n=5)	4.1	45	.86	3.9	21	.80
Treated (n=5)	3.4	33	.74	2.7	52	.09

Effects of HESW on tumor lactate concentration and pH

The absolute lactate concentration in tumor xenografts has not yet been estimated by NMR in vivo. From 8 independent measurements we have calculated an average lactate concentration of 7.1 ± 1.9 mM (pH ≥ 7.0, results not shown). This value is in agreement with the lactate concentration as measured in another tumor model (Maxwell 1988). From two in vitro NMR measurements of PCA extracts of the tumors we estimated the lactate concentration to be 5.4 and 7.8 mM. These observations suggest that our in vivo determination of lactate concentration provides a good approximation for the lactate concentration despite the necessary assumption made for the T_2 of lactate methyl protn spins in the tumor. To rule out initial differences between the sham and treated group, the pH and lactate concentration were determined simultaneously by combining $^{31}P/^1H$ MRS in both groups (fig. 3). Using Wilcoxon's test, no significant differences between the HESW treated or sham treated groups were observed. (each group n=5; p(pH)=0.86; p(lactate)=0.92).
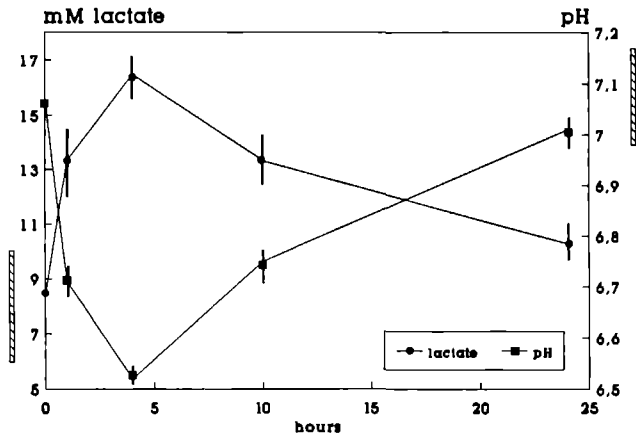
Fig. 3:
Changes in lactate and pH, in the NU-1 kidney cancer xenograft after treatment with 800 HESW, focussed on the center of the tumor. Values are mean ± standard error of the mean, (n=5). The dashed vertical bars represent the range of values after the sham-treatment procedure (n=5).

A maximal increase in the average lactate concentration from 8.8 mM (range 5.9 to 11.5) to 16.5 mM (range 14.9-17.9) was observed 4 hours post treatment. The lactate concentration decreased to pretreatment levels within the following 48 hours. The changes in pH showed a similar, but inverse, temporal pattern. After 4 hours the mean pH was decreased from 7.06 (range 7.12 to 6.97) to 6.52 (range 6.45 to 6.60). Thereafter the pH increased to pretreatment values in a similar time span as the lactate concentration. The Koziol test revealed a significant difference in the temporal pattern between treatment and sham-treatment for the lactate concentration as well as the pH (both $p < 0.001$).

DISCUSSION

Although HESW have been successfully used as an anti-tumor treatment modality in different animal tumor models, the mode of action of HESW is still largely unknown. Recently, in vivo ^{31}P NMR spectroscopy in the NU-1 kidney xenograft showed drastic alterations in tumor cell metabolism, and a temporary tumor growth inhibition after HESW exposure (Smits 1991). Since HESW, generated extra-corporally, can be precisely focussed on a limited area in the body, these findings revealed a new potential application for this form of acoustic energy. At present it is unclear whether the metabolic changes observed are a direct or an indirect effect of the shock waves. The metabolic changes seem to be related to the induction of a temporary ischemia, due to an impaired tumor blood flow and perfusion.

D_2O efflux measurements by ^{2}H NMR can be used to evaluate TBF and perfusion in response to therapeutic interventions (Evelhoch 1988, Hwang 1991, Okunieff 1991).

In our experiments, a bi-exponential tracer residue decay was observed after applying DOH intra-tumorally in non-treated NU-1 tumors. The tracer wash-out was best described by a mathematical model using a fast and slow flow component of DOH decay within the tumor. This wash-out pattern was not influenced significantly by the number of D_2O injection sites. Repeating the experiment after 5 hours also revealed similar DOH wash-outs. Our results are in agreement with similar experiments in the RIF-1 tumor (Kim 1988b) and show that the injury by the micro syringe had no significant effect on DOH wash-out pattern in the NU-1 xenograft. The bi-exponential clearance kinetics are likely due to TBF heterogeneity (Larcombe McDouall 1990).

The studies presented here show a pronounced effect of HESW on the TBF in the NU-1 human kidney cancer xenograft. When the HESW were focussed on the tumors, a mean reduction in TBF of 75% of the initial TBF two hours after HESW treatment was observed. Exposure to 800 HESW focused adjacently to the tumor did not influence TBF significantly. The reduction in TBF was temporary and the DOH wash-out increased to non treated profiles. These results demonstrate that a reduction in TBF by HESW is only effectuated if the tumor (or at least a major part) is subjected to the high pressure focal area.

In this study the major effect was seen in the fast flow component suggesting that the most viable part of the tumor with the highest TBF is most sensitive towards the shock waves.

How can these effects of HESW on TBF be explained? Recent studies indicate that cavitations, presumably associated with the tensile pressure, have a damaging effect at the vascular level (Delius 1990, Prat 1991b). In addition, microscopic studies in the NU-1 xenograft as well as in several other animal tumor models have shown vascular (capillar) disruption, extravasation of erythrocytes, and the formation of thrombosis and necrosis when the tumors were placed in the focal beam with high pressures. (Oosterhof 1990a,b, Debus 1991, Hoshi 1991). Thus, the impact of HESW on functional vascularization (TBF) most likely results from the generation of cavitations which subsequently act on the tumor vascular component (damaging and or activation of endothelial cells). Whether more gas holding nuclei are present and thus cavitations are induced to a greater extent in the well perfused (fast compartment) parts of the tumor is speculative. However this might explain the preferential effects of HESW on the fast flow component and the reduction in volume fraction of the fast component.

The ^{1}H NMR spectroscopy studies showed a temporary increase in lactate concentrations. From this observation one can conclude that the reduction in TBF results in cellular hypoxia and that consequently anaerobic glycolysis becomes the main cellular energy source. Since the TBF is reduced, the increased lactate concentration could also be explained by a disturbed outflow of lactate. However, the concomitant monitoring of ^{31}P NMR revealed a synchronous temporary change in tissue pH (i.e., *intra*-cellular tumor pH), indicating that the acidification is due to an enhanced lactic acid synthesis (Griffiths 1991, Maxwell 1988). The outcome of the ^{31}P/^{1}H NMR studies supports the hypothesis that the HESW induced tumor growth suppression is mediated by an impact on the functionality of the vascular component of the tumor.

Quantitative measurement of TBF and perfusion may not only contribute to the knowledge of HESW induced changes in vascular functionality, moreover this may provide the rational for the use of HESW in a combined treatment setting, i.e., combining HESW with chemo- or immunotherapy.

Until now, as a result of the lack of knowledge on the mode of action, treatment schedules have been determined empirically. The findings here presented can provide a better rational for developing more effective combined treatment modalities, e.g., the use of HESW adjuvant to systemic drugs that have an increased effect in an acid environment, or that block glycolysis. In addition to a diminished drug outflow, a decreased TBF and perfusion may also enhance diffusion processes and thus result in an enhanced drug penetration in the tumor. Due to the substantial destruction of the tumorvascularity it is possible that the interstitial pressures which can be high in tumors (Roh 1991) are reduced considerably and thus result in an increased convection i.e bulk transfer of fluid (containing exogenous molecules) in the interstitial compartment. Further studies using combined Deuterium imaging and interstitial pressure measurement techniques may give more insight in this phenomenon. The extent of modulation of local TBF and perfusion provoked by HESW treatment, with subsequent changes in metabolism, will be of importance in designing adjuvant (local or systemic) anti-cancer therapies.

ACKNOWLEDGEMENTS

REFERENCES

Bendall M.R., Pegg D.T. Magn. Reson. Med., 2, 91, 1985.

Blondet P., Albrand J.D., von Kienlin M., Decorps M. Use of rotating-phase DANTE pulses for in vivo proton NMR spectral editing with a single irradiation facility. J. Magn. Reson., 71, 342, 1987.

Bourgeois D., Decorps M., Remy C., Benabid A.L. High-flux signals and spatial localization in high-resolution ^1H spectroscopy with surface coils. Magn. Res. Med., 11, 275, 1989.

Debus J., Peschke P., Hahn E.W., Lorenz W.J., Lorenz A., Ifflander H., Zabel H.J., van Kaick G., Pfeiler M.: Treatment of the Dunning tumor R3327-AT1 with pulsed high energy ultrasound shock waves (PHEUS): growth delay and histomorphologic changes. J. Urol., 146, 1143, 1991.

Delius M., Weiss N., Gambihler S., Goetz A., Brendel W. Tumor therapy with shock waves requires modified lithotripter shock waves. Naturwissenschaften, 76, 573, 1989.

Delius M., Denk R., Berding C., Liebich H-G., Jordan M., Brendel W. Biological effects of shock waves: cavitation by shock waves in piglet liver. Ultrasound Med. Biol., 16, 467, 1990.

Evelhoch J.L., Bissery M-C., Chabot G.G., Simpson N.E., McCoy C.L., Heilbrun L. K., Corbett T.H. Flavone acetic acid (NSC 347512)-induced modulation of murine tumor physiology monitored by in vivo nuclear magnetic resonance spectroscopy. Cancer Res., 48, 4749, 1988.

Evelhoch J.L., McCoy C.L., Giri B.P. A method for direct in vivo measurements of drug concentration from a single ^2H NMR spectrum. Magn. Res. Med., 9, 402, 1989.

Glickson J.D., Wehrle J.P., Rajan S.S., Li S.J., Steen R.G. NMR spectroscopy of tumors. In: Pettegrew J.W. (ed.) NMR, principles and applications to biomedical research, Springer-Verlag, New York, 1990.

Griffiths J.R. Are cancer cells acidic? Br. J. Cancer, 64, 425, 1991.

Haase A., Frahm J., Haenicke W., Matthei D. Phys. Med. Biol., 30, 341, 1985.

Hanstock C.C., Bendall M.R., Hetherington H.P., Boisvert D.P., Allen P.S. Localized in vivo proton spectroscopy using depth pulse spectral editing. J. Magn. Res., 71, 349, 1987.

Hetherington H.P., Avison M.J., Schulman R.G. ^1H homonuclear editing of rat brain using semiselective pulses. Proc. Natl. Acad. Sci. USA, 82, 3115, 1985.

Hore P.J. J. Magn. Res., 54, 539, 1983.

Hoshi S., Orikasa S., Kuwahara M., Suzuki K., Yoshikawa K., Saitoh S., Ohyama C., Satoh M., Kawamura S., Nose M. High energy under water shock wave treatment on implanted urinary bladder cancer in rabbits. J. Urol., 146, 439, 1991.

Hwang Y., Kim S-G., Evelhoch J.L., Seyedsadr M., Ackerman J.J.H. Modulation of murine radiation-induced fibrosarcoma-1 tumor metabolism and blood flow in situ via glucose and mannitol administration monitored by ^{31}P and ^2H nuclear magnetic resonance spectroscopy. Cancer Res., 51, 3108, 1991.

Kim S-G., Ackerman J.J.H. Multicompartment analysis of blood flow and tissue perfusion employing D_2O as a freely diffussible tracer: a novel deuterium NMR technique demonstrated via application with murine RIF-1 tumors. Magn. Reson. Med., 8, 410, 1988a.

Kim S-G., Ackerman J.J.H. Quantitative determination of tumor blood flow and perfusion via deuterium nuclear magnetic resonance spectroscopy in mice. Cancer Res., 48, 3449, 1988b.

Larcombe McDouall J.B., Evelhoch J.L. Deuterium nuclear magnetic resonance imaging of tracer distribution in D_2O clearance measurements of tumor blood flow in mice. Cancer Res., 50, 363, 1990.

Maxwell R.J., Prysor-Jones R.A., Jenkins J.S., Griffiths J.R. Vasoactive intestinal peptide stimulates glycolysis in pituitary tumours. ^{1}H NMR detection of lactate *in vivo*. Biochim. et Biophys. Acta., 968, 86, 1988.

Okunieff P., Dols S., Lee J., Singer S., Vaupel P., Neuringer L.J., Beshah K. Angiogenesis determines blood flow, metabolism, growth rate, and ATPase kinetics of tumors growing in an irradiated bed: [31]P and ^{2}H nuclear magnetic resonance studies. Cancer Res., 51, 3289, 1991.

Oosterhof G.O.N., Smits G.A.H.J., de Ruyter J.E., Schalken J.A. Debruyne F.M.J. In vivo effects of high energy shock waves on urological tumors, an evaluation of treatment modalities. J. Urol., 144, 785, 1990a.

Oosterhof G.O.N., Smits G.A.H.J., de Ruyter J.E., Schalken J.A. Debruyne F.M.J. Effects of high energy shock waves combined with biological response modifiers or adriamycin on a human kidney cancer xenograft. Urol. Res., 18, 419, 1990b.

Oosterhof G.O.N., Smits G.A.H.J., de Ruyter J.E., Schalken J.A., Debruyne F.M.J. Effects of high energy shock waves combined with biological response modifiers in different human kidney cancer xenografts. Ultrasound in Med. & Biol., 17, 391, 1991.

Pfeiler M., Matura E., Iffländer H., Seyler G. Lithotripsy of renal and biliary calculi: physics, technology, and medical-technical applications. Electromedica, 57, 52, 1989.

Prat F., Ponchon T., Berger F., Chapelon Y., Gagnon P., Cathignol D. Hepatic lesions in the rabbit induced by acoustic cavitation. Gastroenterology, 100, 1345, 1991.

Randazzo R.F., Chaussy C.G., Fuchs G.J., Bhutta S.M., Lovrekovich H., de Kernion J.B. The in vitro and in vivo effects of extracorporeal shock waves on malignant cells. Urol. Res., 16, 419, 1988.

Roh H.D., Boucher Y., Kalnichi S., Buchsbaum R., Bloomer W.D., Jain R.K. Interstitial hypertension in carcinoma of uterine cervix iin patients: possible correlation with tumor oxygenation and radiation response. Cancer Res., 51, 6695, 1991.

Russo P., Heston W.D.W., Fair W.R. Suppression of in vitro and in vivo tumor growth by high energy shock waves. Surg. Forum, 36, 645, 1985.

Shaka A.J., Freeman R. J. Magn. Reson., 64, 145, 1985.

Smits G.A.H.J., Heerschap A., Oosterhof G.O.N., Ruys J.H.J., Hilbers C.W., Debruyne F.M.J., Schalken J.A. Early metabolic response to high energy shock waves in a human tumor kidney xenograft monitored by ^{31}P magnetic resonance spectroscopy. Ultrasound in Med. & Biol., 17, 791, 1991.

Vergunst H., Terpstra O.T., Schröder F.H., Matura E. Assesment of shock wave pressure profiles in vitro: clinical implications. J. Lithotripsy & Stone Dis., 1, 289, 1989.

Weiss N., Delius M., Gambihler S., Dirschedl P., Goetz A., Brendel W. Influence of the shock wave application mode on the growth of A-MEL3 and SSK2 tumors in vivo. Ultrasound in Med. & Biol., 16, 595, 1990.

Williams G.R., Proctor E., Allen K., Gadian D.G., Lockard H.A. Quantitative estimation of lactate in the brain by ^{1}H NMR. Magn. Res. Med., 7, 425, 1988.

Chapter 7

SUMMARY AND CONLUSIONS
PERSPECTIVES

SUMMARY AND CONCLUSIONS

This thesis describes experimental in vitro and in vivo studies with the aim to get insight in (1), the factors influencing the effects of high energy shock waves HESW on (tumor-)cells, (2), the use and efficacy of this form of acoustic energy as an anti-tumor treatment modality, either alone or in combination with other local or systemic therapies, and (3), the way HESW affect tumor growth in vivo, with the final objective to come to an appropriate rational for HESW tumor treatment schedules.

Chapter 1 gives a general description of the physical characteristics of HESW and the technical aspects of the various shock waves generators. Acoustic waves can be generated and focussed in such a way that shock waves are concentrated in a relatively small volume. These HESW are used clinically for extracorporeal shock wave lithotripsy. It has become evident that HESW also affect soft tissues considerably. In the past five years, an increasing number of papers dealing with the biological (side-)effects associated with HESW, were published. The pathophysiologic effects of shock waves on cells and tissue are summarized, and some aspects of the possible mode of action of HESW are described.

Chapter 2 describes the influence of the experimental set-up on the results of in vitro studies. A dose-dependent reduction in viability was observed when various (tumor-)cells were exposed in a suspension or as a pellet on the bottom of the test tube. The sensitivity for the shock waves was not the same in these treatment models. Furthermore, a differential sensitivity in various cell types was found. Interestingly, shock waves had no effect when the cells were fixed and immobilized by gelatine, or when the pellet was placed on a bottom layer of gelatine. These results indicate that damage to cells in vitro depends on the way they are exposed to HESW. The extent of cytotoxicity in vitro apparently results from factors associated with the micro-environment. In this respect, the induction of cavitations can play an important role. The results of this study may be of use to understand the way shock waves act in vivo on (tumor-)cells.

In **Chapter 3** the effects of high energy shock waves alone or in combination with biological response modifiers (interferon-α and/or tumor necrosis factor-α) on the growth of five human kidney cancer xenografts were examined. Synergistic effects in tumor suppression were observed between HESW and TNF-α. A differential sensitivity of the tumors for this combined treatment became evident. Tumors wich

were well vascularized appeared to be most sensitive for this combination.

Extrapolation of the outcome of in vitro studies for the in vivo treatment is difficult (chapter 2). Moreover, HESW can exert their cytotoxic effects indirectly, e.g., by damaging the (tumor) vasculature. For this reason we used in the following studies in vivo nuclear magnetic resonance spectroscopy (MRS) in order to gain information on HESW induced (biological) effects at a cellular level in vivo. This is a non-invasive technique that enables longitudinal evaluation of metabolic changes, and has therefore a great potential to study of progressively changes that accompany (tumor) response to different kinds of therapies.

Using the in vivo ^{31}P MRS we were able to measure changes in the high energy phosphate metabolism and pH simultaneously in HESW-exposed skeletal muscle (calf muscles) of nude mice. In addition, extensive light- and electron- microscopic studies were carried out. In this way, we were able to examine functional and structural effects of HESW in time, and gain information on HESW induced cell-degeneration, cell-death and cell-regeneration in vivo. The observed effects in skeletal muscle (described in Chapter 4) represent a spectrum of (sub)-cellular alterations confined to the focal area of the shock wave generator. Several (ultra)-structural abnormalities were found, e.g., dilatation and disruption of capillaries and damage of peripheral nerves. By defining different stages of myofiber degeneration, it appeared that this process, consisting of disorganization of myofilaments and structural changes in sarcoplasmic organelles, was progressive in time, and reached its maximum about 24 hours after HESW exposure. In addition, it was shown that the transient alterations in inorganic phosphate and acidification could be interpreted as a metabolic event in the (non-synchronous) process of degenerating myofibers. The myofiber degeneration could only partially be explained by HESW induced ischemia, and most likely additional cytotoxic events (at a sub-cellular and (macro)molecular level) occur after HESW treatment. The (ultra-) structural changes were not evident in all myofibers, i.e., between affected degenerating fibers, unaffected intact fibers were seen, suggesting a cellular differential sensitivity for HESW. The degeneration of the pre-existing myofibers was predominantly confined to type 1 fibers and was followed by a regeneration of the muscle tissue with proliferation of myoblasts. A notable amount of myotubes still showed vacuolization. We concluded that in vivo HESW exposure of skeletal muscle tissue results in a degeneration of myofibers, and that ^{31}P MRS is able to monitor accompanying metabolic alterations of the degenerating myofibers.

In order to get more insight in the experimental HESW treatment modalities on in vivo growing tumors, we examined the short term effects of HESW on tumor cell metabolism in vivo, employing ^{31}P MRS. This technique gives information about the metabolic changes that occur in viable tumor cells that may be the target for HESW therapy. The results are described in Chapter 5. HESW treatment of NU-1 human kidney tumor xenografts resulted in a transient dose dependent reduction in concentration of energy rich molecules like phosphocreatine and nucleoside triphosphates, concomitant with a temporal increase of Pi and decrease in pH (i.e. intra-cellular pH) in the tumor. These changes were qualitatively similar to those produced by ischemic inhibition of energy metabolism, and correlated with early histological features like vascular disruption, stasis within capillaries and focal thrombosis. It was concluded that the metabolic inactivation and acidification after HESW treatment is most likely the result of impairment of oxygenation, presumably by a decreased tumor blood flow.

Chapter 6 describes the effects of HESW exposure on tumor blood flow (TBF) and metabolism using multinuclear ^{1}H/^{2}H/^{31}P MRS. Using this technique, we were able to confirm the results of the experiments described in chapter 5. By the ^{2}H MRS monitoring of D$_2$O washout, we could demonstrate that a dramatic, but temporary, reduction in TBF is only seen if the tumor (or at least a major part) is subjected to the high pressure focal area. In addition, the concomitant monitoring of ^{1}H and ^{31}P MRS showed a transient acidification of the tumor and, in the same time interval, an increase in the lactate concentration with a subsequent decrease to pretreatment levels. These studies supported the hypothesis that the vascular functionality of the tumor is the primary target of HESW, i.e., HESW induce the reduction in oxygen and nutrient supply of the tumor, causing a decline in aerobic energy metabolism. It was suggested that the impact of HESW on TBF most likely results from the generation of cavitations with subsequent damage or activation of endothelial cells of the tumor vessels.

In general, from chapter 5 and 6 it was concluded that NMR spectroscopy is a powerful tool to study HESW induced effects on in vivo growing tumors, and that the outcome of these studies provide a logic rational to design HESW (combination) therapy regimens.

We do not know whether high energy shock waves will ever become clinically applicable in (urological) oncology.

In the past three years, hopeful experimental results in animal studies have been published, showing effective tumor growth suppression by HESW application. In these studies, the use of HESW appeared to be of more benefit when used in combination with a local or systemic therapy. At present, no evidence of a HESW induced tumor cell resistance to an additional series of shock waves or adjuvant (systemic or local) treatment has been shown.

Despite these favorable properties of HESW, it is still to early to consider clinical application in oncological patients. Many challenging questions remain to be answered, for instance whether HESW exposure of tumors may result in an induction or enhancement of metastases. Also, the anti-tumor effects of HESW treatments are still sub-optimal and need to be improved. In the first place, this can be achieved by changing factors related to the physical properties of the shock waves. Further studies on shock wave tumor therapy could use more effective shock waves (different wave forms than those generated by current lithotriptors). Secondly, improvement could be obtained by making the tumor tissue more susceptible for the shock waves. Thirdly, it is likely that more effective (combined) treatment strategies and schedules can be developed.

Physical properties of HESW

Recent studies revealed that the in vitro mechanisms of cytotoxicity differ between electrohydraulic and electromagnetic shock waves (Smith 1992). Since the pressure profile of HESW, as measured in the center of the focal area, is distinct concerning its physical parameters like $P_{max/min}$, t_w, etc., these investigations suggest that cytotoxicity is related to specific physical properties of the HESW. Although lacking appropriate pressure measurements, it has been shown that a more effective tumor treatment requires the use of modified shock waves (Delius 1989). Own observations in the NU-1 kidney cancer xenograft revealed that, when using HESW with a higher energy density, i.e., higher P_{max} (and at the same time shorter t_r), an increased tumor suppressive effect became evident.

It has become evident that the bio-effects of HESW are related to the occurrence of cavitations in the focal area (chapter 1 and 2). Tissue damage during shock wave lithotripsy is presumably secondary to cavitation phenomena involving the collapse of gas bubbles (in fluid). In order to increase the impact of HESW it seems logic to increase the number of cavitation nuclei at the target. Recently it has been shown that intravascular infusion of gas micro bubbles into the path of a shock wave generator dramatically enhances tissue damage (Prat 1991). This technique could be potentially useful in the treatment of tumors.

Development of more effective treatment strategies

From our studies (Oosterhof 1990, chapter 3) and those of others (Weiss 1990), it appeared that, by repeating HESW treatments, a more successful tumor growth suppression could be obtained. Shortening the interval between subsequent HESW treatments leads to a more effective tumor growth suppression. In addition, multi-focal exposure of the tumor, i.e., fractionated exposure of the tumor at several places, leads to enhanced anti-tumor effects. As is the case for the pressure profile, the optimal dose or interval between the exposures still need to be defined.

Several attempts were made to improve the effectivity of the HESW treatment, by combining it with other systemic therapies, like chemotherapy or immunotherapy.

Using tumor necrosis factor alfa (TNFα), we were able to provoke synergistic anti-tumor effects in human kidney cancer xenografts that were well vascularized. This may be explained by the fact that both TNFα and HESW act on the microvasculature. TNFα is known to induce an ischemic time period in a tumor similar to HESW. Also, TNFα induces specific morphological and functional alterations in the endothelial cells, described as endothelial cell activation. Microvascular endothelium is a significant target for biological response modifiers such as interferons, TNFα and interleukins. Besides direct cytotoxic effects, indirect immune-mediated anti-tumor effects and enhancement of procoagulant activity, TNFα is known to induce the release of vaso-active substances like nitric oxide, which mediates a vasodilatation and vascular leakage (Kilbourn, 1990). The latter might result in an altered microvascularity that is more susceptible for HESW.

Jones et al. showed that vascular disruption in vivo can be used to produce a localization of parenterally administered autologous erythrocytes loaded with methotrexate (Jones 1990). Using this technique in the NU-1 kidney tumor xenograft, in pilot studies we observed a tremendous tumor growth suppression when HESW were combined with intravenously administration of methotrexate loaded erythrocytes, whereas the administration of loaded erythrocytes alone resulted in no tumor growth suppression at all.

It is known that cavitation processes can induce a release of incorporated substances (Kost 1989). HESW treatment strategies using carriers (liposomes, proteinaceous bubbles or autologous erythrocytes) containing substances with anti-tumor activity to be trapped and released only at the target location, may induce local effects with minimal systemic toxicity.

In conclusion, it has become clear that HESW, generated outside a target location and focussed on a limited area of interest, can be used to alter tumor growth and response to therapy in vivo. It is evident that the most effective HESW treatment protocol still has to be developed. This protocol will depend on tumor specific properties and on the adjuvant therapy used. At the moment we are still at the beginning of a new era of HESW research in tumor biology and tumor treatment.

REFERENCES

Delius M., Weiss N., Gambihler S., Goetz A., Brendel W. Tumor therapy with shock waves requires modified lithotripter shock waves. Naturwissenschaften, 76, 573, 1989.

Jones B.J., McHale A.P., Butler M.R. Oncological applications for high energy shock waves. Eur. Urol., 18, 285, 1990.

Kilbourn R.G., Belloni P. Endothelial cell production of nitrogen oxides in response to interferon gamma in combination with tumor necrosis factor, interleukin-1, or endotoxin. J. Natl. Cancer Inst., 82, 772, 1990.

Kost J., Leong K., Langer R. Ultrasound enhanced polymer degradation and release of incorporated substances. Proc. Natl. Acad. Sci., 86, 7663, 1989.

Oosterhof G.O.N., Smits G.A.H.J., de Ruyter J.E., Schalken J.A., Debruyne F.M.J. In vivo effects of high energy shock waves on urological tumors, an evaluation of treatment modalities. J. Urol., 144, 785, 1990.

Prat F., Ponchon T., Berger F., Chapelon Y., Gagnon P., Cathignol D. Hepatic lesions in the rabbit induced by acoustic cavitation. Gastroenterology 100, 1345, 1991.

Smith F.L. Carper S.W., Hall J.S., Gilligan B.J., Madsen E.L. Storm F.K. Cellular effects of piezoelectric versus electrohydrolic high energy shock waves. J. Urol., 147, 491, 1992.

Weiss N., Delius M., Gambihler S., Dirschedl P., Goetz A., Brendel W. Influence of the shock wave application mode on the growth of A-MEL3 and SSK2 tumors in vivo. Ultrasound Med. Biol., 16, 595, 1990.

SAMENVATTING EN CONCLUSIES

Dit proefschrift beschrijft experimentele in vitro en in vivo studies, met als doel inzicht te verkrijgen in (1), faktoren welke de effecten van hoog energetische schokgolven (HESW) op (tumor)celen beinvloeden, (2), het gebruik en effect van deze vorm van acoustische energie als antitumor behandelings modaliteit, hetzij als monotherapie, hetzij in combinatie met locale of sytemische therapien, en (3), de wijze waarop HESW de tumorgroei in vivo beinvloeden, met als uiteindelijk doel tot rationele en doeltreffende behandelingsschema's te komen.

Hoofdstuk 1 beschrijft de physische karakteristieken van HESW en de technische aspecten van verschillende typen HESW generatoren. Geluidsgolven kunnen op zodanige wijze worden gegenereerd en gefocusserd dat zogenaamde schokgolven in een betrekkelijk beperkt volume ontstaan. HESW worden alszodanig klinisch toegepast in extracorporele schokgolf lithotripsy waarbij concrementen in urine- en gal-wegen kunnen worden vergruisd. Duidelijk is geworden dat HESW ook een effect kunnen bewerkstelligen op weefsel niveau. In de laatste vijf jaren zijn een toenemend aantal publicaties betreffende HESW geassocieerde bijwerkingen en bio-effecten verschenen.

Hoofdstuk 2 beschrijft de invloed van de experimentele opstelling op de uitkomst van in vitro onderzoek. Een dosis-afhankelijke afname van vitale cellen werd waargenomen na blootstelling van verschillende (tumor)cellen in een suspensie of in een centrifugaat op de bodem van een testbuis. De gevoeligheid voor schokgolven was evenwel niet gelijk in deze beide testsituaties. Tevens werd een differentiële gevoeligheid van verschillende celtypes waargenomen. Schokgolven bewerkstelligden geen effect wanneer de cellen in 15% gelatine werden gefixeerd en geïmmobiliseerd, of als het centrifugaat op een bodemlaag van 15% gelatine werd geplaatst. Deze resultaten geven aan dat de beschadiging van cellen in een suspensie afhankelijk is van factoren welke het micromilieu beinvloeden. Hierbij kan de generatie van cavitaties een belangrijke rol spelen. Deze resultaten kunnen van belang zijn om het werkingsmechanisme van schokgolven in vivo te begrijpen.

In hoofdstuk 3 werden de effecten van gecombineerde behandeling met verschillende biological response modifiers (BRM's, interferon-α en tumor necrosis factor-α) in vijf humane niertumoren in het naakte muis model bestudeerd. Toediening van schokgolven alleen had een tijdelijk effect op de tumor groei en BRM's alleen hadden ook een beperkt effect op de groei van gevestigde tumoren.

133

Synergistische remming van de tumor groei, tot zelfs tumor regressie, werd gezien in de gecombineerde behandeling van HESW met tumor necrosis factor-α in goed doorbloede tumoren.

Extrapolatie van in vitro verkregen resultaten naar de in vivo situatie is moeilijk (Hoofdstuk 1). Bovendien kan de cytotoxiciteit van HESW in vivo indirect bewerkstelligt worden door beschadiging, verstoring van de (tumor) vascularisatie.

Derhalve werd in de volgende studies kernspin resonantie spectroscopie (MRS) toegepast om HESW geinduceerde cellulaire effecten in vivo te bestuderen. Deze non-invasieve techniek maakt het mogelijk om metabole veranderingen longitudinaal te evalueren en heeft derhalve een grote potentie om progressieve veranderingen na uiteenlopende tumor therapien te vervolgen.

Simultane veranderingen in hoog energetisch fosfaat metabolisme en pH in HESW blootgesteld spierweefsel in muizen werden met behulp van ^{31}P MRS gemeten. Tevens werd uitgebreid histologisch onderzoek (licht- en electronen-microscopie) verricht. Zodoende werden HESW geinduceerde celdegeneratie, celdood en celregeneratie in de tijd vastgelegd. De resultaten hiervan zijn beschreven in Hoofdstuk 4. Naast dilatatie en disruptie van capillairen en beschadiging aan zenuwweefsel werden verschillende stadia van spiercel degeneratie gezien. Er bleek een differentiele cellulaire gevoeligheid voor HESW te bestaan. De tijdelijke veranderingen in inorganisch fosfaat en pH, welke werden gezien met behulp van de MRS, kon worden geinterpreteerd als metabole veranderingen in het proces van degenererende spiercellen en wij concludeerden dat de ^{31}P MRS in staat is de metabole veranderingen van degenererende spiercellen te monitoren. Deze degeneratie kon slechts gedeeltelijk worden verklaard door tijdelijke ischemie.

Om meer inzicht te krijgen de behandeling van tumoren in vivo met HESW, werd ^{31}P MRS gebruikt en hiermee tumorcelmetabolisme bestudeerd. Deze techniek verschaft informatie over metabole veranderingen in viabele tumorcellen welke ,de target' voor de HESW behandeling zijn.

De resultaten zijn beschreven in Hoofdstuk 5. Blootstelling van NU-1 humane niertumoren in de naakte muis resulteerde in een passagiere dosis-afhankelijke afname van phosphocreatinine en nucleoside trifosfaten en stijging van inorganisch fosfaat met daling van de pH. Deze veranderingen passen bij ischemische veranderingen in the tumor.

Hoofdstuk 6 beschrijft de effecten van HESW op tumor blood flow (TBF) en tumorcelmetabolisme. Er werd gebruikt gemaakt van ^{1}H/^{2}H/^{31}P MRS. Een

dramatische, maar tijdelijke, reductie van de TBF werd gezien. Simultane monitoring met ^{1}H en ^{31}P MRS vertoonde een daling van de pH en stijging in lactaat concentratie in hetzelfde tijdsinterval.

De MRS studies ondersteunen de hypothese dat tumor vascularisatie (zowel structureel als functioneel) het voornaamste aangrijpingspunt is van HESW therapie, mogelijk door het ontstaan van cavitaties ter hoogte van het vasculaire endotheel. De resultaten van deze studies kunnen gebruikt worden voor een rationele benadering in de ontwikkeling van (gecombineerde) HESW tumortherapie.

Woorden van Dank

Bij het verschijnen van dit proefschrift wil ik eenieder die heeft bijgedragen aan de tot standkoming ervan, bedanken voor haar of zijn medewerking.

Mijn bijzondere dank gaat uit naar:

Prof.Dr. F.M.J. Debruyne voor het feit dat hij me in vol vertrouwen de gelegenheid bood om als wetenschappelijk medewerker op het Urologisch Research Laboratorium van zijn afdeling onderzoek te verrichten. Hij heeft enkele waves van zijn nimmer aflatende energie op mij over weten te brengen.

Jack Schalken, voor de wijze waarop hij me als basis-arts heeft laten ontplooien in de (uro-oncologische) fundamentele research.

Gosse Oosterhof voor zijn aimabele ondersteuning en adequate directheid gedurende onze onderzoeksperiode.

Arend Heerschap, voor zijn enthousiaste begeleiding bij het opzetten en uitvoeren van de NMR spectroscopie experimenten en voor de heldere wijze waarop hij de principes en zijn onschatbare know-how in dit onderzoek heeft weten over te dragen.

Erik v.d. Boogaart voor het bouwen van de "home-build" NMR-probes.

Jos Joordens, Gerda Nachtegaal en Jan van Os voor hun altijd oproepbare steun bij de uitvoering en verwerking van de spectroscopie metingen.

Paul Jap, voor zijn joviale begeleiding bij de E.M. studies.

Huub Croes en Mietske Wijers voor het maken van de ultra-dunne coupes.

Georg Borm en Ad Theeuwes voor hun belangrijke bijdrage aan de statistische bewerking van de gegevens.

Monique Derks, Jan Koedam en Piet Spaan, voor de verzorging en behandeling van de naakte muizen en ratten bij de experimenten vanuit het Centraal Dieren Laboratorium.

Alle 22 van het URL, voor ieders aandacht en inzet. In het bijzonder Erik Cornel voor de prettige samenwerking en de voortzetting van het onderzoek. Anja de

Ruiter, voor het aanleren van de weefselkweek technieken en de hulp bij de uitvoering van vele experimenten. Ton Beniers, Jeroen van Moorselaar en Pim Peelen, voor het wegwijs maken in het onderzoek met in vivo tumormodellen. Egbert Oosterwijk, voor zijn opbouwende en glasheldere commentaar.

Frans Huisman voor de cover met shock effect.

Mirjam, ondanks mijn veel afwezig zijn kon ik toch altijd rekenen op je geduld en immer aanwezige steun. Zonder deze had ik mijn experimenten nooit kunnen uitvoeren en was dit proefschrift niet geworden wat het is.

CURRICULUM VITAE

De schrijver van dit proefschrift werd geboren op 25 juni 1961 te Maastricht. In 1979 behaalde hij het diploma VWO b aan het Hertog-Jan College te Valkenswaard. Hij startte de studie Geneeskunde aan de Vrije Universiteit Brussel alwaar hij zijn kandidaatsexamen behaalde in 1984. Hij vervolgde deze studie aan de Rijks Universiteit Utrecht. Het artsexamen werd met goed gevolg afgelegd in februari 1988. Sinds maart 1988 is de auteur verbonden als wetenschappelijk medewerker aan het Urologisch Research Laboratorium (Hoofd: Dr. J.A. Schalken) van de afdeling Urologie (Hoofd: Prof. Dr. F.M.J. Debruyne) van het Academisch Ziekenhuis Nijmegen. Vanaf januari 1992 volgt hij de vooropleiding algemene heelkunde, in het kader van de opleiding tot uroloog, aan het Canisius-Wilhelmina Ziekenhuis te Nijmegen (opleider: Dr. H.F.M. Joosten).